

WOOD THE BEST MATERIAL FOR MANKIND

Jozef KÚDELA & Marian BABIAK, editors

Arbora
Publishers

Proceedings of the annual IAWS meeting “Wood the Best Material for Mankind” and the 5th International Symposium on the “Interaction of Wood with Various Forms of Energy” held on September 26–28, 2012 in Zvolen, Slovakia.

Organizers:

Faculty of Wood Sciences and Technology, Technical University in Zvolen, Slovakia
The International Academy of Wood Science (IAWS)

Guarantees of the Symposium

Lennart SALMÉN, President of IAWS
Marian BABIAK, Technical University in Zvolen, Zvolen, Slovakia

Advisory Committee

Uwe SCHMITT, Vice-President of IAWS
Rob EVANS, Secretary of IAWS
Frank BEALL, Past-President of IAWS
Jozef KÚDELA, Technical University in Zvolen, Zvolen, Slovakia

Scientific Committee

Igor ČUNDERLÍK, Technical University in Zvolen, Zvolen, Slovakia
Janis DOLACIS, Latvian State Institute of Wood Chemistry, Riga, Latvia
Joris Van ACKER, Ghent University, Belgium
Sergej MEDVEĎ, University of Ljubljana, Slovenia
Eva HAVIAROVA, Purdue University, West Lafayette, IN, USA
Petr HORÁČEK, Mendel University of Agriculture and Forestry, Brno, Czech Republic
Bohumil KASAL, Fraunhofer Institute for Wood Research, Braunschweig, Germany
Stanislav KURJATKO, Technical University in Zvolen, Zvolen, Slovakia
Jianxiong LU, Chinese Academy of Forestry, Peking, China
Waldemar MOLIŃSKI, University of Life Sciences in Poznań, Poznań, Poland
Sándor MOLNÁR, University of West Hungary, Sopron, Hungary
Peter NIEMZ, Institut f. Baustoffe (IFB), Zürich, Switzerland
Patrick PERRÉ, École Centrale, Paris, France
Jack N. SADDLER, University of British Columbia, Vancouver, Canada
Pekka SARANPÄÄ, Finnish Forest Research Institute, Vantaa, Finland
Marketta SIPI, University of Helsinki, Helsinki, Finland
Alfred TEISCHINGER, University of Natural Resources and Applied Life Sciences, Vienna, Austria
Boris N. UGOLEV, Moscow State Forestry University, Moscow, Russia

© Jozef Kúdela & Marian Babiak, editors, 2013

© Arbora Publishers, Zvolen, Slovakia, 2013

Printing: Technical University in Zvolen, Zvolen, Slovakia

Technical editor: Antónia Malenká

Number of pages: 117

The manuscripts have been peer-reviewed by the editors and anonymous reviewers and have not been subjected to linguistics revision.

ISBN 978-80-968868-6-9

Preface

The International Academy of Wood Science held its annual meeting on September 26–28, 2012 at the Technical University in Zvolen, Slovakia. The IAWS meeting joined forces with the 5th International Symposium on the Interaction of Wood with Various Forms of Energy. The event was participated by about 50 attendants from 16 countries all over the world.

The International Academy of Wood Science (IAWS) is a non-profit assembly of wood scientists working in all fields of wood science with their associated technological domains. The Academy secures worldwide recognition to respectable wood scientists by selecting them for election as fellows. The Department of Wood Science, Faculty of Wood Sciences and Technology of the Technical University in Zvolen (TUZVO) organizes the International Scientific Symposium dealing with interactions of wood with various forms of energy and with impacts of these interactions on the wood quality. Beginning with the year 1996, the symposium has been organized at regular, four-year intervals. The event provides a very good opportunity for exchange of recent findings in the area.

The last meeting was aimed at better understanding of wood in the sense of the slogan: “We can use wood with intelligence only if we understand wood”. The motto of the conference “Wood the best material for mankind” was also used as the title of the symposium proceedings.

The topics of interest included:

- ~ Interactions in the system wood – water – heat
- ~ Wood’s response to mechanical loading
- ~ Interactions on the wood surface
- ~ Interactions between wood and various forms of radiation
- ~ Wood quality parameters determining its final use
- ~ Ecological and environmental properties of wood
- ~ Properties of wood based materials

These proceedings do not provide the readers with all the papers presented at the symposium, included are only the ones the authors submitted for publication. Some other presentations read during the conference should be accessible at the address www.iaws-web.org if the speakers give us the permission to publish them.

We would like to express our appreciation to all the participants, the reviewers and the organizers. We also thank Ms. Antónia Malenká and Dr. Rastislav Lagaña for their helpful cooperation in compiling the Proceedings.

Editors

Content:

I. VARIVODINA, N. KOSICHENKO, N. NEDELINA Wood porosity depending on histological structure	7
R. HRČKA An application of diffusion of water in wood	11
P. HALACHAN, R. HRČKA The measurement of the transport characteristics of the water movement in wood	15
T. HORVÁTH, Z. PÁSZTORY Modeling of seasonal heat container for wood frame residential homes	21
P. NIEMZ, W. SONDEREGGER, T. OZYHAR A. MARTIENSSEN Mechanical characterisation of sycamore maple (<i>Acer pseudoplatanus</i> L.)	25
B. UGOLEV, G. GORBACHEVA, S. BELKOVSKIY Quantification of wood memory effect	31
B. NANAYAKKARA, M. RIDDELL, G. EMMS, J. HARRINGTON Understanding the clonal response to imposed mechanical stress in <i>Pinus radiata</i> seedlings	39
N. TERZIEV, G. DANIEL Application of high frequency treatments for improved permeability of Norway spruce (<i>Picea abies</i> KARST.) wood	43
M. REŠETKA, J. KÚDELA Influence of pressing parameters on dimensional stability and density	49
R. NÉMETH, M. BAK, B. MBOUYEM YIMMOU, K. CSUPOR, S. MOLNÁR, L. CSÓKA Nano-zink as an agent against wood destroying fungi	59
J. ABOLINS, J. GRAVITIS Environmental limits to sustainable yields of wood for materials and energy	65
Z. PÁSZTORY, M. EDELÉNYI, J. BOROS, Z. KÖVÁRI Developing of new photo analytical method for measuring of wood stacks	69
S. CLAUB, P. WATSON, S. AMMANN, P. NIEMZ Determination of fracture properties under mechanical stress	73
J. GRAVITIS, J. ABOLINS, G. DOBELE, R. TUPCIAUSKAS, A. VEVERIS, M. ANDZS, A. PUTNINA, S. KUKLE Composites of steam exploded biomass	79
I. RONYECZ, Z. PÁSZTORY Thermal insulation capacity of chipped oak bark in different compression level	85
G. A. UPITIS, J. A. DOLACIS Feasibility of reinforcing birch plywood with hemp fibres	89
J. IŽDINSKÝ, V. TÓTH, J. KÚDELA Polyethylene terephthalate recycling in particle board production	93

Abstracts:

K. RUEL Understanding wood at the nanoscale - zooming through wood cell wall ultrastructural organization ...	101
H. SEHAQUI Nanofibrillated cellulose from wood as building block in high toughness materials	102

R. WIMMER, O. KLÄUSLER, P. NIEMZ Sorption isotherms from wood adhesive films	103
M. TRCALA Spectral stochastic modelling of uncertainties in heat and moisture transfer equations	104
SOPUSHYNSKYI I., ZHMURKO I., TEISCHINGER A. Diagnostic criterions of figured wood of European beech (<i>Fagus sylvatica</i> L.) growing in Ukraine	105
A. ANTONS, J. DOLACIS Drying of sifted wood with the pneumo-impulse method	106
P. ČERMÁK, A. DEJMAL The effect of heat and ammonia treatment on colour response of oak heart/sapwood and comparison of physical and mechanical properties	107
V. KOIŠ Microwave radiation effect on axial fluid permeability in false heartwood of beech	108
V. SEBERA, A. NASSWETTROVÁ Numerical analysis of mode stirrer impact on electric field uniformity in a microwave wood dryer	109
J. VAN ACKER, J. VAN DEN BULCKE, N. DEFOIRDT, M. DIERICK High-throughput characterization of wood	110
R. LAGAÑA, J. KÚDELA, J. ĎURKOVIČ Surface properties analyzed by atomic force microscopy	111
Y. S. HADI, T. NURHAYATI, JASNI, H. YAMAMOTO, N. KAMIYAD Smoked wood resistance to subterranean and dry wood termites attack	112
P. PAŘIL, A. DEJMAL Comparison of physical properties of poplar wood vacuum-pressure impregnated with sucrose and sodium chloride	113
I. ŠUCHAŇOVÁ, R. LAGAÑA & M. BABIAK The influence of heat treatment on the rheological properties of beech wood	114

WOOD POROSITY DEPENDING ON HISTOLOGICAL STRUCTURE

I. VARIVODINA, N. KOSICHENKO & N. NEDELINA

Voronezh State Academy of Forestry Engineering, Department of woodscience, Russia
Voronezh, Timiriازهva str., 8, varivodinna@rambler.ru, vgltaewood@yandex.ru

Abstract

Porous structure is an important feature of wood. Total volume of pores and their linear dimensions influence the properties of porous materials. Wood porosity conditions cell cavities, intercellular spaces and sections of cell wall presence in its structure.

Our former experiments showed the relationship between wood porosity and number of growth rings. This dependence is indirectly proportional for pine and birch and directly proportional for oak. It is well known that the change of growth ring occurs during the period of tree growth. Therefore wood histological structure and porosity as one of the main physical properties characteristics depending on the growth rate were investigated.

It turned out that portion of late tracheids increases with the rate of growth reduction of soft wood. As a result the wood density and strength rise. By volume structure of resin ducts, wood parenchyma and medullary rays are constant. The contrary wood forming is observed at ring-porous wood. The change of growth ring happens at the expense of late wood reduction. By volume structure of tracheids, libriform fibers, wood parenchyma and medullary rays are constant.

Keywords: porosity, rate of growth, histological structure, soft wood, ring-porous wood.

INTRODUCTION

Properties of wood are largely determined by its structure, which has a number of distinctive features. Wood has fibrous structure, because the majority of cells refers to prosenchymatous ones. Alternation of early and late wood forms layered structure of wood. Anatomical elements of wood and tissues are oriented in a certain way in the trunk of the tree (fibres, vessels, wood parenchyma, resin ducts). Many properties of wood are directly dependent on the structural direction, which makes wood an anisotropic material. An important feature of wood structure is that it is a porous material. The total volume of cavities and their linear sizes affect the properties of porous materials.

Wood porosity expresses the relative volume of cavities in non-swollen wood, i.e. in the wood which does not contain water. Porosity of wood is explained by the presence of cell cavities, intercellular spaces and non-thickened sites of cell walls (membrane pores), permeated with tiny holes, in its structure. Formed cell wall in non-swollen condition has low porosity (less than 5%).

Wood porosity is defined as the relative volume of emptiness in oven-dry wood and is calculated according to the formula:

$$P = \left[1 - \frac{\rho_0}{\rho_{w.s.}}\right] \cdot 100$$

where P – porosity of wood, [%]; ρ_0 – the density of absolutely dry wood, [g·cm⁻³]; $\rho_{w.s.}$ – density of wood

substance, [g·cm⁻³]; $\rho_{w.s.} = 1.53$ [g·cm⁻³].

It is known that the reduction of growth ring in wood species on different evolutionary levels occurs in different ways. Therefore, the porosity, as one of the important physical parameters, and histological structure of wood were studied depending on the rate of growth.

MATERIAL AND METHODS

The experiment was carried out in the following way. Firstly, samples of the different wood species were taken from the Scientific-educational forestry subdivision of the Voronezh State Academy of Forestry Engineering. The Common pine (*Pinus sylvestris*) was chosen as an example of soft wood, the European silver birch (*Betula pendula*) – of diffuse-porous hardwood and the Common oak (*Quercus robur*) – of ring-porous hardwood. The samples presented all diapason of rate of growth from small-fibred to coarse-ringed. The samples had standard dimensions 20 × 20 × 30 mm according to the national regulatory requirements.

Then their density was defined in oven dry state (ρ_0) and their porosity (P) was calculated according to the shown earlier formula. Then a number of growth rings in one centimeter ($n_{g.r./1\text{ cm}}$) was defined. Histological structure of wood was analyzed using a point integration eyepiece and electric meter of blood cells SFK-MINILAB. This method of analysis was proposed by German researchers Hester and Spring to determine the histological composition of plant

tissues; we used it in relation to the growth rings of wood. Microsections for the analysis of histological composition of wood typical representatives were produced at Technical University in Zvolen at the Department of Wood Science.

RESULTS AND DISCUSSION

As earlier studies showed the relationship between porosity and number of growth rings of pine and birch is linear, inversely proportional, oak wood has the opposite nature of the relationship between the studied parameters - a linear, directly proportional one.

Equation of regression dependence between the porosity of wood and the number of growth rings in 1 cm has the form:

$$\text{for pine: } P = 71.2 - 0.5 \cdot n \quad (1)$$

$$\text{for birch: } P = 61.3 - 0.2 \cdot n \quad (2)$$

$$\text{for oak: } P = 49.5 + 0.5 \cdot n \quad (3)$$

Determination of histological structure of wood will allow to define the true value of wood porosity and to predict changes in physical and mechanical properties of wood, depending on the number of growth rings in 1 cm.

In the rough form wood can be seen as consisting of two terms: from a dense mass (cell walls) and cavities filled with air. However, in determining the

dense mass of wood in the latter one it is necessary to distinguish not two but three components: the cavity of vessels and wood parenchyma, the shell of these elements and rays.

The establishment of a dense mass of wood hence should include, firstly determination of the specific volume occupied by vessels cavities in the wood, secondly, determination of the specific volume of cavities of fibres (and cells of wood parenchyma, although in this case we are forced to neglect their transverse shells); thirdly, determination of specific volume of the vessel shells, fibres, and finally, fourth, determination of the specific volume of medullary rays. At the same time we neglect cell cavities of the rays. However, the summation of cavities of tracheal elements with cavities of ray cells is impractical. Unfortunately, differences in the caliber of vessels and fibres can be seen only in very rare cases and it is unable to perform all operations under one magnification. Therefore, these operations have to be broken up, which certainly not just delays the work, but to some extent, can serve as a source of error.

With the reduction of rate of growth in pine, the proportion of late tracheids increases, hence the density and strength properties of wood increase. Volume composition of resin ducts of associated parenchyma and medullary rays remains constant.

Table 1 Percentage of items of Common pine wood, depending on the rate of growth.

Number of growth rings in 1 cm	Calculated porosity, %	Early tracheids, %	Late tracheids, %	Resin ducts, %	Associated parenchyma, %	Medullary rays, %
11.5	65.4	64.9	28.9	0.5	0.4	5.3
5.5	68.4	67.5	26.2	0.8	0.5	5.0
2.5	70	74.4	18.8	1.1	0.6	5.1

Table 2 Percentage of shells and cavities of Common pine elements.

PINE	Early tracheids, %		Late tracheids, %	
	shell	cavity	shell	cavity
	12		88	80

Table 3 Calculation of the porosity of Common pine wood on histological composition taking into account cell cavities.

Number of growth rings in 1 cm	Calculated porosity, %	Early tracheids, %	Late tracheids, %	Porosity of cell wall, %	Porosity, %	Error, %
11.5	65.7	57.1	5.8	2	64.9	1.3
5.5	68.4	59.4	5.2	2	66.6	2.6
2.5	70	65.5	3.8	2	71.3	1.8

Table 4 Percentage of elements of European silver birch wood, depending on the rate of growth.

Number of growth rings in 1 cm	Porosity, %	Vessels, %	Vessel tracheids, %	Fibre tracheids, %	Libri-form fibre, %	Parenchyma, %	Medullary rays, %
10	59.3	16.2	10.3	28.0	37.8	2.0	5.8
6	60.1	24.5	7.4	24.2	37.8	1.6	6.5
2	60.9	24.0	7.0	22.1	38.3	1.8	6.8

With the reduction of rate of growth in birch, the proportion of vessels decreases. The vessels are solitary, in short chains or in groups of 2 - 3, rarely more. Uniform diffuse distribution of the vessels of medium-diameter is most favorable for processing. It dries uniformly, cut and soak well. Volume composition of fiber tracheids, libriforma fibres, wood parenchyma and medullary rays remains constant.

Common oak has increase of rate of growth due to the late zone, so strength, density and hardness of wood increases. Oak wood is better to bend, as there are large vessels in the early zone which make it

possible for the wood to be indurated without breaking. Hence wood with a large number of growth rings in 1 cm will bend more, since with reduction of growth ring proportion of large vessels in oak is increased. Volume composition of fibrous and vessel tracheids, libriforma fibres, and wood parenchyma, wide and narrow medullary rays remains constant.

This proves that knowing the percentage of the anatomical elements of wood makes it possible to calculate the true value of porosity, which is not significantly different from that calculated by the formula.

Table 5 Percentage of shells and cavities of European silver birch elements.

Birch	Vessels, %		Vessel tracheids, %		Fibre tracheids, %		Libriform fibre, %	
	shell	cavity	shell	cavity	shell	cavity	shell	cavity
	6.7	93.3	40	60	37	63	70	40

Table 6 Calculation of the porosity volume of European silver birch wood on histological composition taking into account % of the cavities and cell walls.

Number of growth rings in 1 cm	Calculated porosity, %	Vessels, %	Vessel tracheids, %	Fibre tracheids, %	Libriform fibre, %	Porosity of cell wall, %	Porosity, %	Error, %
10	59.3	15.1	6.2	17.6	15.1	4	58.0	2.2
6	60.1	22.8	4.4	15.2	15.1	4	61.5	2.3
2	60.9	22.4	4.2	13.9	15.3	4	59.8	1.8

Table 7 Percentage of Common oak wood elements, depending on the rate of growth.

Number of growth rings in 1 cm	Porosity, %	Large vessels, %	Small vessels, %	Wide medullary rays, %	Narrow medullary rays, %	Vessel tracheids, %	Fibre tracheids, %	Libriform fibre, %	Parenchyma, %
12.5	55.7	11.8	9.4	9.0	1.5	21.1	8.1	35	4.1
8	53.5	7.6	10.9	8.5	1.2	24.0	8.0	35.5	4.3
3	51	5.1	12.2	8.1	1.3	25.5	7.0	36.0	4.8

Table 8 Percentage of shells and cavities of Common oak elements.

Oak	Large vessels, %		Small vessels, %		Vessel tracheids, %		Fibre tracheids, %		Libriform fibre, %	
	shell	cavity	shell	cavity	shell	cavity	shell	cavity	shell	cavity
	5.7	94.3	10	80	30	70	40	60	70	30

Table 9 Calculation of the porosity volume of Common oak wood on histological composition taking into account % of cavities and cell walls.

Number of growth rings in 1 cm	Calculated porosity, %	Large vessels, %	Small vessels, %	Vessel tracheids, %	Fibre tracheids, %	Libriform fibre, %	Porosity of cell wall, %	Porosity, %	Error, %
12.5	55.7	11.1	7.5	14.8	4.8	10.5	4	52.7	5.0
8	53.5	7.2	8.7	16.8	4.8	10.7	4	52.2	2.5
3	51.0	5.9	9.7	17.8	4.2	10.8	4	51.3	0.5

CONCLUSIONS

1. With the reduction of rate of growth in the Common pine (*Pinus sylvestris*), the proportion of late tracheids increases, hence the density and strength properties of wood increase. Volume composition of resin ducts of associated parenchyma and medullary rays remains constant.
2. With the reduction of rate of growth in the European silver birch (*Betula pendula*), the proportion of vessels decreases. Volume composition of fiber tracheids, libriforma fibres, wood parenchyma and medullary rays remains constant.
3. The Common oak (*Quercus robur*) has increase of rate of growth due to the late zone, so strength, density and hardness of wood increases. Volume composition of fibrous and vessel tracheids, libriforma fibres, and wood parenchyma, wide and narrow medullary rays remains constant.

REFERENCES

- UGOLEV, B.N. 2007: Wood science and bases of forest commodity science: Textbook for higher educational institution of forestry engineering. Moscow : MGUL, 351 pp.
- KOSICHENKO N.E. 2000: The wood structure and density forming in ontogeny. In: Wood Structure, Properties and Quality'2000», Petrozavodsk, Russia, 2000, pp. 58–61.
- KOSICHENKO N.E., VARIVODINA I.N. & VARIVODIN V.A. 2007: Interconnection between wood porosity and rate of growth. In: Dendrology and forest economy. Krasnoyarsk, Russia, 2007. pp. 69–71.
- VARIVODINA I., KOSICHENKO N., VARIVODIN V. & SEDLIAČIK J. 2010: Interconnections among the rate of growth, porosity and wood water absorption. Wood Research, 2010, 55(1): 59–66.

AN APPLICATION OF DIFFUSION OF WATER IN WOOD

RICHARD HRČKA

Technical University in Zvolen, T. G. Masaryka 24, 960 53 Zvolen, Slovakia

Abstract

Wood - water interaction can result in dimensional changes, wood has ability to shrink or swell. This system can be loaded with external force, or torque, for example in the environment of air. The diffusion equation has been usually used to describe the movement of water in wood with fixed boundaries, but deriving diffusion equation does not forbid the moving boundary, even such equation can be solved analytically under some restrictions. If these restrictions are met then one will find the deformation field inside wood. The recognition of deformation field in wood is a good starting point of finding stresses, which attack wood during the diffusion of water.

Key words: wood, moisture content, diffusion, maximum deformation.

INTRODUCTION

Optimization of the drying process is still real and actual problem. Even diffusion is not a drying; some common features can be seen (BABIÁK *et al.* 1989, SALIN 2010). Applications of diffusion equation solutions were limited to change of amount of diffusing substance mass inside of wood, functions of concentration through the thickness or at given point of wood in time (SIAU 1994, POŽGAJ 1997). In spite of a lot of work was done (LYKOV 1968), connection between diffusion and deformation field inside wood was failed, because description of diffusion of water in wood did not account for dimensional changes of wood during diffusion. The key point is to realise the centre of mass movement of half thickness of specimen. If it is known that wood surface moves (wood can shrink or swell) (STAMM 1964), but if it goes from rest state to rest state, there must be the force acting on the centre of mass of specimen half thickness (symmetric problem). The problem of moving boundary is solved with the help of Math and Physics knowledge but simulated problem is based on knowledge from Wood Science.

The aim of the article is to show the solution of diffusion equation with moving boundary, and its applicability to determining the maximum possible deformation during diffusion of water in wood.

DIFFUSION EQUATION WITH MOVING BOUNDARY

Diffusion is transfer of mass. The 1st Fick's law defines diffusion, for example in the form of differential equation:

$$\vec{q} = -\overline{D} \text{grad}(c)$$

where \mathbf{q} is flux of matter (intensity) [$\text{kg}\cdot\text{m}^{-2}\cdot\text{s}^{-1}$]; $\text{grad}(c)$ is gradient of concentration [$\text{kg}\cdot\text{m}^{-4}$]; D is diffusion coefficient [$\text{m}^2\cdot\text{s}^{-1}$]. The concentration is defined as:

$$c = \frac{m_{\text{H}_2\text{O}}}{V}$$

where $m_{\text{H}_2\text{O}}$ is mass of water [kg] in V wood volume [m^3]. The differential form of the 1st Fick's law does not contain explicitly time t [s], therefore diffusion equation is introduced as combination of the 1st Fick's law and conservation of mass in a domain of wood volume enclosed by surface S [m^2]:

$$-\int_S q dS = \frac{\delta m_{\text{H}_2\text{O}}}{\delta t} \quad (1)$$

The right side of equation (1) is rate of change of water mass in wood. Let us assume other point of this problem – average concentration, which can be connected with rate change of water mass in wood as following expression:

$$\frac{d}{dt} \left(\iiint_V c dx dy dz \right)$$

General analytical solution of equation (1) met problems, so it was convenient to restrict this problem to two spatial dimensions. Let the flux be a function of z -coordinate (thickness T) and dimension can change only in y -coordinate (width R), fig. 1:

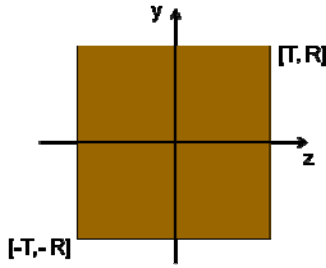


Fig. 1 Board in the coordinate system.

The equation (1) can be arranged after using the Gauss-Ostogradsky theorem:

$$\int_0^T R \frac{\partial}{\partial z} \left(D_T \frac{\partial c}{\partial z} \right) dz = \frac{d}{dt} \int_0^T c R dz$$

and finally diffusion equation with moving boundary has the following form:

$$\frac{\partial}{\partial z} \left(D_T \frac{\partial c}{\partial z} \right) = \frac{\partial c}{\partial t} + \frac{c}{R} \frac{dR}{dt} \quad (2)$$

The concept of diffusion with moving boundary was developed in two dimensions as concentration can change in z coordinate and boundary moves in y coordinate and such movement is evenly distributed in y coordinate finally represented as R width.

DIRECT PROBLEM WITH NON-HOMOGENEOUS BOUNDARY CONDITION

If separation of variables is used, the general solution of equation (2) is obtained. The particular solution is gained after using three conditions. Let the initial condition be constant concentration c_0 over thickness. The flux of concentration in the centre of board is zero (symmetric problem). And the flux at the surface is proportional to surface concentration $c(T,t)$:

$$-D_T \frac{\partial c}{\partial z} \Big|_{z=T} = \alpha (c(T,t) - c_\infty) \quad (3)$$

where α is surface emission coefficient, c_∞ is equilibrium concentration.

The boundary condition (3) is non-homogeneous; therefore it is suitable the concentration space is linear, which is equal to statements: sum of concentrations is also concentration, and multiplying the concentration with real number is also concentration. The consequence of these statements is that surface emission coefficient is function of time in the case of wood. But, there is also another possibility to solve equation (2) according to separation of variables. But, the idea is different. The system of eigenfunctions of the problem will not be complete and equilibrium concentration will depend on the process. Both ideas give the same result:

$$c(z,t) - c_\infty = \frac{2}{T} \frac{R_s}{R} \sum_{n=1}^{\infty} \frac{\mu_n}{\mu_n + \sin(\mu_n) \cos(\mu_n)} e^{-\mu_n^2 \frac{D_T t}{T^2}} \cdot \cos\left(\mu_n \frac{z}{T}\right) \int_0^T (c_s - c_{\infty s}) \cos\left(\mu_n \frac{z}{T}\right) dz$$

with different meaning of symbols included: c_∞ is equilibrium concentration in time t, $c_{\infty s}$ is equilibrium concentration at the beginning, R is width in time t, R_s is width at beginning and μ_n is non-zero n-root of equation:

$$\mu_n \operatorname{tg}(\mu_n) = \frac{\alpha T}{D_T}$$

where μ_n does not depend on time, or

$$\mu_n \operatorname{tg}(\mu_n) = \frac{\alpha T}{D_T} \frac{\frac{1}{R} \frac{dR}{dt}}{\frac{1}{R_s} \frac{dR}{dt} \Big|_{t=0}} = \frac{\alpha_t T}{D_T}$$

where $c_\infty = c_{\infty s}$ then α_t does not depend on the process.

PRODUCT OF CONCENTRATION AND DIMENSION

Concentration c is intensive quantity, width R is extensive one. Their product may be proportional to moisture content. The idea traces the following equation:

$$cR = \frac{1}{L} \frac{dm_{H_2O}}{dz} \frac{dm_0}{dm_0}$$

where L is length, m_0 is oven dry mass. If dm_0 (infinitesimal oven dry mass) and R does not depend on z-coordinate, then cR is proportional to moisture content. It means the concentration will be easily averaged in z coordinate.

DIMENSIONAL CHANGES AND SLICING TEST

The concept recapitulation of moving boundary during diffusion of water in wood is quite clear:

- wood substance, water and air possess the same volume (volume of wood)
- concentration changes in dimension z and time
- width R changes with time
- transport characteristics have constant values

Such concept can be used for determination of deformation in wood during diffusion of water. Let us slice the wood (UGOLEV 2009) in cross section (RT plane) into N equal pieces, fig. 2:

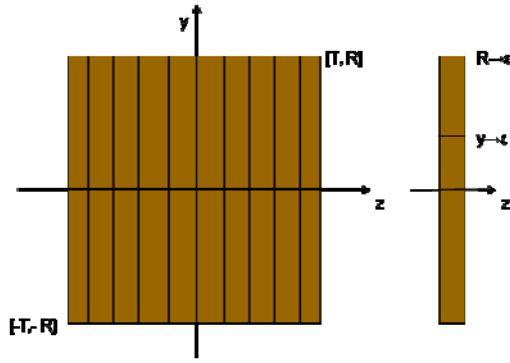


Fig. 2 Slicing test.

Let the strain be equal in y direction in any slice (left side of fig. 2.). Some of slices can show strain after slicing, initially with equal velocity for every slice (R is function only time, rectangular shape of wood prior slicing). Such idea promotes that slicing is a complete inelastic collision. If net external force on a half of specimen is zero during slicing, then momentum conservation principle can be applied:

$$\sum_{j=1}^N (v_{fj} - v_{ij}) \Delta m_j = 0$$

where v_f is final velocity, v_i is initial velocity and Δm_j is mass of slice. Let the masses are known, and after rearrangement and factoring out:

$$\sum_{j=1}^{k-1} (v_{fj} - v_{ij}) \frac{\Delta m_j}{\Delta m_k} + (v_{fk} - v_{ik}) + \sum_{j=k+1}^N (v_{fj} - v_{ij}) \frac{\Delta m_j}{\Delta m_k} = 0$$

for every slice, characteristic matrix is obtained:

$$\begin{pmatrix} 1 & b_{12} & \cdots & b_{1N} \\ \frac{1}{b_{12}} & 1 & \cdots & b_{2N} \\ \vdots & \vdots & \ddots & \vdots \\ \frac{1}{b_{1N}} & \frac{1}{b_{2N}} & \cdots & 1 \end{pmatrix} \begin{pmatrix} v_{f1} - v_{i1} \\ v_{f2} - v_{i2} \\ \vdots \\ v_{fN} - v_{iN} \end{pmatrix} = \begin{pmatrix} 0 \\ 0 \\ \vdots \\ 0 \end{pmatrix} \quad (4)$$

Rewriting the equation (4) to the following form:

$$B(v_f - v_i)_A = 0$$

and if matrix B is equal

$$B = A - E\lambda_A$$

the problem consists of finding the eigenvalues λ_A of matrix A and then to find the eigenvectors of A. It can be shown that eigenvectors of matrixes A and B are related; and moreover if $\lambda_B = N$ then eigenvectors of both matrixes, A and B, are equal. The result is the change of velocity after and before slicing for every slice.

DEFORMATION AND ITS MAXIMUM

Let us assume zero net force acts during cutting in the direction y which means that centre of mass is moving in steady state (motion with constant velocity). Moreover, every point $[R, z]$ moves at the beginning of cutting with the velocity v_i of centre of mass. Then definition of deformation is:

$$\varepsilon = \frac{\int_0^{t_m} v dt - v_i t_m}{v_i t_m + R_i}$$

where v is velocity of slice edge (R) at time t ; t_m is time of cutting duration; v_i is velocity of centre of mass; R_i – initial dimension at the beginning of cutting.

It is obvious that deformation (or strain) depends on details of the process. But there is one special deformation – maximum deformation. Because t_m and R_i are positive constant, maximum deformation is:

$$\varepsilon_{MAX} = \frac{v_f - v_i}{v_i}$$

where v_f is velocity of slice edge (R) just after cutting.

Now, define the process and deformation can be computed. The example is a process with linear restoring force; such matter obeys Hook's law. It can be easily seen that relation between deformation of matter which obeys Hook's law and maximum deformation is:

$$\varepsilon = \frac{1}{2} \varepsilon_{MAX}$$

To confirm the ability of present theory to compute deformation field inside wooden body during diffusion, simulate the process, for example, with data in table 1.

Table 1 Simulated data

Quantity	Value	Unit
starting moisture content	0.30	
equilibrium moisture content	0	
maximum shrinkage	0.10	
T	0.030	m
R	0.060	m
diffusion coefficient	5.0E-09	m ² ·s ⁻¹
surface emission coefficient	1.0E-06	m·s ⁻¹
Biot number=	6.0	
oven dry density	650	kg·m ⁻³
density at starting moisture content=	760	kg·m ⁻³
L	1.00	m

Data in table 1 are suitable for beech wood radial board. The dimension R during shrinkage is computed according the present knowledge in Wood Science

that shrinkage is linear (POŽGAJ *et al.* 1997), descending function of moisture content in interval $\langle 0; 30\% \rangle$ and zero above 30 % until maximum moisture content is reached. But such idea can be overcome with direct prescription of relationship between dimension and moisture content (DUBOVSKÝ *et al.* 1998). Wood does not solute in water. The graph of maximum deformation during diffusion in wooden board sliced to 100 equal pieces is represented on figure 3.

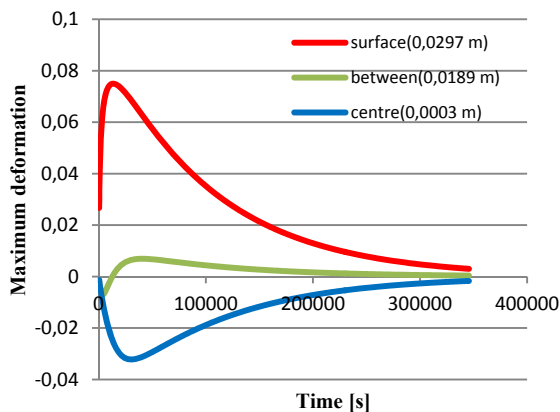


Fig. 3 Graph of maximum deformation in different positions inside wooden board during diffusion of water according presented theory and simulated data.

The largest positive maximum deformation is at the most outer layers of board and the largest negative maximum deformation is at the central layer of the board during the diffusion, which perhaps affects the stresses in wood where water diffuses. But this description is beyond the scope of this article.

CONCLUSIONS

The concept of moving boundary during diffusion leads to two conclusions:

1. moisture content can be a potential of diffusion under some restrictions, but with unchanged diffusion coefficient in the 1st Fick's law.
2. maximum deformation which wood exhibits during diffusion.

The results can be utilized in optimizing the wood drying processes and developing the equipment for performing and control of such processes.

REFERENCES

- BABIAK, M., PAVLÍKOVÁ, M. & JOKEL, J. 1989: Kinetika a termodynamika vlhkého dřeva. [Správa pre priebežnú oponentúru.] Bratislava: ŠDVU, 33 pp.
- DUBOVSKÝ, J., BABIAK, M. & ČUNDERLÍK, I.; 1998: Textúra, štruktúra a úžitkové vlastnosti dřeva. Zvolen: TU vo Zvolene. 106 pp.
- LYKOV, A. V. 1968: Analytical heat diffusion theory. Moscow: Vysshaya Shkola, 685 pp.
- POŽGAJ, A., CHOVANEC, D., KURJATKO, S. & BABIAK, M. 1997: Štruktúra a vlastnosti dřeva. Bratislava: Príroda a.s., 488 pp.
- SIAU, J. F. 1995: Wood: Influence of moisture on physical properties. Department of Wood Science and Forest Products, Virginia Polytechnic Institute and State University. 227 pp.
- SALIN, J. 2010: Problems and Solutions in Wood Drying Modelling – History and Future. In: 11th International IUFRO Wood Drying Conference. Skellefteå: LTU. pp. 103–114.
- STAMM, A. J. 1964: Wood and cellulose science. New York: The Ronald Press Company, 549 pp.
- UGOLEV, B. N. 2009: Wood As Natural Smart Material. Available on Internet: http://www.iaws-web.org/files/file/2009-SaintPetersburg_academy_lecture_ugolev.pdf.

Acknowledgement

This work was supported by the Slovak Research and Development Agency under the contract No. SK-CZ-0045-11.

THE MEASUREMENT OF THE TRANSPORT CHARACTERISTICS OF THE WATER MOVEMENT IN WOOD

PAVOL HALACHAN & RICHARD HRČKA

Technical University in Zvolen, T. G. Masaryka 24, 960 53 Zvolen, Slovakia

Abstract

The paper is divided into two parts. The first part provides experimental diffusion coefficients of non-stationary method for three coniferous species. It refers to factors that affect water movement in wood and their influence on the results of the diffusion properties of wood. The work provides experimental diffusion coefficients of non-stationary method for three coniferous woods [Norway spruce (*Picea abies*, L.), Scots pine (*Pinus sylvestris*, L.), Silver fir (*Abies alba*, Mill.)]. It refers to factors that affect water movement in wood and their influence on the results of the diffusion properties of wood. The second part with capillary elevation was measured after determining the diffusion coefficients. The results of this work were evaluated by Microsoft Excel. We confirmed the fact that with increasing moisture content (MC) the diffusion coefficient increases. The experiment with capillary elevation is based on the measurement of weight changes in time. The aim of the second experiment is to use a capillary action of liquid in the capillaries of species to determine their porosity, determine the dimensions and the number of capillaries which are in our chosen three woods.

Keywords: coniferous species, diffusion coefficient, water in wood, bound water, capillary elevation, capillarity, free water.

INTRODUCITON

Diffusion is one of the processes, which influence changes of MC in wood. Fick's laws describe diffusion. We can use Fick's laws to find moisture content of some point inside a solid in exact time and amount of accepted or evaporated water from whole solid and amount of water that diffused through wood (HRČKA 2008). Diffusion coefficient is the number that describes water movement of bound water in wood. It is an integral parameter which quantitatively characterizes the physical, respectively physical-chemical action. The aim of this paper is to determine diffusion coefficients for three coniferous woods and to compare them with older results and methods. Dimensions of capillaries for every wood are very important for gluing technology, impregnation of wood etc. Porosity of our chosen woods was determined by capillary elevation. These experiments are much cheaper than mercury porosimetry and nitrogen adsorption method, but the results and graphs of this experiment still have large reporting ability.

MATERIAL AND METHODS

Bound water

For experiments we used wood of three coniferous species [Norway spruce (*Picea abies*, L.), Scots pine (*Pinus sylvestris*, L.), Silver Fir (*Abies alba*, Mill.)]. We used samples with dimensions $3 \times 3 \times 1 \text{ cm}^3$ and ten samples for every principal anatomical direction. We used for non-stationary method aquarium with

$\phi = 98 \%$ humidity. At first, samples were dried to 0% and placed to $\phi = 98 \%$ relative humidity (RH). Aquarium was placed in a conditioning chamber with constant temperature ($20 \text{ }^\circ\text{C}$). KURJATKO (1990) measured weight in time intervals: 0h, 1h, 2h, 4h, 8h, 1d, 3d, 5d, 7d, 14d, 28d. But in our experiment we measured samples on balances in ascending time intervals (at beginning every half hour), when we had samples full with bound water we prepared the second experiment. The samples were measured on balances for three decimal places. For nonlinear regression we used Excel (procedure Solver).

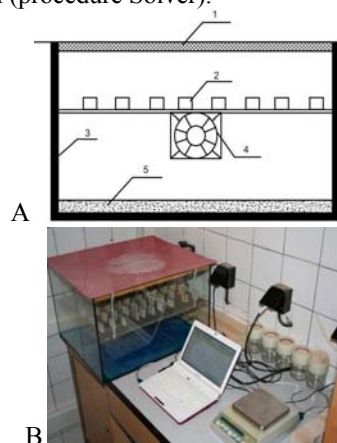


Fig. 1 A: Schematic representation of aquarium with $\phi = 98 \%$ RH. 1 – top with insulation, 2 – sample, 3 – desiccator, 4 – fan, 5 – aqueous solution of $\text{CuSO}_4 \cdot 5\text{H}_2\text{O}$ [$\phi = 98 \%$], B: Work place.

Non- stationary methods are based on Fick's second law:

$$\frac{\partial c}{\partial t} = D \frac{\partial^2 c}{\partial x^2} \quad (1)$$

Equation (1) is only for one direction, on condition that the diffusion coefficient is constant. The concentration is a potential of transport in wood:

$$c = \rho_{rw} \cdot w \quad c \approx \rho_0 \cdot w \quad (2)$$

ρ_{rw} - basic density,
 ρ_0 - oven dry density.

We used boundary condition in the form:

$$\left. \frac{\partial c}{\partial t} \right|_{x=s} = \alpha(c_r - c(s, t)) \quad (3)$$

s- half the thickness of the sample, α - mass transfer coefficient, c_r - equilibrium concentration

We used average concentration:

$$\bar{c}(t) = \frac{1}{S} \int_0^S c(x, t) dx \quad (4)$$

The solution is (POŽGAJ *et al.* 1997):

$$\frac{c(x, t) - c_0}{c_r - c_0} = 1 - 2 \sum_{n=1}^{\infty} \frac{\cos\left(\frac{\delta_n x}{a}\right) Bi}{\delta_n^2 (\delta_n^2 + Bi^2 + Bi) \cos \delta_n} e^{-\delta_n^2 \frac{Dt}{S^2}} \quad (5)$$

Biot criterion is defined as:

$$Bi = \frac{\alpha S}{D} \quad (6)$$

Standardized average solution is (HRČKA 2008):

$$D \frac{w}{w_r} = 1 - \sum_{n=1}^{\infty} \frac{2Bi^2}{\delta_n^2 (\delta_n^2 + Bi^2 + Bi)} e^{-\delta_n^2 \frac{Dt}{S^2}} \quad (7)$$

D and α are unknown. D and α can be determined by least squares method. Solver uses least-squares criterion in the following form:

$$Q(D, \alpha) = \sum_{i=1}^N \left(\left. \frac{w_t}{w_{\infty}} \right|_{teor.} - \left. \frac{w_t}{w_{\infty}} \right|_{exp.} \right)^2 \quad (8)$$

Free water

The second part was the experiment with free water. Specimens saturated with bound water were prepared. This experiment is based on weight changes in time. We can see (Fig. 2) measurement of capillary elevation. The theoretical base is as follows:

The expression of the total weight of water means:

$$N_1 \pi_L R_1^2 \cdot L \cdot \rho_{H_2O} + N_2 \pi_L R_2^2 \cdot h \cdot \rho_{H_2O} = m \quad (9)$$

Where: N_1 - number of full, N_2 - number of capillaries which are not full with water, R_1 - radius of capillary, R_2 - radius of capillary in which water elevates, L - high of sample, h - high of water in some time, m - mass of water.

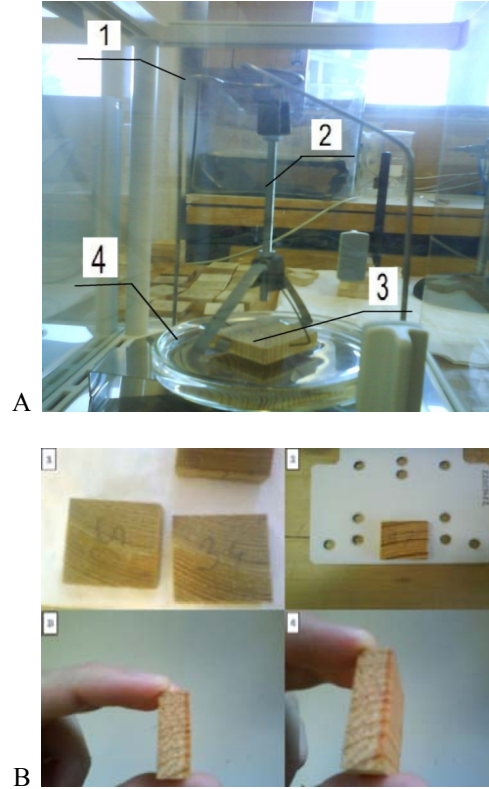


Fig. 2 A: Experiment of capillary elevation. 1 – Tripod for a sample, 2 – holder, 3 – sample, 4 – petri dish with distilled water. B: After experiment with capillary elevation. 1 – Scots pine heartwood, 2 – silver fir, 3, 4 – silver fir - tangential direction.

For the initial condition $h(0s) = 0m$ we found the implicit analytic form (FRIES & DREYER 2008):

$$t = -\frac{h}{b} - \frac{a}{b^2} \ln\left(1 - \frac{bh}{a}\right) \quad (10)$$

The equation h - height of the fluid in the capillary means:

$$h = \frac{m - N_1 \pi R_1^2 L \rho_{H_2O}}{N_2 \pi R_2^2 \rho_{H_2O}} \quad (11)$$

Substituting into the relation (11):

$$t = -\frac{m_1 \delta \eta}{\rho^2 \rho_{H_2O}^2 g R_2^4 N_2 \pi} - \frac{16 \eta \sigma \cos \vartheta}{R_2^3 \rho_{H_2O}^2 g^2} \cdot \ln\left(1 - \frac{m_1 g}{2 \sigma \cos \vartheta R_2 \pi N_2}\right) \quad (12)$$

The solution that forms the basis for solver, relation between the constants:

$$t = -m \cdot A - B \ln(1 - m \cdot C) \Rightarrow \frac{A}{B} = C \Rightarrow C \cdot B = A \quad (13)$$

The equations determining the constants:

$$B = \frac{16 \eta \sigma \cos \vartheta}{R_2^3 \rho_{H_2O}^2} \quad (14)$$

$$R_2^3 = \frac{16\mu\sigma \cdot \cos \vartheta}{\rho_{H_2O} \cdot g^2 \cdot B} \quad (15)$$

$$C = \frac{g}{2\sigma \cos \vartheta \cdot R_2^2 \pi N_2} \quad (16)$$

$$N_2 = \frac{g}{2\sigma \cos \vartheta \cdot R_2 \pi \cdot C} \quad (17)$$

The basic principle of evaluation of theoretical and experimental data is written in relation (18):

$$Q = \sum_{i=1}^N (t_{exp.} - t_{teor.})^2 \quad (18)$$

RESULTS AND DISCUSSION

Here we presented only the main results of the experiments. All charts, graphs and results are in work HALACHAN (2012).

Bound water

The samples of Pine sapwood show a great similarity of diffusion coefficients in all anatomical directions but at different moisture content. The diffusion coefficient reached the highest value at moisture of 20 % in the longitudinal direction (Fig. 3).

In the samples of Pine heartwood, the diffusion coefficient in the longitudinal direction is significantly different from radial and tangential direction. Radial and tangential directions are almost identic (Fig. 4).

Silver fir samples are very unique and the only one that show large difference between anatomical directions (Fig. 5). Silver fir confirms theoretical differences in diffusion coefficient values between anatomical directions. Diffusion coefficient reaches maximal value at 13 % MC in longitudinal direction. After 13 % MC, further towards EMC, diffusion coefficient decreased.

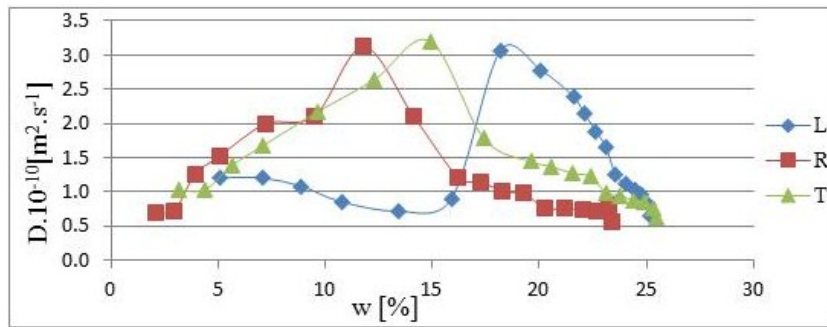


Fig. 3 Graph of diffusion coefficient depending on the moisture for pine sapwood.

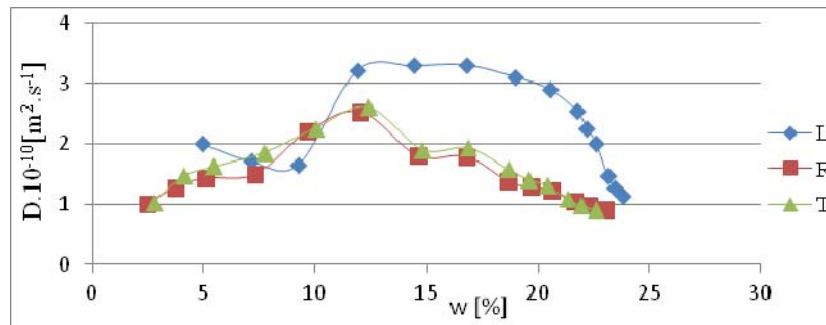


Fig. 4 Graph of diffusion coefficient depending on the moisture for pine heartwood.

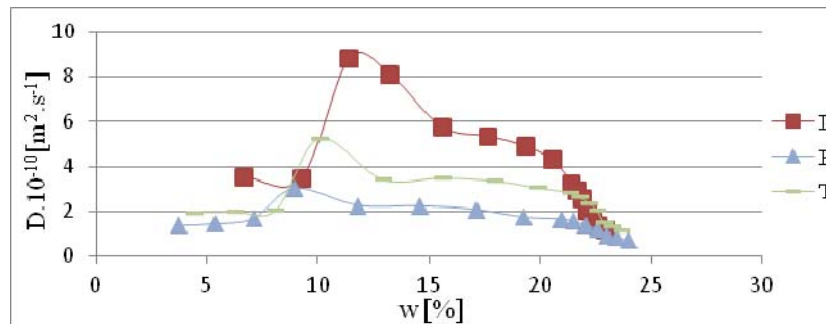


Fig. 5 Graph of diffusion coefficient depending on the moisture for silver fir.

With the increase of density, the diffusion coefficient decreases. (REGINÁČ *et al.* 1990, POŽGAJ *et al.* 1997). We confirmed this fact, only when we compared pine and spruce. The results show that extractives do not affect the diffusion in our case. Older publications (REGINÁČ *et al.* 1990) write that diffusion coefficient in longitudinal direction can be 12-18 times higher than in the radial direction, but our results were different. If the coefficients increase with increasing MC and if this relationship is strong, we should observe decreasing D during the first stage of desorption and increasing D during the absorption (BABIÁK 1998). The diffusion coefficients in longitudinal direction are several times higher than in transverse directions (KURJATKO & KÚDELA 1990). According to KURJATKO & KÚDELA (1990) their experiments with sorption method (spruce) confirm no statistical differences between radial and tangential direction. Silver fir confirms this fact in our experiments. The non-stationary method does not confirm this fact in our case. We also used the statistical analysis F-tests and t-tests. These analyses do not show large differences between different samples.

Free water

Graphs of capillary elevation consist of y logarithmic axes which describes number of capillaries per 1 mm² and x axis which describes radius of capillaries.

The graph (Fig. 7) shows the distribution of pores in radial and tangential directions. This experiments show that elevation, flow and permeability in this directions are much more complicated than in longitudinal directions. For example, in pine sapwood (green triangles), water rapidly elevated. In this sample, most of capillaries had smaller radius then $1 \cdot 10^{-5}$ m.

According to the literature (POŽGAJ *et al.* 1997), the average tracheid widths are about $4 \cdot 10^{-5}$ m for early wood and $2 \cdot 10^{-5}$ m for latewood tracheids. Our values in graphs show the early wood tracheid radius range approximately from $4 \cdot 10^{-5}$ m to about $1 \cdot 10^{-5}$ m (Fig. 6 and Fig. 7). According to the literature (POŽGAJ *et al.* 1997) limit of micro pores is the radius of $1 \cdot 10^{-7}$ m. The graphs confirm this fact.

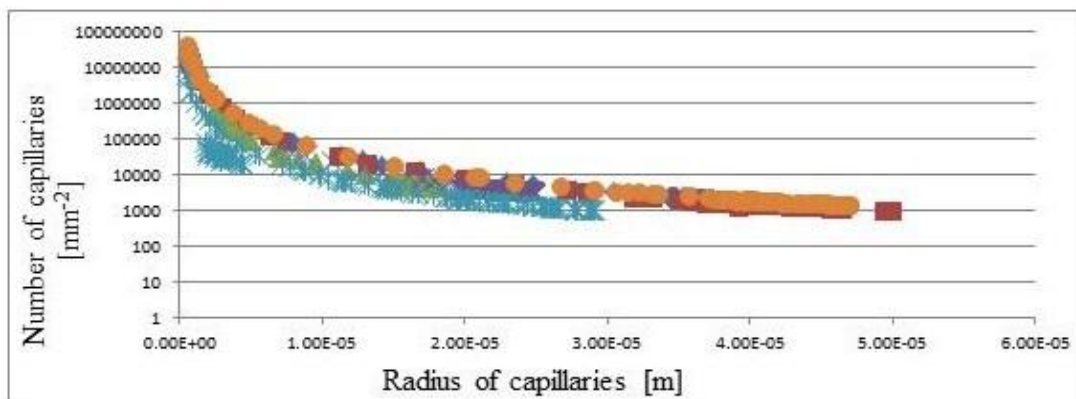


Fig. 6 Graph of capillary elevation in Norway spruce, distribution function.

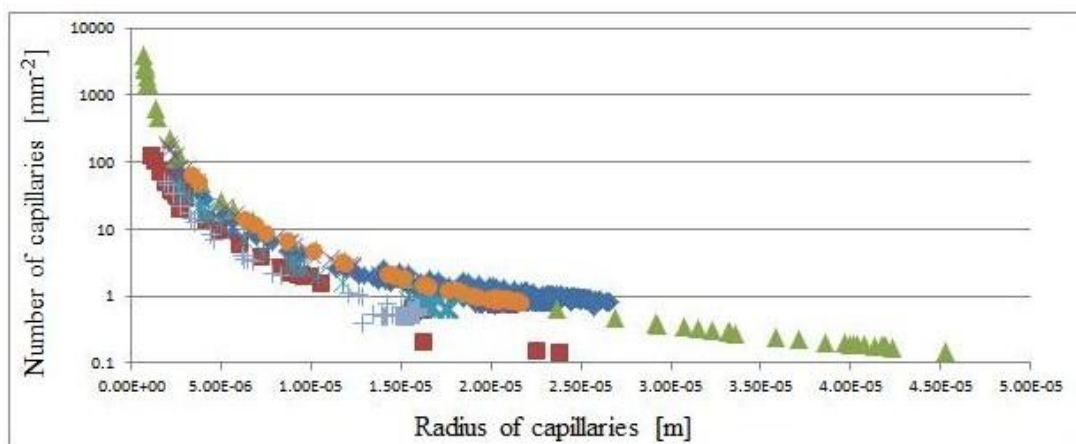


Fig. 7 Graph of capillary elevation, radial and tangential directions, distribution function.

CONCLUSIONS

Older stationary methods in literature show only that that the diffusion coefficient value increases with increasing MC. The experiment with bound water confirms this fact only for some MC in wood. The experiment with free water shows that radii of capillaries measured by capillary elevation are almost equal to those in literature which were measured with other methods.

REFERENCES

BABIAK, M. 1998: Diffusion coefficients of beech and black locust wood. Wood structure and properties '98, Zvolen: Arbora Publishers, pp. 65–70.

FREIS, N. & DREYER, M. 2008: An analytic solution of capillary rise restrained by gravity. Science direct, Bremen: University of Bremen, pp. 259–263.

HALACHAN, P. 2012: Measurement of transport characteristics of wood, [The Diploma thesis]. Zvolen: Technical University in Zvolen, 67 pp.

HRČKA, R. 2008: Diffusion of water in wood of diffuse-porous species in longitudinal direction. Acta facultatis Xylogiae Zvolen, 50: 57–59.

KURJATKO, S. 1970: Návodny na cvičenia z fyzikálnych vlastností dreva a drevných materiálov. (Physical properties of wood and wood based materials, Guides exercises). Zvolen : VŠLD, 90 pp.

KURJATKO, S. & KÚDELA, J. 1990: Bound water diffusion coefficients based on the sorption method. In.: Latest achievements in research of wood structure and physics. Zvolen: VŠLD Zvolen 1990, pp. 187–198.

POŽGAJ, A., CHOVANEC, D., KURJATKO, S. & BABIAK, M. 1997: Wood structure and properties. (in Slovak) Bratislava: Príroda, 486 pp.

REGINÁČ, L. a kol. 1990. Náuka o dreve II. (Wood science) 5 vyd. Zvolen: VŠLD, 1990. 424 s.

Acknowledgement

This work was supported by the Slovak Research and Development Agency under the contract No. SK-CZ-0045-11.

MODELING OF SEASONAL HEAT CONTAINER FOR WOOD FRAME RESIDENTIAL HOMES

TIBOR HORVÁTH & ZOLTÁN PÁSZTORY

University of West Hungary, H-9400 Sopron, Bajcsy Zs. u. 4., horvath.tibor@emk.nyme.hu, pasztory@fmk.nyme.hu

Abstract

In temperate and cold regions seasonal Thermal Energy Storage (TES) systems have got a growing interest in the last few decades. Several researches have done especially the ones of latent heat and chemical storage mechanisms, but for residential space heating and hot water production sensible heat storage systems have been the most advanced in practice.

In this paper the authors present a novel method of seasonal sensible heat storage for residential space heating in a wood frame building using solar thermal energy. A sample heat storage system has been built in Sopron (West-Hungary) and numerous data have been recorded at several measure points in the storage system and building related to some physical parameters e.g., temperature distribution, heat flux density. Thermal processes were investigated and modeled using finite element method software COMSOL Multiphysics.

Keywords: TES, sensible heat storage, space heating, solar energy, wood frame building.

INTRODUCTION

In Europe, energy needs of space heating and hot water production come out at about 82 % of total energy consumption in a residential building (LINDER & BHAR 2007). In the last few decades the tendency of energy prices have been constantly growing and because of this in present days energy savings have become an important factor in building industry. For this reason, national standards in Europe have been requiring lower and lower U-values (overall coefficient of heat transmission) of building elements, and there have been government programs for renovating existing buildings to improve their insulation and space heating systems. To have proper information on energy efficiency of a house, in several countries there has been introduced some type of energy certification of buildings. For example, from 1 January 2012 it is mandatory to provide Energy Performance Certificate (EPC) for all homes for sale and to let in Hungary.

Besides revising existing insulation systems and developing new ones, space heating applications' efficiency must also be improved to achieve an economically and at the same time ecologically better system. In the last centuries fossil energy resources have been dominating on energy market, however increasing consumption of them led to significant pollution of environment. This fact and their limited availability makes necessary to prefer renewable resources to fossil energy carriers in energy production, for the sake of sustainable development.

To reduce ecological footprint (e.g., CO₂ emission) of residential buildings, it seems to be a good decision using solar energy for space heating. As far as we are thinking at daily scale in warmer periods (spring and fall), this type of primer energy source may solely cover the demands because the structure elements of buildings normally have adequate thermal mass which helps damping exterior temperature fluctuations. However in temperate and cold regions of our planet, there is a time offset in seasonal variations of temperature and solar irradiation i.e., maximum amount of solar energy is available at summer and peak demand of space heating occurs at winter. In this case immediate solar irradiation usually cannot cover space heating demands in colder periods. It seems to be logical to store surplus energy from summer in some way and reuse it when needed in the other half of the year. There have been researches on developing such seasonal storage systems for a long while, and some of them have been already implemented successfully in practice.

Overall objectives

The overall aim of authors' research was to develop a new type of seasonal thermal energy storage system for a wood frame residential building with minimal energy demand, using solar energy as primary source for space heating. The system aimed at to store and reuse surplus solar energy collected (mainly) in the summer. This paper focuses on the thermal energy storage system developed in the research but it outlines some information of the building, too. It was intended to investigate heat

Wood the Best Material for Mankind

J. Kúdela & M. Babiak (eds.), 2013, pp. 21–24

© Arbora Publishers, Zvolen, Slovakia

ISBN 978-80-968868-6-9

conditions of thermal energy storage by collecting and interpreting experimental data and by simulating thermal processes using finite element analysis software COMSOL Multiphysics. After validating the numerical model, it could be possible to estimate and optimize parameters of seasonal thermal energy storage system for a wood frame residential home.

Thermal energy storage systems

Several researches have done in the last few decades about TES systems. A number of books and hundreds of articles have been released on the topic with some very good review between them (e.g., DINCER & ROSEN 2002, PINEL *et al.* 2011, AGYENIM *et al.* 2010). In this section we give a brief overview of classifying and characterizing these systems.

By storage concept there are active and passive TES systems (PINEL *et al.* 2011). While in active thermal storage systems the storage material circulates itself by forced convection, in passive thermal storage systems there is a heat transport medium (liquid or gas) which transfer energy from and to the storage system, flowing through the storage material (solid or liquid). Active TES systems can be subdivided into two categories: direct (or closed loop) systems, and indirect (or open loop) systems. In the former case heat storage material flow through the heating system (e.g., solar collector), while in the latter case there are two mediums: one for collecting heat from solar system and one for storing thermal energy.

Classifying TES systems by storage mechanism, there are (thermo-)chemical, latent and sensible heat storage systems (DINCER 2002). In (thermo-)chemical TES systems heat storage medium participates in a reversible endothermic chemical reaction, and the energy needed for this reaction comes from solar applications. Reversing the reaction (often with an appropriate catalyst), heat stored as chemical energy can be recovered and used for residential applications. This type of TES systems has some advantages e.g., very high storage density, good control of chemical reactions (with catalysts), low storage temperature, but it has disadvantages too, such as expensive materials which do not have the right properties and the lack of adequate numerical models for simulation and optimization. Researches done about (thermo-)chemical TES systems focused mainly on diurnal heat storage possibilities, for seasonal heat storage further investigations are needed (PINEL *et al.* 2011).

Latent heat storage systems operate using Phase Change Materials (PCMs) as heat storage medium. Heat fed into the TES system is stored mainly as latent heat of phase change of the PCM material. Storage medium can be classified as organic (e.g., paraffin, fatty acids, alkanes) and inorganic (e.g.,

melting ice, salts). This type of TES systems has the advantages such as relatively small size and weight because of its high storage density and relatively narrow operating and storage temperature range. However, storage materials are usually expensive, and both organic and inorganic ones have some disadvantageous properties (ZALBA *et al.* 2003). Organic PCMs are inflammable and they have rather low thermal conductivity so extraction of heat from the container at high rate can be difficult. Encapsulating storage material increases its total surface area thus we can speed up heat transfer process. Disadvantages of inorganic PCMs are phase separation, phase segregation, undercooling, thermal instability and corrosiveness. Some of them has considerably high operating temperature e.g., NaCl: $T_{\text{fusion}} = 800 \text{ }^{\circ}\text{C}$ (PINEL *et al.* 2011), LiF-CaF₂ 80.5:19.5 mixture: $T_{\text{fusion}} = 767 \text{ }^{\circ}\text{C}$ (GONG & MUJUMDAR 1997), KNO₃: $T_{\text{fusion}} = 330 \text{ }^{\circ}\text{C}$, KOH: $T_{\text{fusion}} = 380 \text{ }^{\circ}\text{C}$ (ZALBA *et al.* 2003). This can be lead to a notable heat leakage if insulation system of heat storage is not sufficient. Besides of these disadvantages latent TES systems seem to be promising solutions and with better PCMs and operating technologies (like subcooling) they could reach the market.

Sensible TES systems operate in a wider temperature range as (thermo-)chemical and latent ones, because they store energy in a sensible form of heat. The storage medium can be liquid (e.g., water, salt solutions, oil) or solid (e.g., rock, soil, concrete, graphite, pellets or balls of iron and iron oxide), and in the latter case there is a heat transport medium, which is liquid (usually water) or gas (mostly air). In practice, the most widely used materials are water and rock, so in general it could be say that sensible heat storage systems are cheaper than the others. However, heat storage density of the storage medium is considerably lower, and for this reason sensible TES systems are larger and heavier than chemical and latent ones. To reduce the significant heat loss appearing at high storage temperature, there must be achieved very well insulation system and low surface over volume ratio. In water based systems, system efficiency can be improved by achieving and increasing thermal stratification. This type of heat storage system operates on scale of district heating and single detached house, either. In practice, there is a variety of solutions for seasonal sensible TES systems, e.g., water tanks, aquifers, solar ponds, rock beds, soil or rock ground, etc. (PINEL *et al.* 2011).

MATERIALS AND METHODS

For experimental studies, in the last year a sample wood frame residential home was built in Sopron (West-Hungary) (Fig. 1). To fill the requirement of high energy efficiency, it was vital to use the best

insulation system available and yet affordable. For this reason, a special advanced insulation wall system was applied and a three-layered window system was used with a U-value of $0.8 \text{ W/m}^2\text{K}$. The calculated overall coefficient of heat transmission for the building wall is under $0.1 \text{ W/m}^2\text{K}$. To collect solar energy, 16 solar panels have been mounted onto the southern side of the roof.



Fig. 1 Sample wood frame house in Sopron (West-Hungary)

To effectively utilize solar thermal energy for space heating in the sample building, it was inevitable to design and assemble a heat container system which was then placed inside a separated room of the house. During planning, one of the primary aspects was to hold down initial costs of the system, thus sensible heat storage mechanism has been selected due to the relatively inexpensive available storage materials. The chosen medium was a silicate based solid material, with a density of approximately 2200 kg/m^3 . Because of the relatively large height of the box-shaped heat container and high density of the storage medium, it was necessary to reinforce the floor under the heat storage unit to distribute the load. Volumetric heat capacity of the chosen material is nearly half of the water's. While operating temperature range of water is about 70 K in liquid state on normal pressure, the one of the heat storage medium used in the project is 200 K. Accordingly, the amount of heat stored in a cubic meter water is less than that of the chosen material.

Considering the high operating temperature (30–230 °C) especially at full charge, it was vital to apply the best available and at the same time yet affordable insulation around the heat storage medium in order to minimize heat losses. For this reason, a three-layered system has been developed. Feeding energy in the heat container is utilized by eight U-shaped resistance heating filament connected to the solar photovoltaic system, and which are placed nearly in the center horizontal plane of the storage unit. Recuperating heat for

space heating can be obtained by an air ventilation system mounted on the top of the storage medium, under the insulation layers of the upper side of heat container.

During the assembling of heat storage, a number of thermocouples and several heat flux sensors were placed in the system. Thus it is possible to monitor temperature distribution in the heat container, and heat transfer rate on its surfaces. Collecting data is an automatized process, and recorded information can be saved from the data acquisition system to an appropriate device using a USB port. Before further application, experimental data must be investigated and erroneous ones must be excluded.

Besides acquisition experimental data, authors planned to build up a computer model of the seasonal heat storage system. With modeling thermal processes in the storage unit (e.g., heat propagation, temperature distribution), main factors of heat storing and heat transfer could be determined and moreover, planning and optimizing such a system could be achieved. In the model the following parameters must be given:

- size, shape, structure and material properties of heat container;
- size, structure and material properties of insulation layers;
- placement, number, shape and material properties of heat input / extraction elements.

Since the numerical model can take into consideration just a finite number of factors affecting the heat process, it must be refined by an iterative way, using experimental filtered data for validation. This can be a long process, and for this reason it seems to be logical to start with a simplified model and develop it into a more advanced one.

Up to now a simplified seasonal heat container has been modeled using finite element method software. Its significant advantage is that it has a Heat Transfer module which utilizes the appropriate underlying differential equation system for heat propagation. A dynamic (transient) model with 3D geometry was built up and material properties as well as initial and boundary conditions were determined. Heating of the system was modeled using an experimental function which was derived from the output power data of heat feeding system, collected during a given period. First the computer simulation model was preheated to a determined temperature condition in accordance with the real thermal energy storage system, and then its thermal behavior was compared with the experimental one. Comparison was done by a heating/cooling cyclic process in which both systems were heated intermittently for 160 hours according to a schedule plan (Table 1).

Table 1 Schedule plan for intermittent heating of models.

Time interval (hours)	Power (W)
16	1500
16	0
16	1500
16	0
8	1500
8	1500
16	0
16	1500
32	0

Under computer simulation process, at each time step temperature values were calculated at given points of the geometry according to the thermocouple (e.g., T18, T19) placement in real thermal storage system. Experimental (Fig. 2) and numerical temperature data (Fig. 3) were then plotted and compared.

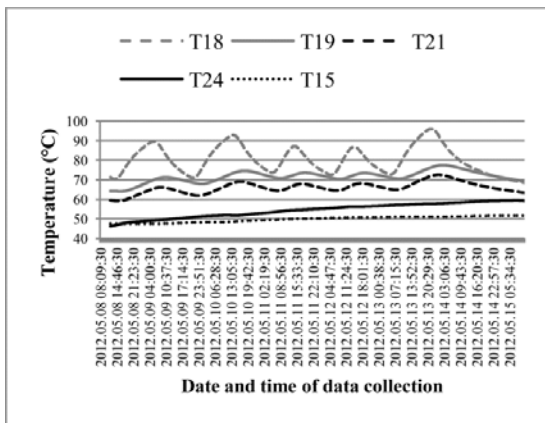


Fig. 2 Temperature change of selected thermocouples in the experimental TES system during a 160 hours long intermittent heating process.

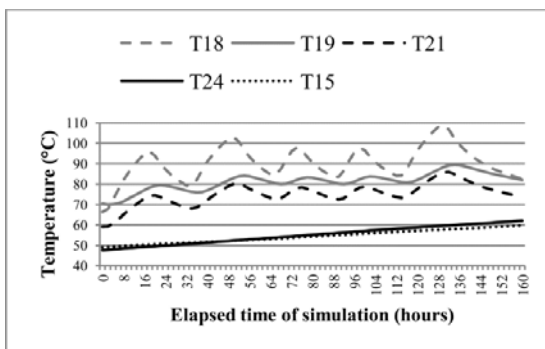


Fig. 3 Temperature change at given points (notation according to the corresponding thermocouples) of the numerical model during a 160 hours long intermittent heating simulation.

DISCUSSION

After comparing temperature data of the numerical and experimental model, it can be seen that tendency in thermal changes are very similar but not the same. Computer model must be improved by correcting initial and boundary conditions as well as adjusting some parameters. Taking into account the temperature and moisture dependency of (thermo)physical properties of materials involved in the thermal storage system will certainly give more accurate solution. The speed of the convergence process could be improved significantly by determining which factors have the largest impact of deviation from experimental data. COMSOL Multiphysics gives proper tools for this type of examination (e.g., in the form of parametric studies).

REFERENCES

- AGYENIM F., HEWITT N., EAMES P. & SMYTH M. 2010: A review of materials, heat transfer and phase change problem formulation for latent heat thermal energy storage systems (LHTESS). *Renewable and Sustainable Energy Reviews*, 14: 615–628.
- DINCER I. 2002: On thermal energy storage systems and applications in buildings. *Energy and Buildings*, 34(4): 377–388.
- DINCER I. & ROSEN M. A. 2002: *Thermal Energy Storage: Systems and Applications*. London: John Wiley & Sons, 580 pp.
- GONG Z. & MUJUMDAR AS. 1997: Finite-element analysis of cyclic heat transfer in a shell and tube latent heat energy storage exchanger. *Applied Thermal Engineering*, 17(4): 583–591.
- LINDER S. & BHAR R. 2007: Space conditioning in the residential sector in Europe. Deliverable 1. Ground Reach EU project. Ecofys.
- PINCEMIN S., OLIVES R., PY X. & CHRIST M. 2008: Highly conductive composites made of phase change materials and graphite for thermal storage. *Solar Energy Materials & Solar Cells*, 92(6): 603–613.
- PINEL P., CRUICKSHANK C. A., BEAUSOLEIL-MORRISON I. & WILLS A. 2011: A review of available methods for seasonal storage of solar thermal energy in residential applications. *Renewable and Sustainable Energy Reviews*, 15: 3341–3359.
- ZALBA B., MARÍN J. M., CABEZA L. F. & MEHLING H. 2003: Review on thermal energy storage with phase change: materials, heat transfer analysis and applications. *Applied Thermal Engineering*, 23(3): 251–283.

MECHANICAL CHARACTERISATION OF SYCAMORE MAPLE (*ACER PSEUDOPLATANUS L.*)

PETER NIEMZ, WALTER SONDEREGGER, TOMASZ OZYHAR & ANNE MARTIENSSEN

Swiss Federal Institute of Technology, Wood Physics Group

Abstract

Selected mechanical properties of sycamore maple (*Acer pseudoplatanus L.*) were investigated as a basis for three-dimensional material modelling for structural simulations (e.g. with the finite element method). Young's moduli, Poisson's ratios and strength parameters, determined in tension, compression and bending tests, as well as the fracture toughness are presented. Mechanical tests were carried out at different moisture conditions with respect to the three main anatomical directions.

Key words: bending, compression, fracture toughness, mechanical properties, Poisson's ratios, sycamore maple, tension, Young's moduli, strength.

INTRODUCTION

Sycamore (*Acer pseudoplatanus L.*) is one of the most common hardwoods in Central Europe. Currently, the population in Switzerland totals 11.8 Mio m³ according to the Swiss National Forest Inventory (BRÄNDLI 2010) and is the third most common species after beech (73.3 Mio m³) and ash (14.8 Mio m³).

Therefore, hardwood is used among conventional applications like parquetry, interior joinery, furniture and musical instruments and also more and more for wood constructions (glue lam). Well-founded knowledge of the material properties of these species is becoming necessary since calculation and simulation of material behaviour are being increasingly carried out with the finite element method (for example for calculation of boards). Among the strength properties, the complete elastic parameter-set (3 moduli of elasticity (MOE), 3 shear moduli (G) and 6 Poisson's ratios) within the three main directions (longitudinal (L), radial (R) and tangential (T)) is required. Analogously, the influences of grain angle (LR, LT) and ring angle (RT) on the parameters mentioned above have to be known. Ideally, the parameters of the plastic deformation should also be known since this topic is increasingly studied (e.g. SCHMIDT 2008, HERING 2011).

Altogether, very complex measurements are required to allocate all essential data in a numerical simulation. The following parameters are necessary for a comprehensive material characterization:

- Elastic parameters (including properties on cyclic load and on hysteresis effects)
- Strength
- Viscoelastic and plastic parameters
- Mechano-sorptive parameters
- Creep and relaxation
- Thermal and moisture dependent behaviour

The total stress under real conditions (external load and cycling climatic conditions), according to equation (1), consists of:

- Mechanical stresses
- Climatically induced stresses like shrinkage and swelling

The total strain is composed accumulatively as

$$\varepsilon_{\text{tot}} = \varepsilon_{\text{el}} + \varepsilon_{\text{m}} + \varepsilon_{\text{ms}} + \varepsilon_{\text{ve}} + \varepsilon_{\text{pl}} \quad (1)$$

where ε_{tot} is the total strain constituted of ε_{el} the elastic strain, ε_{m} the moisture induced strain, ε_{ms} the mechano-sorptive strain, ε_{ve} the viscoelastic strain and ε_{pl} the plastic strain.

The three-dimensional elastic behaviour of an orthotropic material can be described with the generalised Hooke's law. Equation (2) shows the compliance matrix using the engineering elastic parameters.

$$\begin{bmatrix} \varepsilon_{11} \\ \varepsilon_{22} \\ \varepsilon_{33} \\ \gamma_{23} \\ \gamma_{13} \\ \gamma_{12} \end{bmatrix} = \begin{bmatrix} \frac{1}{E_{11}} & -\frac{\mu_{21}}{E_{22}} & -\frac{\mu_{31}}{E_{33}} & 0 & 0 & 0 \\ -\frac{\mu_{12}}{E_{11}} & \frac{1}{E_{22}} & -\frac{\mu_{32}}{E_{33}} & 0 & 0 & 0 \\ -\frac{\mu_{13}}{E_{11}} & -\frac{\mu_{23}}{E_{22}} & \frac{1}{E_{33}} & 0 & 0 & 0 \\ \hline 0 & 0 & 0 & \frac{1}{G_{23}} & 0 & 0 \\ 0 & 0 & 0 & 0 & \frac{1}{G_{13}} & 0 \\ 0 & 0 & 0 & 0 & 0 & \frac{1}{G_{12}} \end{bmatrix} \begin{bmatrix} \sigma_{11} \\ \sigma_{22} \\ \sigma_{33} \\ \tau_{23} \\ \tau_{13} \\ \tau_{12} \end{bmatrix} \quad (2)$$

where ε_{ii} are the normal strains, γ_{ij} the shear strains, σ_{ii} the normal stresses and τ_{ij} the shear stresses, E_{ii} the moduli of elasticity, G_{ij} the shear moduli and μ_{ij} the Poisson's ratios. Thereby, the first index signifies the

strain direction and the second index the stress direction.

Selected property parameters of hardwood have been published by KOLLMANN (1951), BODIG and JAYNE (1993), SZALAI (1994), POZGAJ *et al.* (1997), SELL (1997), WAGENFÜHR (2007), KURJATKO *et al.* (2010) and ROSS (2011), amongst others. However complete data sets for the three main wood directions that are sufficient for static calculations and modulations in wood construction and also for calculations on multi-layered boards, parquet or musical instruments with the finite element method rarely exist. Mostly, investigations on tension, compression and bending are carried out only parallel to the grain and the parameters for the other main directions (R, T), which are required for finite element calculations, as well as the influences of grain and ring angle are lacking. Equally, the influence of the load type (tension, compression, bending) and of MC on the elastic constants and the Poisson's ratio are scarcely investigated. Also for the rheological characteristics (creep, relaxation, mechano-sorptive effects), the parameters are lacking for the most part. For hardwoods, the most comprehensive dataset of moisture-dependent elastic and strength parameters so far was recently presented for beech wood in compression by HERING (2011) and in tension by OZYHAR *et al.* (2012). For softwood, most investigations were carried out on Norway spruce since it is the most commonly used wood for construction (e.g. NEUHAUS 1981). For sycamore maple, WEDEL (1964) determined in detail the swelling, tension, compression, bending, impact bending and shear properties in the fibre direction.

Sycamore maple wood is particularly applied in furniture-making, parquetry and interior joinery, but also in musical instruments and pattern making as well as turnery (WEDEL 1964, SONNABEND 1989 and 1990). Thereby, calculations and optimizations are helpful to simulate, for example, stresses in multi-layered parquet or musical instruments and furniture.

The aim of this work is to generate a preferable complete dataset of the mechanical properties of sycamore maple.

MATERIAL AND METHODS

Material

All test specimens for the determination of the physical and mechanical properties were cut from logs of a sycamore tree (*Acer pseudoplatanus* L.) from Eastern Switzerland with a mean normal density of 626 kg/m³ (at a MC of about 12%) and oven-dry density of 563 kg/m³.

The following mechanical properties were tested at climates 20/35 (20°C and 35% relative humidity (RH)), 20/65, 20/85 and 20/95:

- Bending strength with static MOE
- Tensile strength

- Compression strength
- MOE and Poisson's ratio from tensile and compression tests
- Fracture toughness K_{IC}

Methods

Determination of the mechanical properties

Bending strength and static MOE

Bending strength and static MOE were determined according to DIN 52186:1978-06 on 18-26 specimens sized 20 mm (R) × 20 mm (T) × 400 mm (L).

Tensile strength

Tensile strength was determined parallel to the grain according to DIN 52187:1979-05. Perpendicular to the grain tensile strength determinations were made using 95 mm long dog-bone-shaped specimens (cross-sectional area: max. 28 mm × 28 mm, min. 14 mm × 14 mm) according to HERING *et al.* (2012). 13–16 specimens were tested per direction and climate.

Compression strength

Compression strength parallel to the grain was determined according to DIN 52185:1976-09 and perpendicular to the grain according to DIN 52192:1979-05. Deviating from the norm, a reduced specimen size (15 mm × 15 mm × 45 mm) was employed. 16–21 specimens were tested per direction and climate.

MOE and Poisson's ratio from tensile and compression tests

MOE and Poisson's ratio were determined on the tensile and compression test specimens by means of a video image correlation system (Vic 2D, LIMESS Messtechnik & Software GmbH, Krefeld) for the determination of the longitudinal and transverse elongation. The method is described in detail by KEUNECKE *et al.* (2008) and HERING *et al.* (2012). The Poisson's ratio was determined according to

$$\mu_{ij} = -\frac{\varepsilon_i}{\varepsilon_j} \quad (3)$$

where μ_{ij} is Poisson's ratio, ε_i the transverse elongation and ε_j the longitudinal elongation.

Fracture toughness K_{IC}

Fracture toughness K_{IC} was determined according to DIN EN ISO 12737:2011-04 on compact specimens in the RL, TL, RT and TR directions (first index = direction normal to the crack plane, second index = direction of crack propagation). 5-14 specimens were tested per direction and climate.

The static tests were carried out with a Zwick Z010 universal testing machine for tension and compression perpendicular to the grain as well as fracture toughness, and a Zwick Z100 machine for tension, bending and compression parallel to the grain as well as shearing.

RESULTS AND DISCUSSION

Tensile, bending and compression tests

The results are summarized in Table 1 and visualised in Figures 1 and 2. The strength is highly influenced both by the test mode and the wood direction. Parallel to the fibre, the ratio of tensile strength to bending and compression strength is, at normal climate, about 1.8 : 1.7 : 1 and corresponds well with the literature data of Table 1. The influence of MC within the tested RH range is least for tensile strength (with a reduction of about 10 %), whereas bending strength is reduced by about 33 % and compression strength by about 40 % (Fig. 1a). However, in contrast, results perpendicular to the grain show only small differences between tensile and compression strength. All values are reduced with increasing MC by about 33 % (Fig. 1b). For the wood directions at normal climate, the strength ratio of L, R, T is for tension 13 : 1.8 : 1 and for compression 6 : 1.5 : 1.

In contrast to strength, the MOEs (Fig. 2) parallel to the fibre show rather different ratios with regard to the test mode. The highest MOE was determined at compression whereas bending MOEs were similar to tensile MOEs except at climate 20/35. An explanation of the high compression MOE may be the influence of the bimodularity of the material, which differs according to the wood species. CONNERS and MEDVECZ (1992), for example, show similar behaviour for yellow poplar. The influence of MC on MOE is, with the exception of tension, lower compared to strength. Perpendicular to the grain, there

are only small differences between tensile and compression MOE. The reduction of MOE with increasing MC is similar to the reduction in strength.

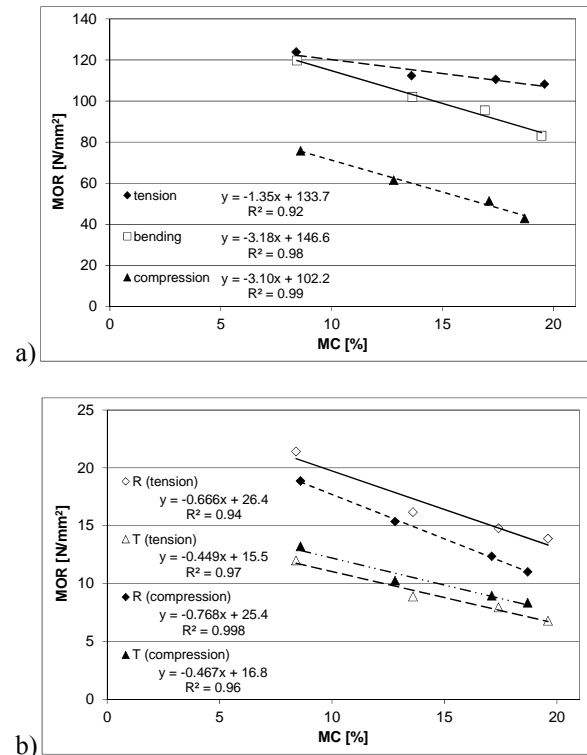


Fig. 1 MOR (= Module of Rupture) in L-direction (a) and in R- and T-direction (b) dependent on moisture content (MC).

Table 1 Mechanical properties of sycamore maple at climate 20/65; σ = strength in tension (t), bending (b) and compression (c), MOE = modulus of elasticity, τ = shear strength, w = impact bending strength, K_{IC} = critical stress intensity factor, L = longitudinal, R = radial, T = tangential, ρ = density, V = coefficient of variation.

Property	Direction	No.	ρ [kg/m ³]	Mean value	V [%]
σ_t [N/mm ²]	L	15	633	112.4	20.1
	R	14	630	16.2	8.8
	T	15	630	8.9	7.2
σ_b [N/mm ²]	L	18	634	102.1	7.8
	R	16	657	15.4	4.7
		21	657	10.3	5.4
σ_c [N/mm ²]	L	19	657	61.5	6.1
	R	16	657	15.4	4.7
	T	21	657	10.3	5.4
MOE _t [N/mm ²]	L	15	633	11450	23.5
	R	15	630	1205	10.0
	T	15	630	688	3.8
MOE _b [N/mm ²]	L	18	634	10920	15.9
MOE _c [N/mm ²]	L	15	657	14480	21.7
	R	19	657	1140	14.9
	T	16	657	789	3.9
K_{IC} [MPa·m ^{0.5}]	RL	6	670	1.08	18.3
	TL	9	620	0.70	11.4
	RT	6	690	0.91	10.7
	TR	7	589	0.54	17.0

Table 2 Poisson's ratio (μ) at normal climate (20/65) for tension and compression. V = coefficient of variation, R^2 = coefficient of determination.

Direction	Tension		Compression		Mean μ	Literature data	
	μ	V	μ	V		$\mu^{(1)}$	$\mu^{(2)}$
	[–]	[%]	[–]	[%]	[–]	[–]	[–]
RL	0.489	15.3	0.340	44.3	0.420	0.490	0.370
TL	–	–	0.421	30.6	0.440	0.470	0.500
TR	0.646	4.3	0.680	11.1	0.690	0.760	0.670
LR	0.059	36.1	0.161	32.2	0.091	0.074	0.044
RT	0.378	9.7	0.403	6.9	0.390	0.440	0.330
LT	0.043	29.8	0.049	53.1	0.061	0.041	0.027

1) Sycamore maple (MC = 9.6): STAMER and SIEGLERSCHMIDT in KOLLMANN (1951)

2) Hardwood: BODIG and JAYNE (1993)

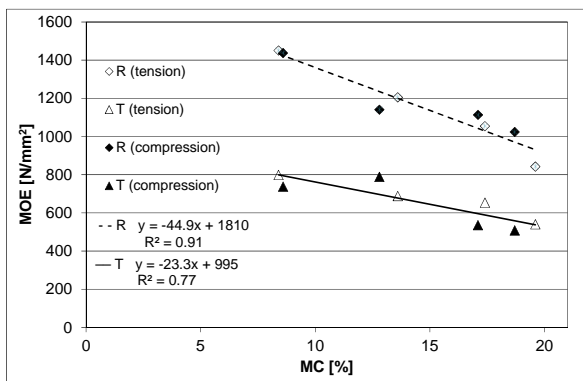


Fig. 2 Modulus of elasticity (MOE) in the L-direction dependent on moisture content (MC).

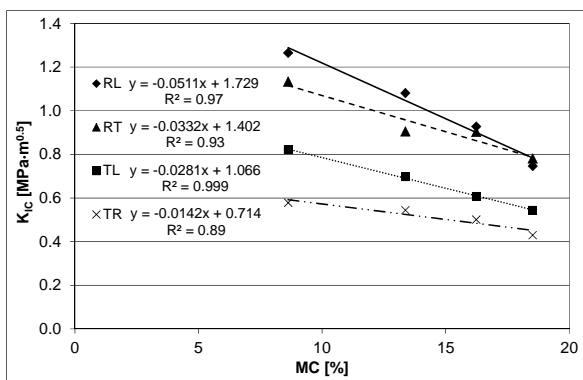


Fig. 3 Fracture toughness (K_{IC}) dependent on moisture content (MC).

Poisson's ratio

Table 2 shows the Poisson's ratio (μ) at normal climate (20/65) determined from the tension and compression tests. At normal climate, the values from the tension and compression tests differ only marginally except for the RL and LR directions. The mean Poisson's ratios from tension and compression over all climates coincide quite well with values determined by STAMER and SIEGLERSCHMIDT in KOLLMANN (1951) for sycamore maple and with values of BODIG and JAYNE (1993) for hardwood. The influence of MC on Poisson's ratio is not uniform so that the values increase or decrease depending on the

direction. In contrast, HERING *et al.* (2012) observed a decrease of Poisson's ratio for beech with increasing MC in all directions.

Fracture toughness

Table 1 shows the fracture toughness K_{IC} of the different loads at climate 20/65. The values are very high compared with other wood species, like oak and beech, and also higher compared to sugar maple (STANZL-TSCHEGG *et al.* 2011) and are similar to ash in the RL and TL directions (REITERER *et al.* 2002). Tests in the RL and RT directions result in clearly higher values compared to the TL and TR directions, which can be attributed to the influence of the rays. The fracture toughness within a crack plane was higher for crack propagation in the fibre direction than perpendicular to the grain, which is in contrast to the behaviour of different soft woods (STANZL-TSCHEGG *et al.* 2011). All K_{IC} values are highly influenced by MC, with the greatest percentage decrease in the RL and TL directions (Fig. 3). In contrast, LOGEMANN and SCHELLING (1992) found only a low MC influence for spruce in the TL direction.

CONCLUSIONS

A dataset of mechanical properties in the three main directions was established for sycamore maple wood. Until now, such complex data sets for hardwoods (ash, oak, beech) are rare, despite becoming more and more important in parallel with the increasing silvicultural availability of these species. The dataset allows, within the elastic range, the calculation and simulation of multi-layered and three-dimensional wood structures with finite element methods. Still, investigations have to be carried out to determine the physical (sorption, swelling, diffusion, thermal conductivity) and rheological properties and the mechano-sorptive behaviour. Equally, further research is needed to analyse the plastic behaviour, which is particularly important in regard to compression perpendicular to the fibre. Investigations from HERING (2011) and SCHMIDT (2009) could provide a basis for this.

LITERATURE

- BODIG, J. & JAYNE, B. 1993: Mechanics of Wood and wood composites. 2nd edition, Malabar: Krieger Publishing, 712 pp.
- BRÄNDLI, U. B. (ed.) 2010: Schweizerisches Landesforstinventar. Ergebnisse der dritten Erhebung 2004–2006. Birmensdorf, Eidgenössische Forschungsanstalt für Wald, Schnee und Landschaft WSL. Bern, Bundesamt für Umwelt, BAFU. 312 pp.
- CONNERS, T. E. & MEDVEZ, P. J. 1992: Wood as a bimodular material. *Wood Fiber Sci.*, 24(4): 413–423.
- HERING, S. 2011: Charakterisierung und Modellierung der Materialeigenschaften von Rotbuchenholz zur Simulation von Holzverklebungen. Dissertation, ETH Zürich.
- HERING, S., KEUNECKE, D. & NIEMZ, P. 2012: Moisture-dependent orthotropic elasticity of beech wood. *Wood Sci Technol.*, (first online), DOI 10.1007/s00226-011-0449-4.
- KEUNECKE, D., SONDEREGGER, W., PERETEANU, K., LÜTHI, T. & NIEMZ, P. 2007: Determination of Young's and shear moduli of common yew and Norway spruce by means of ultrasonic waves. *Wood Sci Technol.*, 41(4): 309–327.
- KEUNECKE, D., HERING, S. & NIEMZ, P. 2008: Three-dimensional elastic behaviour of common yew and Norway spruce. *Wood Sci Technol.*, 42(8): 633–647.
- KOLLMANN, F. 1951: Technologie des Holzes und der Holzwerkstoffe. 2nd edn., vol 1. Springer, Berlin.
- KRACKLER, V., KEUNECKE, D. & NIEMZ, P. 2010: Verarbeitung und Verwendungsmöglichkeiten von Laubholz und Laubholzresten. ETH Zürich, Eigenverlag, 151 pp.
- KURJATKO, S. *et al.* 2010: Parametre kvality dreva určujúce jeho finálne použitie. Zvolen: TU vo Zvolene, 351 s.
- LOGEMANN, M. & SCHELLING, W. 1992: Die Bruchzähigkeit der Fichte und ihre wesentlichen Einflussparameter. *Untersuchungen in Mode-I. Holz Roh- Werkst.*, 50(2): 47–52.
- NEUHAUS, F.H. (1981) Elastizitätszahlen von Fichtenholz in Abhängigkeit von der Holzfeuchtigkeit. Dissertation, Ruhr-Universität Bochum, 162 pp.
- OZYHAR, T., HERING S. & NIEMZ P. 2012: Moisture-dependent elastic and strength anisotropy of European beech wood in tension. *Journal of Material Science* (first online), DOI: 10.1007/s10853-012-6534-8.
- POZGAJ, A., CHONAVEC, D., KURJATKO, S., BABIAK, M. 1997: Štruktúra a vlastnosti dreva. 2nd ed. Bratislava: Príroda, 485 pp.
- REITERER, A., SINN, G. & STANZL-TSCHEGG, S. E. 2002: Fracture characteristics of different wood species under mode I loading perpendicular to the grain. *Mater Sci Eng A* 332: 29–36.
- ROSS, R.J. (ed.) 2011: Wood Handbook. 2010 edition. Forest Products Society, Madison WI.
- SCHMIDT, J. 2008: Modellierung und numerische Analyse von Strukturen aus Holz. Habilitation, TU Dresden.
- SELL, J. 1997: Eigenschaften und Kenngrößen von Holzarten. 4th edn. Baufachverlag, Dietikon, 87 pp.
- SONNABEND, J. 1989: Das Holz des Ahorns und seine heutige Verwendung. Parts 1-2. *Holz-Zentralblatt* 115:1680, 1683, 2020, 2024.
- SONNABEND, J. 1990: Das Holz des Ahorns und seine heutige Verwendung. Part 3. *Holz-Zentralblatt*, 116: 26–27.
- STANZL-TSCHEGG, S.E., KEUNECKE, D. & TSCHEGG, E.K. 2011: Fracture tolerance of reaction wood (yew and spruce wood in the TR crack propagation system). *Journal of the Mechanical Behavior of Biomedical Materials*, 4: 688–698.
- SZALAI, J. 1994: A faanyag és faalapú anyagok anizotrop rugalmasság- és szilárdságtana (Book title in English: Anisotropic strength and elasticity of wood and wood based composites), University of West Hungary, Sopron [in Hungarian].
- WAGENFÜHR, R. 2007: Holzatlas. 6th edn. Fachbuchverlag, Leipzig.
- WEDEL, K. VON 1964: Untersuchungen über Eigenschaften, Verwertung und Verwendung des Ahornholzes. Dissertation, Georg-August-Universität Göttingen, Hann. Münden, 176 pp.

Acknowledgement

The authors thank the Händel- Haus foundation, Halle for the co-financing of this work.

QUANTIFICATION OF WOOD MEMORY EFFECT

BORIS UGOLEV, GALINA GORBACHEVA & SERAFIM BELKOVSKIY

Moscow State Forest University, 141005, Mytischki-5, Moscow Region, Russia
ugolev@mgul.ac.ru, gorbacheva-g@yandex.ru, belkovskiy@ro.ru

Abstract

Wood is a complex of polymers and is the natural smart material. The dominant feature of smart materials is «shape-memory effect». The last decade is characterized by intense researches in the field of forming of artificial smart materials as polymers with shape memory effect. Therefore it is expedient to use the accepted quantities of this effect of polymers, such as R_r (strain recovery rate), R_f (strain fixity rate) for memory effect of wood. Loading of wood induces reversible elastic-viscous and irreversible plastic strains. Based on the integral law of wood deforming under loading and moisture content and/or temperature changing (UGOLEV & LAPSHIN 1971) and the model of hygro-thermo-mechanical strains of wood as an elastic-viscous-plastic material, the frozen strains ε_f , set strains ε_s and residual, plastic strains $\varepsilon_c = \varepsilon_p$ have been determined. Results of experimental research of the parameters R_r and R_f of several wood species expressed through the components of the model of hygro-thermo-mechanical strains are presented. Besides results of experimental research multi-shape memory effect of wood are presented also.

Key words: memory effect of wood, frozen strain, set-strain, strain recovery rate, strain fixity rate.

INTRODUCTION

The memory effect of wood was experimentally discovered at the end of the 1970-x (UGOLEV 1980, 1986). Further researches of various aspects of this phenomenon were mostly qualitative character. Overview of the results was given in the IAWS Academy lecture (UGOLEV 2009) and subsequent researches of MSFU (UGOLEV *et al.* 2010, UGOLEV 2011). For a quantitative assessment of this dominant feature of wood as natural smart material the quantities used for shape memory polymers can be applied. For this purpose, a convenient method for visualization of wood memory effect and measuring procedure should be developed.

BACKGROUND

Wood deformative conversions at changing of loading, moisture content and/or temperature

As it is well known, loading of wood induces recoverable (elastic ε_e and viscous ε_v) strains and irreversible plastic strain ε_p .

$$\varepsilon = \varepsilon_e + \varepsilon_v + \varepsilon_p \quad (1)$$

At changing of moisture content and/or temperature of loaded wood the deformative conversions occur and frozen strains are formed. They were detected by us in wood fastened specimen at drying in the early 1960s (UGOLEV 1961). Later the integral law of wood deforming under loading and moisture content and/or temperature changing was formulated (UGOLEV & LAPSHIN 1971, UGOLEV 1976):

$$\varepsilon = H_1 \int_0^{\bar{t}} \frac{\dot{\sigma}}{E(\bar{w}, \bar{t})} d\tau + H_2 \frac{\sigma}{E(\bar{w}, \bar{t})} \quad (2)$$

where ε – strain, σ – stress, E – stiffness modulus, \bar{w} – moisture content decrease from limit saturation of cell walls (FSP), \bar{t} – temperature decrease from 100 °C, $\bar{w}(\tau)$, $\bar{t}(\tau)$ and $\dot{\sigma}(\tau)$ are functions of time τ . H_1 and H_2 are Havisade's functions accordingly for drying (cooling) and wetting (heating).

This law describes the formation of frozen strains of wood as an elastic-viscous body. The model of hygro(thermo)-mechanical strains of wood (Fig. 1) which takes into account formation as elastic-viscous (eq. 2) and plastic strains had been proposed (UGOLEV 1997).

This scheme shows wood behavior at transition from wet to dry states and vice versa. Here: σ – stress; ε – strain; $\Delta w = \bar{w}$ – drop of moisture content. Short-time loading of wet wood leads to the formation of elastic – viscous strain ε_{ev1} (0-1). Long-term loading adds creep ε_{c1} (1-2). Continuous, slow loading (0-2) and unloading (2-3) remain residual strain $\varepsilon_r = \varepsilon_c = \varepsilon_p$ (0-3).

It is possible to consider various histories of wood behavior. For example: wetting (4-0) and loading (0-2) leads to forming of total strain ε_{ev1} (0-2'). At drying under load (2-10) this strain is constant although wood stiffness increases. While unloading of dry wood elastic-viscous strain ε_{ev2} recovers (10'-11). Set ε_s (4-11) includes frozen strain ε_f (4-9) and residual strain ε_r (9-11) which is equal to creep of wet wood ε_{c1} i.e. plastic strain ε_{p1} .

Wood the Best Material for Mankind

J. Kúdela & M. Babiak (eds.), 2013, pp. 31–37

© Arbora Publishers, Zvolen, Slovakia

ISBN 978-80-968868-6-9

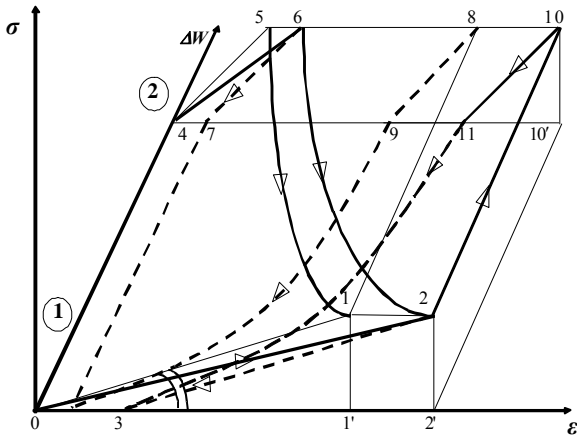


Fig. 1 Changes of wood elastic, viscous and plastic strains at drying and wetting.

Taking into account temperature – moisture analogy, the model can be used for the description of strains at heating and cooling of loaded wood. The important consequence following from the model – constancy of total strains at drying of bended spruce specimens and cooling of stretched ones was discovered by us at the beginning of the 70^{ies} (UGOLEV *et. al* 1980). This phenomenon has been revealed in other works - at cooling spruce, beech, hornbeam bended specimens (PASSARD & PERRE 2001), and at drying loaded wood (TORATTI & SVENSSON 2000, HANHIJARVI 1997, MIRIANON *et al.* 2008 and others). This is explained by the formation of frozen elastic-viscous strains. The model shows that plastic strains of wet wood $\varepsilon_{c1} = \varepsilon_{p1}$ remain constant at drying. Hence, the constancy of the total strains also remains.

The main statements of the model were confirmed experimentally.

Consequently, frozen strains are equal to:

$$\varepsilon_f = \varepsilon_{ev1} - \varepsilon_{ev2} = \frac{\sigma}{E_1} - \frac{\sigma}{E_2} = \sigma \left(\frac{E_2 - E_1}{E_2 \cdot E_1} \right) \quad (3)$$

Thus, quazi-residual frozen strains are the result of temporary reconstruction of wood nanostructure. It takes place under the controlling load influence while wood stiffness increases at drying or cooling.

Because frozen strains are reversible strains, they are a carrier of the memory effect of wood.

Since wood is a complex biological object, one should develop a fairly simple way to visualize the memory effect of wood. This method should allow to focus on the major factors while eliminating side factors (anisotropy, shrinkage, swelling and others).

The quantities of shape-memory effects of polymers

Recently the polymers with shape memory effect have become widespread among artificial smart materials (HILTZ 2002; KAUYMOV & STRAHOV 2011; LENDLEIN & KELCH 2002; SCHUH *et al.* 2010; XIE 2010).

Two important quantities are used to describe shape-memory effects of polymers (LENDLEIN & KELCH 2002):

- R_r is the strain recovery rate, it describes the ability of the material to memorize its permanent shape and is a measure of how far a strain that was applied in the course of the programming is recovered.
- R_f is strain fixity rate, it describes the ability to fix the mechanical deformation which has been applied during the programming process and so memorize its temporary shape.

The strain recovery rate R_r reflects the degree of recovery of the permanent shape of the sample:

$$R_r = \frac{\varepsilon_m - \varepsilon_p}{\varepsilon_m}, \quad (4)$$

where ε_m is the maximum strain imposed on the material; ε_p is irreversible plastic strain.

The strain fixity rate R_f is given by the ratio of the strain in the stress-free state after the retraction of the tensile stress in the maximum strain.

$$R_f = \frac{\varepsilon_u}{\varepsilon_m}, \quad (5)$$

where ε_u is strain in the stress-free state after the retraction of the stress.

Range of variation of parameters R_r and R_f is regulated depending on purpose of polymer (SCHUH *et al.* 2010).

Currently, several polymers which memorize three forms were proposed (LENDLEIN & KELCH 2002), and there were data on polymer, which can remember 4 forms (XIE 2010).

MATERIAL AND METHODS

Earlier researches of wood memory effect were carried out at change of temperature on the bent samples of birch wood as well as sliced veneer (UGOLEV 2005). This technique was used in subsequent studies of the memory effect on bent wood veneer samples at temperature and moisture content change. The samples of sliced, rotary-cut and fine-line veneer of birch, beech, pine and obeche were used. The temperature was varied in the range of 0–100 °C, moisture content of 0–150 %. In Table 1 the characteristic of test specimens is presented.

Table 1 The characteristic of test specimens.

Wood species	Type of veneer	The sample sizes, mm
Beech (<i>Fagus sylvatica</i> L.)	Sliced veneer	200 × 15 × 0.6
Pine (<i>Pinus sylvestris</i> L.)	Sliced veneer	200 × 15 × 0.6
Obeche (<i>Triplochiton scleroxylon</i> K. Schum.)	Fine-line veneer	200 × 15 × 0.6
Birch (<i>Betula</i> L.)	Rotary-cut veneer	250 × 15 × 1.5

RESULTS AND DISCUSSION

Using the model of hygro(thermo)-mechanical strains of wood, equations for the calculation of the shape memory effect quantities at a single change of temperature or moisture content of the loaded wood were obtained.

The strain recovery rate R_r is determined as follows:

$$R_r = \frac{\varepsilon_{evp} - \varepsilon_p}{\varepsilon_{evp}}, \quad (6)$$

Here ε_{evp} is the total hygro(thermo)-mechanical strain, ε_p is irreversible, plastic strain $\varepsilon_r = \varepsilon_c = \varepsilon_p$.

The strain fixity rate R_f is calculated by the formula:

$$R_f = \frac{\varepsilon_s}{\varepsilon_{evp}} = \frac{\varepsilon_f + \varepsilon_p}{\varepsilon_{evp}}. \quad (7)$$

The value of frozen strain is determined by the memory effect quantities as follows:

$$\varepsilon_f = \varepsilon_{evp}(R_r + R_f - 1). \quad (8)$$

The scheme of interrelation of shape memory effect quantities for polymers and for wood is shown on Fig. 2. Here: 0-1 – slow loading at θ_1 , all three types of strains are formed; 1-1 – cooling to θ_2 at $\sigma = \text{const}$; 1-2- unloading at θ_2 ; 2-3 – heating at $\sigma = 0$.

Results of experiments are presented in Table 2. The comparative assessment of quantities R_r and R_f at temperature and moisture content changing is shown on Fig. 3 and Fig. 4.

The obtained data shows that the quantities R_r^l , reflecting ability of wood to recover its permanent shape in the direction along the grain for samples of a pine and a beech sliced veneer have quite high values (0.9244–0.9729). For all types of veneer at change of moisture content the high value of R_r^w also are noted (0.789–0.948). In the direction across the grain the quantities R_r^t and R_r^w are lower due to the specifics of veneer manufacturing technology (availability of rotary peeling cracks, drying cracks, glue joints). In the fine-line veneer the ability to remember its permanent shape is revealed less. Low values of R_r^t for fine-line veneer are due to the complexity of technology, the presence of adhesive joints.

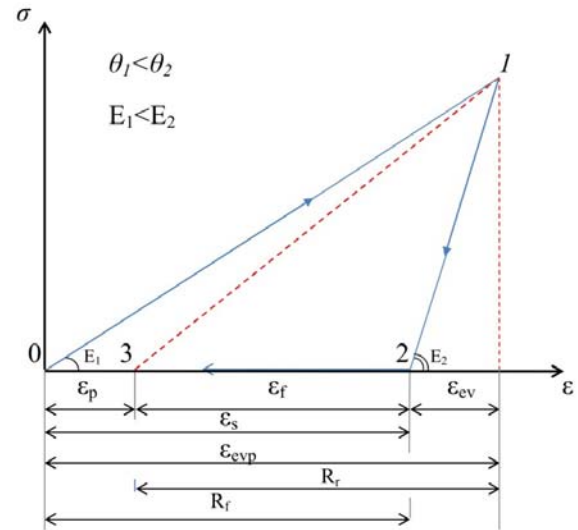


Fig. 2 Shape memory polymer quantities, characterizing deformative conversions of wood.

Table 2 Influence of wood species and veneer type on quantities of the wood memory effect at temperature changing

Quantities of the wood memory effect	Statistical characteristics	Wood species, type of veneer		
		Pine, Sliced veneer	Beech, Sliced veneer	Obeche, Fine-line veneer
R_r^l along the grain	x	0.9244	0.9729	0.5721
	±s	0.0844	0.0137	0.0509
	v; %	9.2	1.4	8.8
R_r^t across the grain	x	0.5438	0.7824	0.4331
	±s	0.1766	0.0170	0.1670
	v; %	32	2.1	38
R_r^f along the grain	x	0.5776	0.5044	0.8055
	±s	0.0624	0.0640	0.11
	v; %	10.8	12.6	13.5
R_r^f across the grain	x	0.7180	0.7793	0.7011
	±s	0.1720	0.1854	0.0374
	v; %	23.4	23.3	5.3

The quantities R_f^w characterizing ability to remember the temporary shape in the direction along and across the grain for all wood species and veneer types have also high values (0.923–0.943 and 0.833–0.8927, respectively). At temperature change the quantities R_f^t are slightly lower.

More visually the process of recovering of the permanent shape can be traced on the video made with the use of digital camera. On Fig. 5 the storyboard of the process and the timing of the wood sample restoring of its permanent shape at wetting are shown. Fig. 6 shows the recovery of the initial (permanent) shape of the beech sliced veneer sample in the direction along the grain at heating.

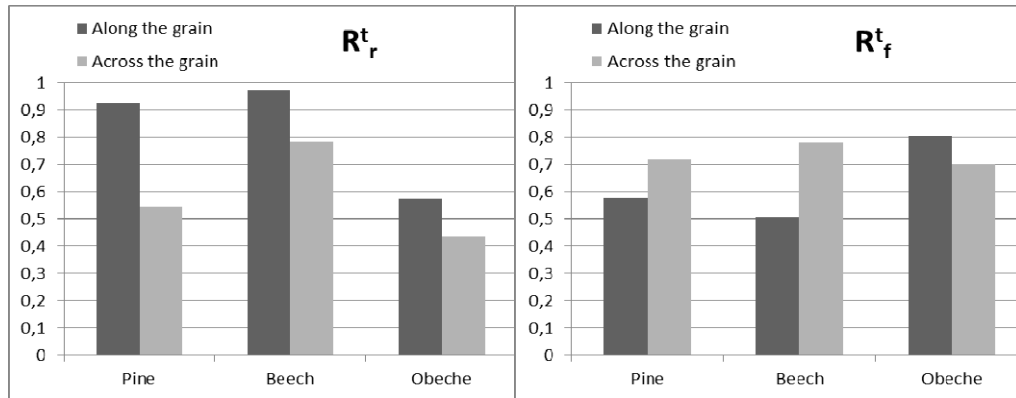


Fig. 3 The mean values of quantities R_r^t and R_f^t at temperature change.

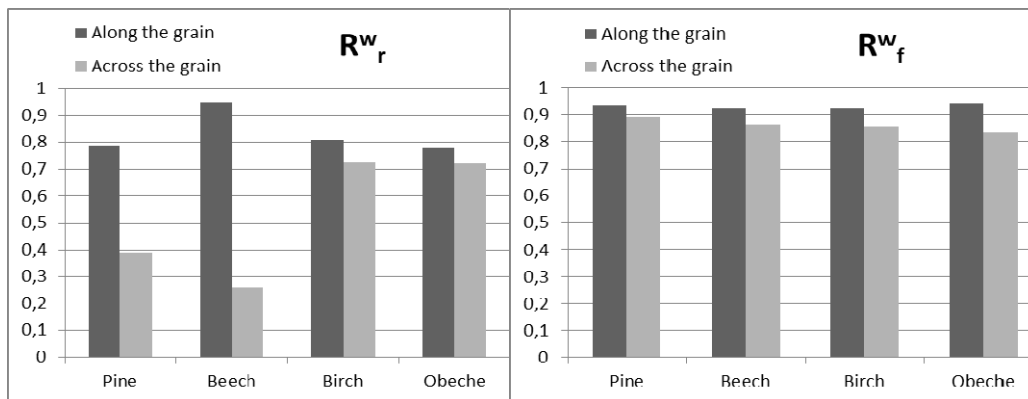


Fig. 4 The mean values of quantities R_r^w and R_f^w at moisture content change.

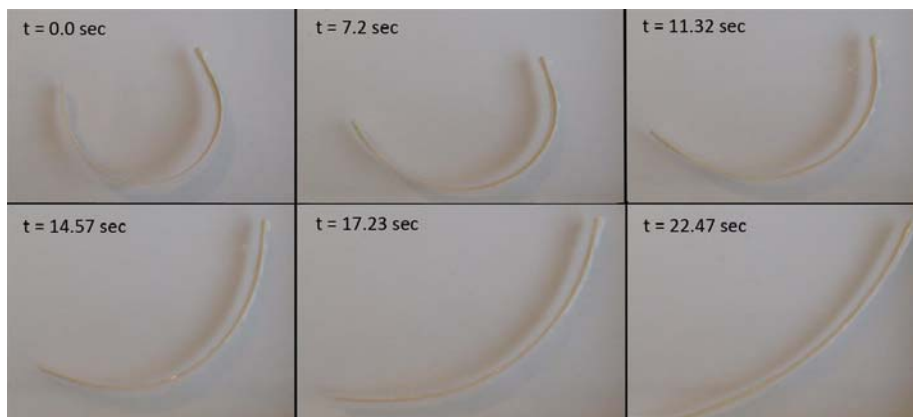


Fig. 5 Recovering of the initial (permanent) shape of the sample of pine sliced veneer in the direction along the grain at wetting.

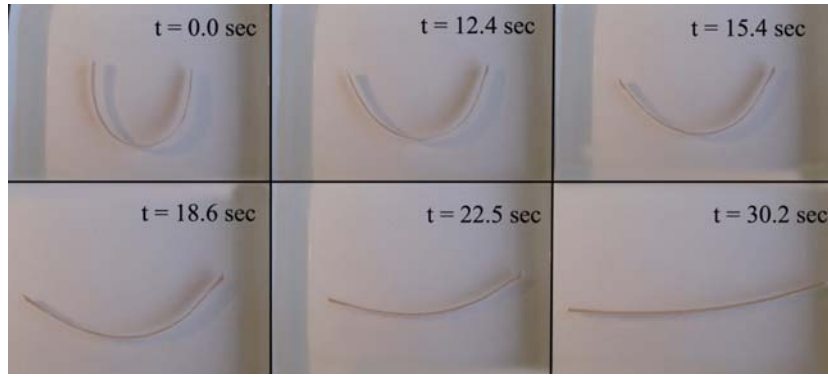


Fig. 6 Recovering of the initial (permanent) shape of the beech sliced veneer sample in the direction along the grain at heating.

The multi-shape memory effect of wood reveals that wood, as well as polymers can remember some forms. Let us consider wood deformative conversions at deformation history which allows to investigate multi-shape memory effect of wood. On Fig. 7 the scheme of deformative conversions in coordinates $\sigma - \varepsilon - \theta$ is presented. $\theta = \bar{t}$ is temperature decrease from 100 °C. As the carrier of the memory effect of wood are elastic-viscous strains, the scheme doesn't include the plastic strains. All stress-strain relationships are linearized.

On fig. 7 the following history of deforming is shown: heating up to 100 °C (0-1), loading of the right side of the sample (see also fig. 10) at 100 °C to $\varepsilon_0 = \varepsilon_{ev1}$ (1-2), cooling (2-3) to 60 °C at constant loading, $\varepsilon_0 = \text{const}$; unloading (3-4) the right side of the sample at 60 °C occurs after loading and cooling of the left side, frozen strain after cooling to 60°C ε_f the right side of the sample (4-5), loading the left side of the sample at 60 °C (5-6), cooling the left side of the sample from 60 °C to 0 °C (6-7), unloading (7-8) the left side of the sample at $t = 0$ °C, frozen deformation ε_f (60-0 °C) (0-8), disappearing of frozen strain ε_f of the left side at heating from 0 to 60 °C (8-5); disappearing of frozen strains ε_f of the right side at heating from 60 to 100 °C (4-1).

On Fig. 8 three forms memorized at multi-shape memory effect are considered on the combined scheme for a single sample.

Shape 1.

$\theta_1 = 0$, $\varepsilon_{f1} = 0$. 0-1 - loading, 1-2 – time exposure, 2-3 – unloading, section 0-3 is equal to ε_p .

$E = E_0(1 + \gamma\theta)$, where γ is coefficient.

$\sigma_1 = E_1\varepsilon_1$, $\varepsilon_{c1} = \varepsilon_p = \text{const}$, $\varepsilon_{evp} = \text{const}$

Section 3-2' $R_r = \frac{\varepsilon_{evp} - \varepsilon_p}{\varepsilon_{evp}}$ Section 0-4 $R_f = \frac{\varepsilon_s}{\varepsilon_{evp}} = \frac{\varepsilon_f + \varepsilon_p}{\varepsilon_{evp}}$

Shape 2

θ_2 , $\varepsilon_{f2} = \frac{\varepsilon_1\gamma(\theta_2 - \theta_1)}{1 + \gamma\theta_2}$, loading at the same σ_1 at θ_1 (0-1), time exposure 1-2, cooling to θ_2 , unloading 2-4, section 4-5 is equal to ε_p , section 5-0 is equal to ε_{f2}

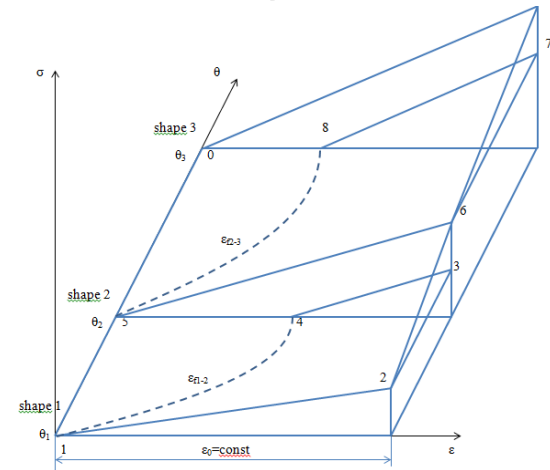


Fig. 7 The scheme of deformative conversions at multi-shape memory effect of wood.

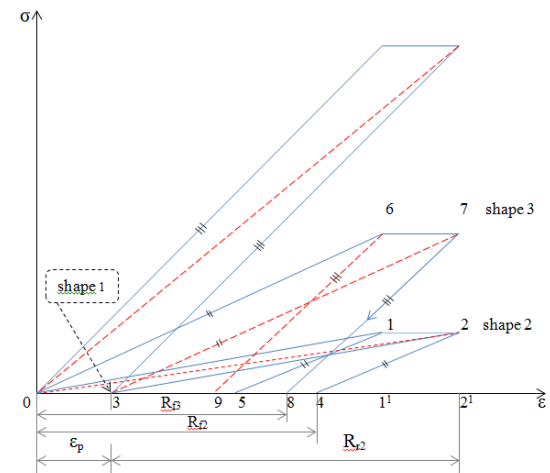


Fig. 8 Stress-strain state at multi-shape memory effect of wood.

$$\text{Section } 3-2' \quad R_{r2} = \frac{\varepsilon_{evp} - \varepsilon_p}{\varepsilon_{evp}} \quad \text{Section } 0-4 \quad R_{f2} = \frac{\varepsilon_1 \gamma (\theta_2 - \theta_1)}{1 + \gamma \theta_2} + \frac{\varepsilon_p}{\varepsilon_{evp}}$$

Shape 3 θ_3 , $\varepsilon_{f3} = \frac{\varepsilon_1 \gamma (\theta_3 - \theta_2)}{1 + \gamma \theta_3}$, loading to σ_2 at θ_2 (0-6), time exposure, approximately equal to the duration of cooling (6-7), cooling to θ_3 (7-7), unloading (7-8), section 8-9 corresponds to ε_p , section 9-0 corresponds to ε_{f3} .

$$\text{Section } 3-2' \quad R_{r3} = \frac{\varepsilon_{evp} - \varepsilon_p}{\varepsilon_{evp}} \quad \text{Section } 0-8 \quad R_{f3} = \frac{\varepsilon_1 \gamma (\theta_3 - \theta_2)}{1 + \gamma \theta_3} + \frac{\varepsilon_p}{\varepsilon_{evp}}$$

On fig. 9 change of strains at multi-shape memory effect is shown.

Shape 1 $\theta_1=0$ Slow loading (0-1) to σ_1 and ε_{evp1} , after unloading $R_r = \varepsilon_{ev1}$ (1-1'), $R_f = \varepsilon_p$ (1'-1'').

Shape 2 θ_2 Loading (0-1) to σ_1 and ε_{evp1} at θ_1 , cooling to θ_2 (1-2), after unloading ε_{ev2} (2-2'), ε_f (2'-2''), R_r (2-2''), $R_f = \varepsilon_s$ (2'-2'''), $\varepsilon_{p2} = \varepsilon_{p1}$ (2''-2''').

Shape 3 θ_3 Loading 2'''-2 to σ_2 and ε_{evp2} at θ_2 , cooling to θ_3 (2-3), after unloading ε_{ev3} (3-3'), ε_f (3'-3''), R_r (3-3''), R_f (3'-3'''), $\varepsilon_{p2} = \varepsilon_{p1} = \varepsilon_{p3}$ (3''-3''').

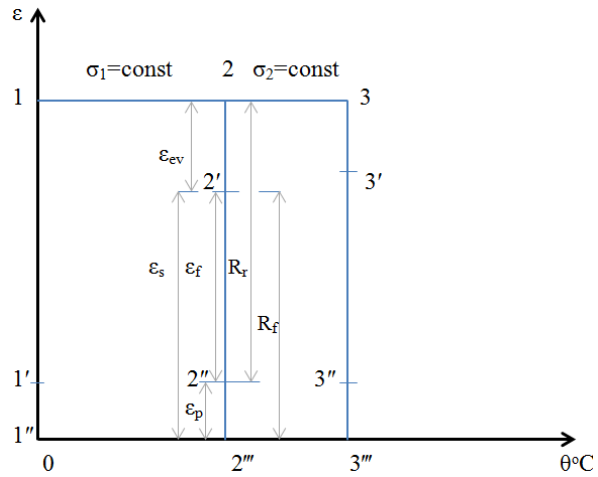


Fig. 9 The combined scheme of influence of temperature on quantities of shape-memory effect of wood.

Visualization of multi-shape memory effect of wood is presented on Fig. 10.

It is possible to notice that the recovery of the initial (permanent) shape is step by step, wood gradually remembers its initial form. When wood is heated from 0 to 60 ° C thermofrozen strains of the left side disappear, with further increase in temperature from 60 to 100 ° C the right side restores its shape.

Thus, the proposed experimental method of visualization allows to look deeper into the memory effect of wood, investigate its deformative conversions.

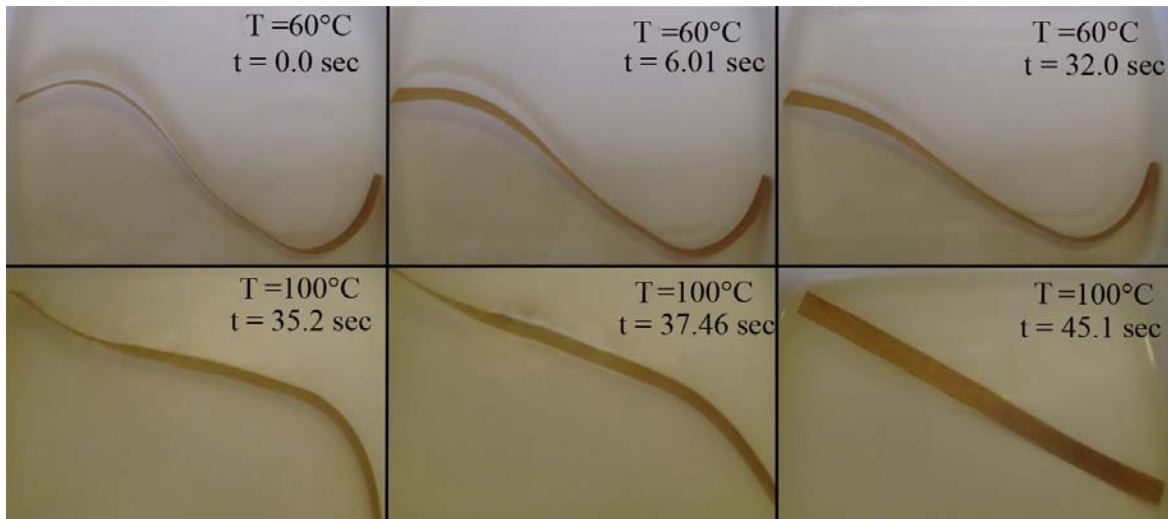


Fig. 10 Visualization of multi-shape memory effect for a sample of beech sliced veneer ($W > 100\%$) in the direction along the grain at heating.

CONCLUSION

The shape memory effect is a dominant feature of wood as a natural smart material. Although it was found by us in 60s of the last century, so far we have confined ourselves to just stating the existence of this unique property of wood. However, modern materials science approaches require quantification of a qualitative phenomena. Visualization and application of generally accepted system of quantities for polymers allow to expand areas of effective use of this phenomenon for the improvement of existing technologies and the development of new nanocomposite polymer materials based on wood.

REFERENCES

- HANHJÄRVI, A. 1997: Perpendicular-to-grain creep of Finnish softwoods in high temperature drying conditions. Espoo. VTT Publications 301, 94 pp.
- HILTZ, J. A. 2002: Shape Memory Polymers. Literature Review. Technical Memorandum DRDC Atlantic TM 2002-127 August 2002.
- KAUYMOV, R.A.& STRAHOV, D.E. 2011: Prediction of deformation in time of high polyethylene fibers with different temperatures. *Izvestija KGASU*, 2(16): 196–199. (In Russian).
- LENDLEIN, A.& KELCH, S. 2002: Shape-Memory Polymers. *Reviews. Angew. Chem. Int. Ed.*41: 2034–2057.
- MIRIANON, F. et. al. 2008: A method to model wood by using ABAQUS finite element software. Part 1. Constitutive model and computational details Espoo. VTT Publications 687. 51 pp.
- PASSARD, J.& PERRÉ, P. 2001: Creep test under water-saturated conditions: do the anisotropy ratios of wood change with temperature and time dependency. *Proc. of 7th Inter. IUFRO Wood drying conf.* Tsukuba, Japan, pp. 230–237.
- SCHUH, C., SCHUH, K., LECHMANN, M. C., GARNIER, L. & KRAFT, A. 2010: Shape-Memory Properties of Segmented Polymers Containing Aramid Hard Segments and Polycaprolactone Soft Segments. *Polymers*, 2: 71–85.
- TORATTI, T.& SVENSSON, S. 2000: Mechano-sorptive experiments perpendicular to grain under tensile and compressive loads. *Wood Science and Technology*, 34: 317–326.
- UGOLEV, B.N. 1961: Method of research of wood rheological properties at changing moisture content. *Zavodskaja laboratoria* 27(2): 199–203 (In Russian).
- UGOLEV, B.N. & LAPSHIN, JU.G. 1971: On deforming of wood when loaded in the condition of drying. *Lesnoy Zhurnal*, 3: 63–65 (In Russian).
- UGOLEV, B.N. 1976: General laws of wood deformation and rheological properties of hardwood. *Wood Science and Technology*, 10(3): 169–181.
- UGOLEV, B.N. 1980: Peculiarity of wood deforming and simulation methods for drying stresses, *Proc. of 3rd Int. Symposium on fundamental research of wood*, Grillenburg, Germany 2: 116–120 (In Russian).
- UGOLEV, B.N., LAPSHIN, JU.G. & KROTOV, E.V. 1980: Measuring and monitoring of stresses at drying. *Lesn. Prom. Moscow*, 208 pp. (In Russian).
- UGOLEV, B.N. 1986: Effect of “freezing” wood deformations at complex force and heat actions. *The 2nd Int. Symposium on wood rheology*, Rydzina, Poland, pp. 5–14.
- UGOLEV, B.N. 1997: History and prospects of wood drying stresses research's development. In: *Wood structure, properties & quality*, Moscow-Mytischki, Russia, pp. 230–238 (In Russian).
- UGOLEV, B.N. 2005: Wood Drying Strains. *Proc. of 9th Inter. IUFRO Wood drying conference*, Nanjing, China, pp. 13–23.
- UGOLEV, B.N. 2009: Academy lecture «Wood as natural smart material», http://www.iaws-web.org/files/file/2009-SaintPetersburg_academy_lecture_ugolev.pdf
- UGOLEV, B. N., GALKIN, V. P., GORBACHEVA, G. A. & KALININA, A. A. 2010: Frozen shrinkage of wood. In: *Wood Structure and Properties'10*, Zvolen: Arbora Publishers, pp. 73–77.
- UGOLEV, B.N. 2011: Nanotechnology and nanomaterials in forestry complex. *M, MGUL*, 221 p. (In Russian).
- XIE, T. 2010: Tunable polymer multi-shape memory effect. <http://www.nature.com/nature/journal/v464/n7286/full/nature08863.html>

UNDERSTANDING THE CLONAL RESPONSE TO IMPOSED MECHANICAL STRESS IN *PINUS RADIATA* SEEDLINGS

BERNADETTE NANAYAKKARA, MARK RIDDELL, GRANT EMMS & JONATHAN HARRINGTON

Scion, Private Bag 3020, Rotorua 3046, New Zealand

Abstract

For the purpose of genetic improvement, it is useful to study whether genotypes differ in their response to mechanical stress, and if so, whether these differences in response can be used for assessment of stem straightness at very early ages. Mechanical stress was imposed on 8 genotypes of 1-year-old *Pinus radiata* by tilting planter bags by a 30 degree angle and staking them to maintain the lean. Effects of mechanical stress on genotypes after one year of imposed stress on seedling growth, root/shoot ratio, in situ acoustics velocity, resonance velocity, longitudinal shrinkage, compression wood percentage and severity, and chemical composition were determined. The genotypes differed in their growth rate, root:shoot ratio and stiffness estimated by acoustics velocity. While mechanical treatment did not affect the growth rate and root:shoot ratio, it resulted in lower acoustics velocity and higher longitudinal shrinkage compared to the controls. Compared to the control trees, percentage of compression wood was much greater in the stressed ones, with differences also present among the genotypes. This implies that the formation and extent of compression wood is genetically influenced.

Key words: *Pinus radiata*, clone, acoustics velocity, resonance velocity, longitudinal shrinkage, compression wood, chemical composition.

INTRODUCTION

There is a growing interest for selecting genotypes with superior wood quality, at very early stages of tree growth. Traits such as DBH, density, stiffness (MOE) and Mfa are commonly used in breeding programs. Compression wood forms in all conifer species commonly in young saplings which are prone to develop compression wood (TIMELL 1986). Log piles from almost any *P. radiata* forest in New Zealand likely to contain batches of logs in which CW occupies up to 20% of the total log volume, causing significant loss of volume recovery of planted forests (HARRIS 1977). Genotypes showed differences in their propensity to form compression wood at age 12 months (BURDON 1975). Exploiting genotypes propensity to form compression wood through mechanical perturbation for selection purposes, under one year of age is a concept that has been reported previously (NAKADA 2007; TELEWSKI and JAFFE 1986). The rationale for this selection method is that genetic differences in young plant's ability to control stem form will continue throughout the life of the tree. The heritability of compression wood has been reported to be significantly high ranging from 0.3–0.9 (APIOLAZA *et al.* 2011b; SHELBOURNE *et al.* 1969). Therefore, inducing compression wood and studying tree's biomechanical response to this stimulus can be useful for early age selection (APIOLAZA *et al.* 2011a; SIERRA-DE-GRADO *et al.* 2008). This presentation describes a research program under taken at Scion to

test if genotypes differ in their response to various stresses, and if so can these differences in response be used to assess stem straightness at very early ages.

METHODS

Mechanical stress was imposed on 8 genotypes of 1 year old *Pinus radiata* by tilting the seedlings by a 30 degree angle and staking them to maintain the lean along with a control treatment. Effects of mechanical stress on genotypes after one year of imposed stress on seedling growth, root/shoot ratio, whole stem green resonance velocity, green xylem resonance velocity, dry xylem resonance velocity, longitudinal shrinkage, compression wood percentage and severity and chemical composition were determined. Acoustics velocity was measured by the resonance method, longitudinal shrinkage by pin method and amount of mostly severe CW was assessed from 2 RGB images made of freshly cut and wet cross ends scanned on a flat bed scanner. Compression wood areas were visually identified and estimated as a % of the whole stem cross sectional area using GYMP 2.8 image analysis program.

RESULTS

Both clonal and treatment differences were evident. There were clonal differences in the growth rates. Height growth was significantly affected by the mechanical treatment but diameter was not affected

Wood the Best Material for Mankind

J. Kúdela & M. Babiak (eds.), 2013, pp. 39–41

© Arbora Publishers, Zvolen, Slovakia

ISBN 978-80-968868-6-9

(Fig. 1a, b). Root:shoot ratios varied from 0.51–0.73 between clones and was significantly affected by the mechanical treatment (Fig. 1c).

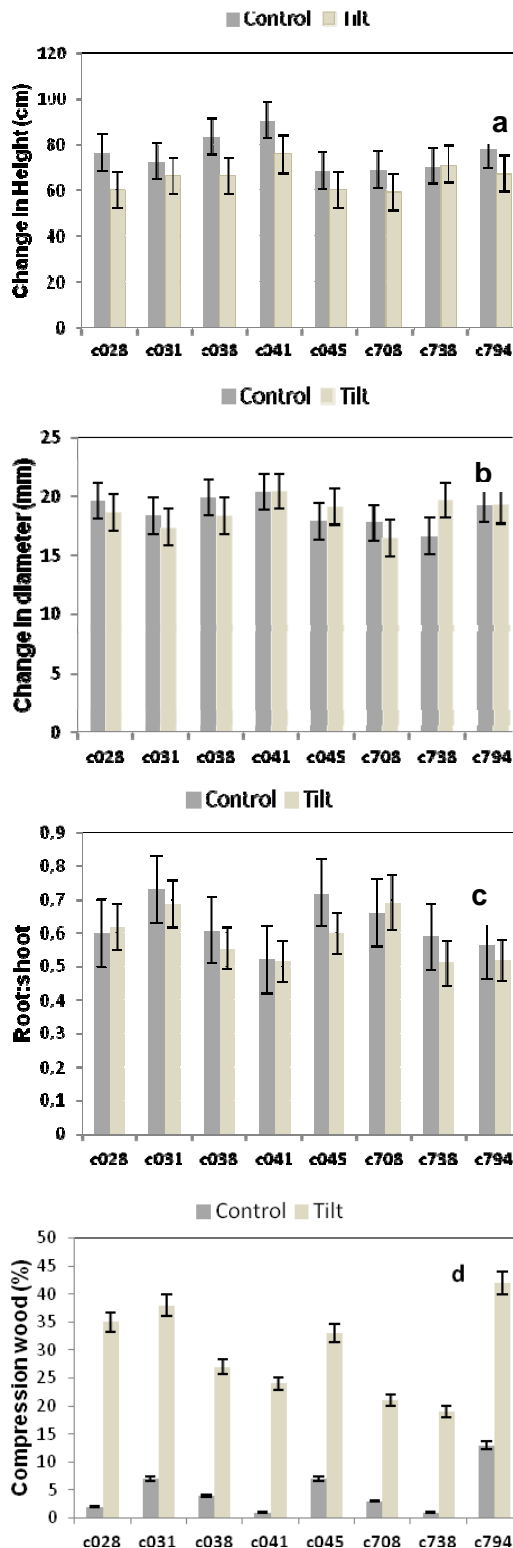


Fig. 1 Morphological features of control and perturbed clones. Values are clone*treatment means \pm SE.

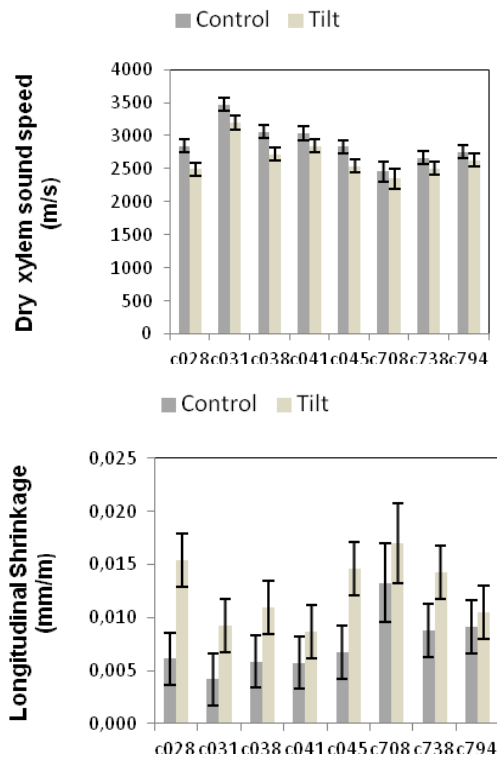


Fig. 2 Mechanical properties of control and perturbed clones. Values are clone*treatment means \pm SE.

Percentage of compression wood varied significantly between genotypes and between treatments as expected and the interaction between genotype and treatment was significant. Genotypes that produced small amounts of compression wood when grown straight produced smaller amounts of compression wood when induced (Fig. 1d). Associated with elevated presence of compression wood in mechanical treatment was lower acoustics velocity and higher longitudinal shrinkage compared to controls (Fig. 2a, b). Longitudinal shrinkage showed significant differences between genotypes, specially clone 708 with the highest shrinkage out of all clones. Shrinkage values were almost doubled in mechanical treatment compared to control treatment. Dry xylem sound speed was negatively correlated with shrinkage (Fig. 3). Whole section green sound speed and green xylem sound speed were closely correlated with dry xylem sound speed (Fig. 4).

CONCLUSION

Genetic variability enhanced by mechanical perturbation can be used to differentiate between genotypes in early age as young as 2 years. Advantages of this approach shorter time span, young stems are easier to handle and analyse, large number of individuals can be tested and a better control of environment conditions.

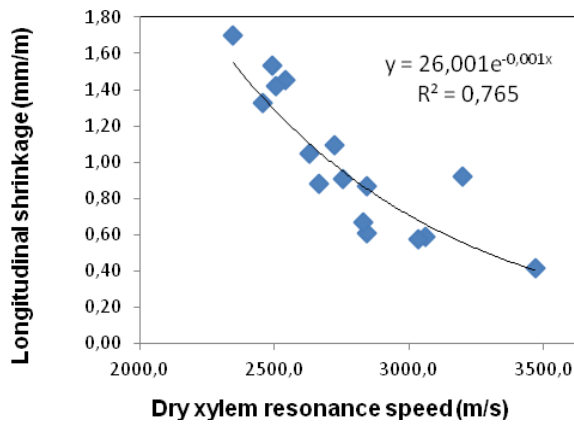


Fig. 3 The relationship between dry xylem resonance speed and longitudinal shrinkage.

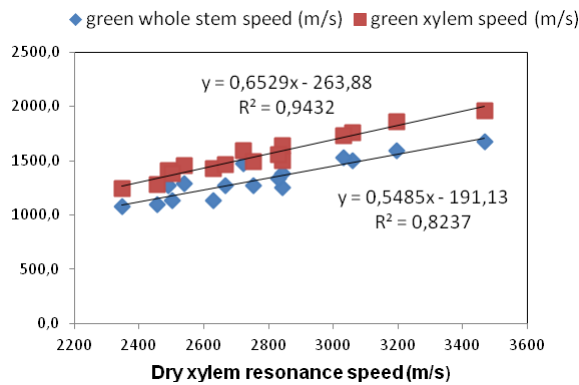


Fig. 4 The relationship between dry xylem resonance speed, green xylem and green whole stem resonance speeds.

REFERENCES

- APIOLAZA L.A., BUTTERFIELD B.G., CHAUHAN S.S. & WALKER J.C.F. 2011a: Characterization of mechanically perturbed young stems: can it be used for wood quality screening? *Annals of Forest Science* 68(2): 407–414.
- APIOLAZA L.A., CHAUHAN S.S. & WALKER J.C.F. 2011b: Genetic control of very early compression and opposite wood in *Pinus radiata* and its implications for selection. *Tree Genet. Genom.* 7:563–571.
- BURDON R.D. 1975: Compression wood in *Pinus radiata* clones on four different sites. *New Zealand Journal of Forestry Science* 5:152–164.
- HARRIS J.M. 1977: Shrinkage and density of radiata pine compression wood in relation to its anatomy and mode of formation. *New Zealand Journal of Forestry Science* 7(1): 91–106.
- NAKADA R. 2007: Within-tree variation of wood characteristics in conifers and the anatomical characteristics specific to very young trees. In: *Within-tree variation of wood characteristics in conifers and the anatomical characteristics specific to very young trees.* pp 51–67.
- SHELBOURNE C.J., ZOBEL B.J. & STONECYPHER R.W. 1969: The inheritance of compression wood and its genetic and phenotypic correlations with six other traits in 5-year-old loblolly pine. *Silvae Genet* 18: 43–47.
- SIERRA-DE-GRADO R., PANDO V., MARTINEZ-ZURIMENDI P., PENALVO A., BASCONES E. & MOULIA B. 2008: Biomechanical differences in the stem straightening process among *Pinus pinaster* provenances. A new approach for early selection of stem straightness. *Tree Physiol.* 28(6): 835–846.
- TELEWSKI F.W. & JAFFE M.J. 1986: Thigmomorphogenesis: anatomical, morphological and mechanical analysis of genetically different sibs of *Pinus taeda* in response to mechanical perturbation. *Physiol. Plant.* 66: 219–226.
- TIMELL T.E. 1986: Ecology of compression wood formation. In: *Compression Wood in Gymnosperms* Volume 3. Springer-Verlag, Berlin. pp 1358–1360.

APPLICATION OF HIGH FREQUENCY TREATMENTS FOR IMPROVED PERMEABILITY OF NORWAY SPRUCE (*Picea abies* KARST.) WOOD

NASKO TERZIEV & GEOFFREY DANIEL

Swedish University of Agricultural Sciences, Department of Forest Products, Box 7008, 750 07 Uppsala, Sweden

Abstract

Samples of Norway spruce (*Picea abies* Karst.) were treated by microwaves (MW). The treatment of spruce samples was performed in a wave guide under various frequency and treatment time. After treatment, samples were taken and modulus of elasticity and water uptake studied. Scanning electron microscope (SEM) was used to reveal the changes in the wood structure caused by the treatment.

The most probable way of “checking” due to HF treatment is along the middle lamella and secondary wall S1 interphases that represent weak points in the cell wall structure and where obvious cleavage occurred. The checks in the middle lamella/S1 interphases of the cell walls were narrow, i.e. 1–2 µm and often followed the entire circumference of the cell. In general the lumen surface seems not modified due to the high frequency and temperature. It is probable that certain modifications in the structure of the wood polymer complex also occurred due to hemicellulose thermal degradation.

The above mentioned structural changes facilitated the penetration of liquids. The water uptake of the treated samples was doubled compared to the untreated controls. As expected, some changes of the modulus of elasticity were inevitable, i.e. the modulus of elasticity decreased with 10% after the treatment. The studied MW energy has also potential in the pulp and paper industry where spruce chips can be more easily impregnated with chemicals after MW treatment. This for examples can save treatment time and energy for refining and defibration of chips.

Keywords: Bordered pits, mechanical properties, microwave impulse mode, microwave treatments, permeability, wood anatomy.

INTRODUCTION

The Northern countries are rich in forests, thus being an important manufacturer of timber, pulp and paper for the local and international markets. Traditionally, more than 55 % of the sawn timber production in Sweden (i.e. 9–10 mill. m³) is Norway spruce (STALAND *et al.* 2000) that is of great commercial interest. When pulp and paper industry is considered the volume of spruce exceeds 40 mill. m³.

Development of wood-based materials and technology becomes up-to-date and important research work from both scientific and industrial points of view. Main challenge in the pulp technology is to intensify the processes while the energy consumption must be decreased. Uptake of chemicals can be faster if spruce chips have better permeability. Novel treatments, e.g. prior MW treatment can facilitate the mechanical defibrillation of wood, thus saving both energy and time.

Significant volume of spruce timber (ca. 600 000 m³) is “impregnated” for export (BERGMAN 2007) but not sold on the Nordic market. This is explained by the fact that spruce is a refractory wood species and cannot be classified according to the impregnation classes approved by the Nordic Wood Preservation Council as it is very difficult to achieve the

recommended retentions of preservatives and uniform penetration into the wood. Some industrial attempts to impregnate spruce timber by supercritical fluid impregnation (i.e. using CO₂ as preservative carrier and pressure of 8–12 MPa) have high production cost. Improvement of depth and uniformity of spruce impregnation by MW and classical or environmentally friendly preservatives will promote a new product (impregnated spruce timber) and improve the service life of material at reasonable cost.

Studies on interaction between wood and microwaves devoted to understand and explain the physical processes of heating and drying have been carried out since 50's of the last century. One of the most comprehensive studies are those of TORGOVNIKOV (1993), PERRE and TURNER (1999, 2004) and ZHAO and TURNER (2000). Two main applications of MW energy can be defined as *MW drying of wood* and *MW treatments to increase wood permeability*.

MW drying of wood: A comprehensive literature review on the MW applications for wood drying can be found in the study of HANSSON (2007). Drying methods for industrial processing based on high-frequency (HF) electromagnetic fields are microwaves (MW), a combination of vacuum and MW (LEIKER and ADAMSKA 2004) or radio frequency

(RF) and vacuum (AVRAMIDIS *et al.* 1994, AVRAMIDIS and ZWICK 1994). An RF drying system creates an alternating electric field between two electrodes. The frequencies of 13.56, 27.12 and 40.68 MHz corresponding to wavelengths of about 22.1, 11.1 and 7.4 m were used because shorter wavelengths cannot penetrate deeply into the material. In contrast to conventional drying, MW and RF drying techniques are based on the principle of instant absorption throughout wet wood. Combining RF and vacuum for heating enables a lower boiling point with decreasing pressure, i.e. lower temperature to vaporize water in wood. In order not to disturb other MW applications, e.g. telecommunications, two particular frequencies have been adopted for MW heating, i.e. 0.915 and 2.45 GHz having wavelengths of 33 and 12 cm.

All MW systems consist of microwave source and application system. The most commonly used microwave generators are magnetrons. The application system consists of a box or waveguides through which the MW are guided and reflected by aluminum walls. The MW resonates and forms standing waves. The position of the nodes and antinodes of the waves in the application system depends entirely on its design and dimensions. The nodes and antinodes make the heating uneven, i.e. hotter and colder spots will be developed in the material. If MW heating technology is used for drying, then a consequence of this uneven heating will be uneven drying, which in turn may cause drying stresses.

At a frequency of 2.45 GHz, the drying rate of spruce and beech boards (EGNER and JAGFELD 1964) was higher than that of conventional drying. With a frequency of 915 MHz and hot air, 25-mm-thick pine planks were dried in less than 3 h (MCALISTER and RESCH 1971) without drying defects. ANTTI (1999) has shown that it is possible to dry Scots pine and spruce wood significantly faster than with conventional drying methods. Concerning other wood species, 50-mm-thick hemlock and Douglas fir planks were dried for less than 10 h with small drying defects (BARNES *et al.* 1976).

The main problem in using this technique in wood drying is the non-uniform MW field. In order to reduce the problems of uneven field distribution and power intensity, an industrial-scale online microwave drier for wood components has been adapted for wood (ANTTI *et al.* 1999, ANTTI and PERRE 1999) to achieve a fairly uniform heating of the load in order to prevent stress development. Too high energy absorption may cause steam expansion checks. OLOYEDE and GROOMBRIDGE (2000) demonstrated that microwave heating reduced the strength of dried wood by 60%. TORGOVNIKOV and VINDEN (2000) use the steam expansion caused by microwaves of high intensity to modify selected hardwoods by increasing

their permeability. They also revealed a decrease of wood strength.

MW treatments for improved permeability: MW applications to increase permeability of refractory wood species have been developed up to industrial scale at Melbourne University, Australia (TORGOVNIKOV and VINDEN 2005, 2006, 2007). Intensive MW power applied to green wood generates steam pressure within the wood cells. Under high internal pressure the pit membranes in cell walls, tyloses in vessels and weak ray cells are ruptured to form pathways for easy transportation of liquids and vapours. A several thousand-fold increase in wood permeability in the radial and longitudinal directions can be achieved in species previously found to be impermeable to liquids and gases. Structural changes in wood after MW modification, their effect on wood properties and process parameters required for different degrees of wood modification are described by TORGOVNIKOV and VINDEN (2009). Typical commodities that have been treated by MW are poles, posts, lumber, railway sleepers, peeler cores, garden sleepers, cross-arms, bridge timbers etc. Experiments with hardwood species, e.g. blue gum (*Eucalyptus globulus*), shining gum (*Eucalyptus nitens*), stringybark (*Eucalyptus muellerana*), messmate (*Eucalyptus obliqua*), Paulownia (*Paulownia fortunei* and *Paulownia elongata*) and softwood species such as Sitka spruce (*Picea sitchensis*), radiata pine (*Pinus radiata*) and Douglas-fir (*Pseudotsuga taxifloria*) heartwood show that full cross section preservative penetration can be achieved.

TORGOVNIKOV and VINDEN (2000) used the steam expansion caused by MW of high intensity to modify selected hardwoods by increasing their permeability. According to the authors, MW processing of heartwood of radiata pine, Douglas-fir and Sitka spruce species using 69–111 kWh·m⁻³ energy facilitates the uptake of water-based preservatives by a factor of 2.9–5.3 compared to control timber. Refractory hardwood species (such as messmate, yellow stringybark and blue gum) showed an increase of a water-based preservative uptake by a factor ranging from 8–14 times following microwave modification using an applied MW energy of 158–236 kWh·m⁻³.

Very few studies concerning MW treatment of other species are available. Experiments with the MW processing of Norway spruce (*Picea abies*) demonstrated a significant increase in the uptake of a 2 % copper-based preservative after wood modification by 2.45 GHz MW frequency and energy greater than 50 kWh·m⁻³ (TREU and GJØLSJØ 2008). Larch (*Larix olgensis*) wood modification by applying intensive MW irradiation (LIU HONG-HAI *et al.* 2005) showed a 2.5–3.3 fold increase in water uptake compared to untreated wood while the MOE and MOR remain practically unchanged.

The objectives of the work were to *study* two MW application of high frequency treatments and their effect on structure and properties of Norway spruce wood. The project was focused on improving the permeability of Norway spruce (*Picea abies* (L.) Karst.) wood by high frequency treatments and studying the impact of treatments on structure and properties of wood to select the optimal treatment parameters with regard to specific processing afterwards.

MATERIALS AND METHODS

Wood of Norway spruce (dowels with diam. 25 mm and 20 cm long) was used in the study. The samples had average initial moisture content of 85% and average basic density of $420 \text{ kg}\cdot\text{m}^{-3}$. A microwave power generator operating at frequencies in the MHz-GHz range and supplying power of 20 kW via a special waveguide to the sample was used. Two MW treatments at 2.45 GHz frequency were studied; the former in impulse mode where the duration of treatment was some milliseconds, while the latter was ordinary constant MW treatment.

After treatment, samples were taken and studied using scanning electron microscopy (SEM). The SEM allowed examination of features like wood cell wall, pits, etc. Semi-thin sections (i.e. TS, TLS, RLS) were cut using a Leitz microtome, air-dried, mounted on stubs, coated with gold and observed using a Philips XL30 ESEM at 15 kV (DANIEL *et al.* 2004). Features from the SEM observations were used to discuss the effect of MW on the anatomical features.

Samples treated in impulse mode were subjected to dynamic testing prior to water uptake test. The wood longitudinal resonance frequency was measured using a Rion SA-77 FFT signal analyser coupled with an accelerometer. Samples were hit with a hammer and the accelerometer picked up the signal pattern from the resonating sample. The signal pattern was displayed with a graphical interface where a cursor was used to mark the peak position of the fundamental resonance frequency, which was recorded to the closest 10 Hz. Using the recorded sample length, fundamental resonance frequency and wood density, the dynamic modulus of elasticity was calculated. The difference between the dynamic MOE of untreated and treated samples was calculated as percentage of the initial modulus. A hypothesis that the permeability of treated samples is increased was further studied by carrying out a water absorption test. The dowels were dried at room temperature and immersed in water and their weight measured after 5, 10, 20, 30, 40, 50, 60 min and 24 h.

Small, free of defects specimens, were cut from the untreated spruce boards and these exposed to MW

treatments in constant mode at various schedules and durations and used further for determination of selected mechanical properties. The specimens were conditioned at $20\pm 2^\circ\text{C}$ and $65\pm 5\%$ RH until reaching constant weight. The ultimate strength in bending, modulus of elasticity, compression perpendicular to grain and shear parallel to grain were measured according to the standards ISO 3133, 3349, 3132 (1975) and ISO 3347 (1976) respectively. The measured wood properties are shown in Table 1.

RESULTS AND DISCUSSION

Treatment at 2.45 GHz frequency in impulse mode

As a step in the project, treatment at 2.45 GHz in impulse mode was tested. Spruce tracheids are connected by bordered pits which are open in fresh undried sapwood. The pit's torus is suspended to the periphery of the pit chamber by margo consisting of strands of cellulose microfibrils. The membrane (i.e. torus and margo) oscillates when pressure is applied alternatively to each side of the membrane. Alternation of the pressure application with required frequency is achieved by MW power that causes rapid water expansion in the pit chamber. For example, a MW generator sends a portion of energy sufficient to expand water in the pit chamber for a very short period of time. Water applies pressure to the membrane which is deflected. After the energy reaches the next cell the water in the first cell achieves lower pressure that deflects the membrane to the reverse direction. In this way the membrane oscillates. Coefficient of water thermal expansion is approximately $5\times 10^{-4} \text{ 1/K}$. If the water temperature is increased with 50°C in a closed volume (i.e. pit chamber) a pressure of $\Delta P = \alpha\Delta TE = 5\times 10^{-4} \times 50 \times 2 \times 10^4 = 500 \text{ kg}\cdot\text{m}^{-2}$ (where E is Young's modulus) can be achieved. The tensile strength of the wood perpendicular to grain does not exceed $100 \text{ kg}\cdot\text{m}^{-2}$. Repetition of the oscillations with a defined frequency destroys the cell wall or pit membrane, i.e. the permeability increases. Such a MW schedule uses ordinary MW frequency but high specific power.

Observations on irradiated spruce samples showed that at least part of the high frequency energy was concentrated in the middle lamella regions between tracheids which showed considerable disruption while the tracheid wall structure appeared relatively undamaged (Fig. 1). The water absorption of the treated samples was increased significantly from $150\text{--}180 \text{ kg}\cdot\text{m}^{-3}$ for the untreated controls to $360\text{--}380 \text{ kg}\cdot\text{m}^{-3}$ for MW treated spruce wood. MOE was measured by ultrasound and decreased by 5–10 % after MW treatments compared to the initial non-treated material.

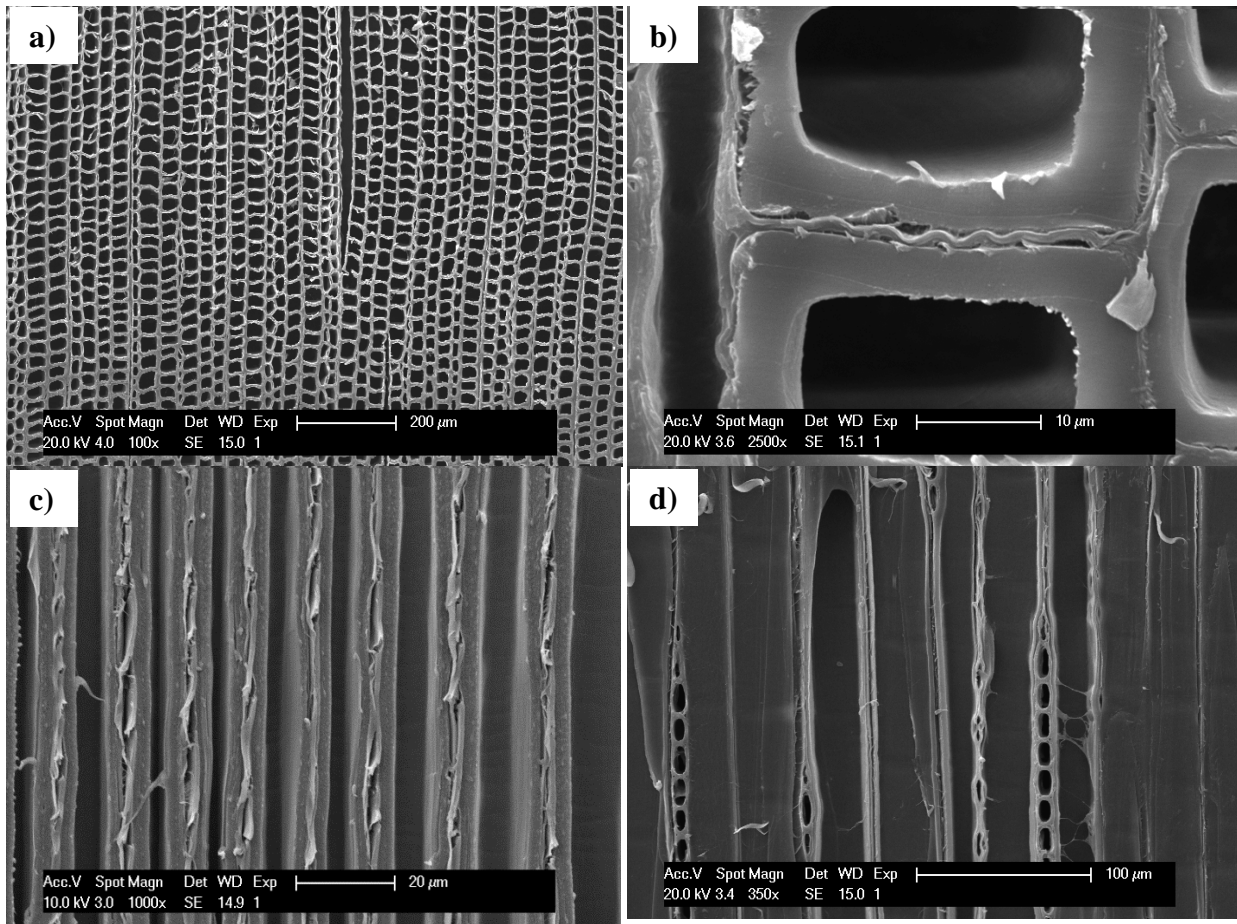


Fig. 1 SEM images of fresh spruce after MW irradiation. a) TS section showing a general loss of tracheid integrity and fractures in the ray canals; b) TS section of late wood tracheid showing modification of the middle lamella between adjacent tracheids; c) RLS sections showing disruption of the middle lamella regions between axial tracheids; d) TLS section with ruptures in the middle lamella regions between axial tracheids and ray/tracheid interphases.

Table 1 MW treatments in constant mode and selected mechanical properties of Norway spruce wood.

Treatment 2.45 GHz, constant mode	Density, $\text{kg}\cdot\text{m}^{-3}$	MOR, N/mm^2	MOE, N/mm^2	Compression \perp grain, N/mm^2	Share tang., N/mm^2	48 h water abs., g
Literature reference (BOUTELJE & RYDEL 1986)	480	66–84	8300–13000	35–44	6–10	–
Untreated	512.5 (14.9)	58.8 (5.0)	9181.2 (925.6)	31.2 (14.4)	9.1 (0.9)	39.3
Power 20 kW, speed 24 mm·sec	456.4 (43.4)	63.1 (26.4)	8607.1 (3163.4)	8.8 (3.2)	8.5 (1.9)	55.2
Power 20 kW, speed 17 mm·sec	444.4 (42.0)	31.9 (20.2)	4517.8 (3431.3)	8.1 (1.9)	6.2 (2.4)	63.4
Power 24 kW, speed 14 mm·sec	422.9 (61.3)	16.8 (10.6)	2444.6 (2312.1)	7.5 (2.4)	4.8 (1.7)	87.0

*Standard deviations in parentheses

Treatment at 2.45 GHz frequency in constant mode

Selected mechanical properties of spruce wood treated in constant mode under various powers and durations are shown in Table 1. The results are in line with previous studies and characterized by significant decrease of the mechanical properties. The effect of

the treatment could be summarised in the single word "checks". Severe checks along the rays are observed, particularly in wood samples treated at speed of 17 and 14 mm/sec. The most probable way of checking due to microwave treatment is along the rays. The middle lamella is the weakest point in the cell wall and cleavage occurs almost always there. The above

mentioned structural changes facilitated the penetration of the preservative during impregnation but also decrease the mechanical properties after the microwave treatment. The density of wood is gradually decreased with increased duration of the treatment thus contributing to the lower strength of the treated wood. The observed changes are proportional to the applied power and duration of treatment.

CONCLUSIONS

The main objective of the study was to improve the permeability of Norway spruce wood by MW treatments and determine changes in the structure and properties of the treated wood. MW treatment is most effective when impulse schedules are used. Alternation of pressure application with required frequency is achieved by HF energy that causes rapid water expansion in the wood pit chambers. Water applies pressure to the pit membranes and wood cell wall. The middle lamella of the cell wall becomes attacked and modified providing for permeability increases while the decrease of strength of the wood is less than 10 %.

MW treatment in ordinary mode caused severe checks along the rays, the density and consequently the mechanical features were influenced negatively. Impulse MW treatment was found to be the most effective treatment with regard to improved spruce permeability and retained mechanical properties. High energy ultrasound treatment, ordinary and impulse MW treatments are also suitable for pulping of wood. The permeability of spruce timber can be significantly improved by the impulse HF treatment and presumably, by HF power pulsation frequency.

REFERENCES

- ANTTI, A. 1999: Heating and drying wood using microwave power. PhD thesis, Vol. 35. Luleå Univ. of Technology, Division of Wood Physics.
- ANTTI, A. L. & PERRÉ, P. 1999: A microwave applicator for on-line wood drying: Temperature and moisture distribution in wood. *Wood Sci. Technol.*, 33: 123–138.
- ANTTI, A. L., ZHAO, H. & TURNER, T. 1999: Investigation of the heating of wood in an industrial microwave applicator: theory and practice. *Drying Technology* 18(8): 1665–1676.
- AVRAMIDIS, S., ZWICK, R. L. & NEILSON, B. J. 1994: Commercial scale RF/V drying of softwoods. Part I. Basic kiln design considerations. *Forest Prod. J.*, 46(5): 44–51.
- AVRAMIDIS, S. & ZWICK, R. L. 1994: Commercial scale RF/V drying of softwoods. Part II. Drying characteristics and degrade. *Forest Prod. J.* 46(6): 27–36.
- BARNES, D., ADMIRAAL, L., PIKE, R. L. & MATHUR, V. N. P. 1976: Continuous system for the drying of lumber with microwave energy. *Forest Prod. J.* 26(5): 31–42.
- BERGMAN, Ö. 2007: Träimpregneringindustrin i Sverige, produktionsåret 2005. Rapport, Svenska Träskyddsinstitutet.
- BOUTELJE, J. & RYDEL R. 1986: Trä fakta – 44 träslag i ord och bild.
- DANIEL, G., DUCHESNE, I., TOKOH, C. & BARDAGE, S. 2004: The surface and intracellular nanostructure of wood fibres: Electron microscope methods and observations. In *Proceedings of COST Action: Wood Fibre Cell Walls: Methods to study their formation, structure and properties*, pp. 87–104. Eds. U. Schmit, P. Ander, J.C. Barnett, A.M.C. Emmons, G. Jeromidis, P. Saranpää, S. Tschegg (available at <http://www-wurc.slu.se>).
- EGNER, K. & JAGFELD, P. 1964: Versuche zur künstlichen Trocknung von Holz durch Mikrowellen. *Holtz-Zentralblatt* 129:297–300.
- HANSSON, L. 2007: Microwave treatment of wood. PhD thesis, Vol. 40. Luleå Univ. of Technology, Division of Wood Physics.
- ISO 3132 (1975) Wood – Testing in compression perpendicular to grain.
- ISO 3133 (1975) Wood – Determination of ultimate strength in static bending.
- ISO 3347 (1976) Wood – Determination of ultimate shearing stress parallel to grain.
- ISO 3349 (1975) Wood – Determination of modulus of elasticity in static bending.
- LEIKER, M. & ADAMSKA, M. 2004: Energy efficiency and drying rates during vacuum microwave drying of Wood. *Holz Roh- u. Werkstoff*, 62: 203–208.
- LIU H-H., WANG Q-W., YANG L. & CAI Y-C. 2005: Modification of larch wood by intensive microwave irradiation. *J. Forest. Res.*, 16(3): 237–240.
- MCALISTER, W. R. & RESCH, H. 1971: Drying 1-inch ponderosa pine lumber with a combination of microwave power and hot air. *Forest Prod. J.* 21(3): 26–34.
- OLOYEDE, A. & GROOMBRIDGE, P. 2000: The influence of microwave heating on mechanical properties of wood. *Journal of Material Processing Technology* 100: 67–73.
- PERRÉ, P. & TURNER, I. W. 1999: The use of numerical simulation as a cognitive tool for studying the microwave drying of softwood in an over-sized waveguide. *Wood Science and Technology* 33(6): 445–464.
- PERRÉ, P. & TURNER, I. W. 2004: Environmental and Energy Engineering Microwave drying of softwood in an oversized waveguide: Theory and experiment. *AIChE Journal* 43(10): 2579–2595.
- STALAND, J., NAVREN, M. & NYLINDER, M. 2002: Såg 2000: Resultat från sågverksinventeringen. Report nr. 3, Inst. För skogens produkter och marknader ISSN 1651–0704.
- TORGOVNIKOV, G. I. 1993: *Dielectric Properties of Wood and Wood-Based Materials*. New York: Springer-Verlag.
- TORGOVNIKOV, G. & VINDEN, P. 2000: New Wood Based Materials Torgvin and Vintorg. In: *Proc. 5th Pacific Rim Bio-Based Composite Symposium*, 10–13 December 2000, Canberra, Australia: 756–764.
- TORGOVNIKOV, G. & VINDEN, P. 2005: New equipment for microwave wood modification. In: *Proc. 10th International Conference on Microwave and High Frequency Heating*, Modena, Italy: 293–297.
- Torgovnikov, G. & Vinden, P. 2006: New 300 kW plant for microwave wood modification. In: *Proc. IMPI's 40th Annual International Symposium*. Aug. 9–11, 2006. Boston, USA: 260–263.
- TORGOVNIKOV, G. & VINDEN, P. 2007: Microwave applicator for intensive timber radiation to modify wood structure. In: *Proc. 11th International Conference on Microwave and High Frequency Heating*, Sept. 3–6, 2007. Oradea, Romania: 335–338.

- TORGOVNIKOV, G. & VINDEN, P. 2009: High intensity microwave wood modification for increasing permeability. *Forest Prod. J.* 59(4): 84–92.
- TREU, A. & GJØLSJØ, S. 2008: Spruce impregnation, finally a breakthrough by means of microwave radiation? *In: Proc. 4th Meeting of the Nordic Baltic Network in Wood Material Science & Engineering (WSE)*, Nov. 13–14, 2008. Riga, Latvia. pp. 42–48.
- ZHAO, H. & TURNER, I. W. 2000: The use of a coupled computational model for studying the microwave heating of wood. *Applied Mathematical Modeling* 24: 183–197.

Acknowledgements

The authors gratefully acknowledge Ångpanneföreningens Forskningsstiftelse for the financial support of project "Application of HF energy for improved impregnation and development of novel properties of spruce timber". Part of this work was carried out within the framework of the "Branschforskningsprogram för skogs- och träindustrin" and program "Process and product developments through unique knowledge of wood fiber ultrastructure" (2007-03230) financed by VINNOVA and six forest based industries (Eka Chemicals, Holmen, SCA, Smurfit Kappa Kraftliner, StoraEnso and Södra Cell).

INFLUENCE OF PRESSING PARAMETERS ON DIMENSIONAL STABILITY AND DENSITY

MAREK REŠETKA & JOZEF KÚDELA

Faculty of Wood Science and Technology, Technical University in Zvolen, Slovak Republic

Abstract

This work was aimed at investigation of the influence of pressing parameters (pressing temperature, pressing time, and compression degree) on dimensional stability and density of poplar wood specimens. The specimens, with an initial moisture content of 15.6 %, were pressed in radial direction. The results show that the dimensional stability significantly improved with increasing pressing temperature and time. With prolonged pressing time and increasing temperature, wood sorption capacity decreased significantly, too.

The measured density profiles suggest that no pressing regimen could guarantee the specimens uniformly pressed across their cross section in the pressing direction. The density increase was the most pronounced in the surface layers and decreased towards the centre.

Keywords: pressing, poplar wood, temperature, pressing time, dimensional stability, density profiles.

INTRODUCTION

The native wood is pressed with the purpose to increase its density, to improve its mechanical properties, and to shape its relief. The performance of compressed wood is affected by a range of factors such as wood moisture content and temperature under pressing, pressing time, pressing pressure or the degree of compression.

The compressed wood density has been recognised primarily dependent on the pressing degree and on the wood species (BLOMBERG *et al.* 2006). Accorded to these authors, the average density values of seven wood species pressed under a constant pressure, ranged (according to the woody plant) between 750–1100 kg·m⁻³. For beech wood compressed by 20 % KÚDELA and REŠETKA (2012a) report an average density ranging 765–957 kg·m⁻³ and for a 40% compression 874–1010 kg·m⁻³. The last cited work suggests that under the same compression degree, the beech wood density raised with raising temperature and prolonged pressing time, as the result of dimensional stability improved by the pressing.

WANG and COOPER (2005), KÚDELA and REŠETKA (2012b) show non-uniform density patterns across the cross-cut (in pressing direction). The variable density profiles confirm that the compression of the pressed body in the pressing direction is not uniform. This is negatively reflected in the dimensional stability of the pressed wood (KÚDELA and REŠETKA 2012a). There arises a question about pressing parameters guaranteeing an appropriate dimensional stability and uniform density of the compressed wood.

Former works (CHUCHRĽANSKIĽ 1953, STAMM and SEBORG 1941 and SEBORG *et al.* 1962) report that wood with moisture content below 13 %, pressed at 150 °C, was not stable; and after repeated wetting and

heating, it returned almost to the original state. To ensure the dimensional stability of the pressed wood, the wood was fixed chemically, physically or mechanically. The mechanism, however, underlying densification of hydrothermally treated wood, has not been sufficiently recognised yet. So, there have been launched thorough studies of the hydrothermal treatment itself, with the purpose to attain good malleability and better stability of the compressed wood (ITO *et al.* 1998a, b, INOUE *et al.* 1998, DWIANTO *et al.* 1999, HIGASHIHARA *et al.* 2000, NAVI and GIRARDET 2000, REINPRECHT and VIDHOLDOVÁ 2011, PALKO and ZEMĽAR 2012, KÚDELA and REŠETKA 2012a and others). Another incentive to restart the research was due to new possibilities and tools in study changes occurring in wood induced by heat and moisture.

ITO *et al.* (1998) obtained, after preliminary plasticization, high dimensional stability for wood pressing temperatures above 180 °C. Temperatures exceeding 180 °C are also preferred by KÚDELA and REŠETKA (2012a), who point at significant influence of pressing time on wood dimensional stability. One of facts underlying improvement of dimensional stability under pressing temperature above 180 °C is distinctly reduced wood sorption capacity (JOHANSSON *et al.* 2006, BÄCHLE 2007). INOUE *et al.* (1998) fixed compressed wood by high-frequency heating, reducing, in such a way the instant reversible deformation.

Dimensional stability is also noticeably affected by interaction between moisture and temperature. NAVI and GIRARDET (2000) show that better results can be obtained for beech wood pressed at 150 °C in saturated steam (thermo-hydro-mechanical treatment – THM) than for the same wood pressed at low

Wood the Best Material for Mankind

J. Kúdela & M. Babiak (eds.), 2013, pp. 49–57

© Arbora Publishers, Zvolen, Slovakia

ISBN 978-80-968868-6-9

moisture contents (thermo-mechanical treatment – TM). The authors also demonstrated that, in comparison with compressed wood, THM compressed wood exhibited significantly reduced sorption capacity and better dimensional stability after repeated wetting in water. There is evidence for a range of other factors improving the dimensional stability in THM beech wood. Under given conditions, the destruction of lignin-carbohydrate matrix is more advanced, and after removal of the moisture and heat load, the matrix molecules are cross-linked due to restoration of hydrogen bonds distorted by wood plasticization and shaping. The stresses in the matrix are relaxed; the hygrophilous cell wall components (primarily hemicelluloses) form polymers showing more resistance against water. There were also observed different mechanisms driving deformation of cell elements. On the other hand, high wood moisture content has also negative impacts – and for higher pressing temperatures, a moisture content range of 15–20 % is recommended.

The results of the cited works do not allow specification of the optimum moisture content and temperature for wood during pressing, due to the influence of a range of other factors. KÚDELA (2005), CLAIR *et al.* (2003) and ESTEVES and PEREIRA (2009) show that molecular mechanisms underlying changes in wood are very diverse and complex. Several changes to wood structure have been explained satisfyingly (changes to chemical structure, degradation of hemicelluloses and of amorphous cellulose, lignin networking, reduction of the number of hydroxyl groups followed by changes in sorption properties); many several, nevertheless, are still waiting for clarification (CLAIR *et al.* 2003, KAČÍKOVÁ and KAČÍK 2011).

The aim of our work was to find out, by experiments, the influence of selected pressing parameters (high temperature, varying pressing time and varying compression degree) on the density and dimensional stability of poplar wood after pressing followed by conditioning to various moisture contents.

MATERIAL AND METHODS

The experiments were performed with test specimens of poplar (*Populus tremula*, L.), with dimensions of 50 × 50 × 20 mm (T × L × R), pressed in radial direction – Fig. 1.

The test specimens were conditioned at a temperature of 20 °C to an equilibrium moisture content of 15 %. This value was set after having considered the results from literature and the results of our former experiments. The acclimated specimens were weighed with an accuracy of 0.01 g and measured with an accuracy of 0.01 mm.

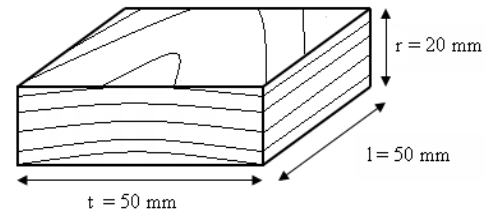


Fig. 1 Test specimen, dimensions and shape.

The pressing appliance was equipped with two pressing plates, with controlled heating. The heating was electric, controlled with a thermostat whose gauge was inserted directly in the pressing plate. The specimens were pressed by 20 % and 40 %. For the pressing process, we choose four temperature regimens: 160, 180, 200 and 220 °C and three pressing periods: for wood compressed by 20 % it was 8, 10 and 12 min and for wood compressed by 40 % it was 6, 8 and 10 minutes.

The required compression extent was obtained with the aid of restraining metal mats with the thickness corresponding to the desired compression (20 % => 16 mm; 40 % => 12 mm). By combining these factors, we obtained 24 different pressing regimens. For each regimen, there were used 12 specimens, altogether 288.

After the pressing finished, the specimens were taken out from the pressing equipment, and weighed and measured again, with the same accuracy as before. Then they were stored in a conditioning box with a relative air humidity of 65 % and a temperature of 20 °C until reaching the equilibrium state. Further conditioning of the specimens was pursued at $\phi = 80$ % and $t = 20$ °C. The conditioned specimens were weighed and measured again. Finally, the specimens were dried out to zero moisture content – to obtain the dry mass m_0 .

The dimensional change of the test specimens in the pressing direction was calculated two times: immediately after the removal from the pressing equipment, according to the equation:

$$D_1 = \frac{H_1 - H_0}{H_0} \cdot 100 \quad (1)$$

and after the conditioning of the test specimens in an environment with parameters (ϕ , t), according to the equation

$$D_2 = \frac{H_{2(3)} - H_0}{H_0} \cdot 100, \quad (2)$$

where H_0 is the thickness of specimen after compression (16 or 12 mm), H_1 – is the thickness of specimen taken out from the pressing equipment, H_2 – is thickness of specimen after conditioning at $\phi = 65$ %.

Wood density at given moisture content was derived from the ratio of the specimen mass and volume (STN

490108). The specimen moisture content before pressing, after pressing and after re-acclimation was determined gravimetrically according to the Standard STN 490103.

Apart from the average density of the compressed wood specimens, we also investigated their density profiles across the thickness (parallel with compression), as the density profiles provide information about profiles for other compressed wood properties dependent on density, in the relevant direction,

For this purpose we used an analyser of density profile. The equipment measures the material density indirectly: by measuring the dampening of a narrow beam of low-energy γ radiation Am^{241} after passing through the material. The radiation intensity I after passing through the material is

$$I = I_0 \exp\left(-\frac{\mu}{\rho} \cdot \rho \cdot d\right), \quad (3)$$

where I_0 is the original radiation intensity, d – is the material thickness and μ/ρ – dampening coefficient.

The material density value $\rho(x)$ at a distance of x mm from the specimen's edge perpendicular to the radiation direction is

$$\rho(x) = \frac{\log \frac{I_0}{I(x)}}{\frac{\mu}{\rho} \cdot d}. \quad (4)$$

The values I_0 and $I(x)$ are calculated from the number of radiation signals detected, according to the equations

$$I_0 = N_0 - N_P \quad (5)$$

$$I(x) = N(x) - N_P \quad (6)$$

where N_0 is the number of signals recorded by the detector under open aperture, N_P is the number of background signals (the aperture closed), $N(x)$ is the number of signals generated by quanta γ having passed through the specimen at position of aperture x mm from the specimen's edge.

Rearranging equations (4), (5) and (6) we obtain

$$\rho(x) = \frac{\log \frac{N_0 - N_P}{N(x) - N_P}}{\frac{\mu}{\rho} \cdot d}. \quad (7)$$

All the variables in Eq. (7) are easy to measure, with exception of the damping coefficient μ/ρ . This coefficient was determined for each specimen separately, according the methods proposed by BAHYL (1992). The sketch of the equipment is in Fig. 2. The density profile was measured at the mid-width of compressed specimens conditioned at $\phi = 65\%$ and 20°C .

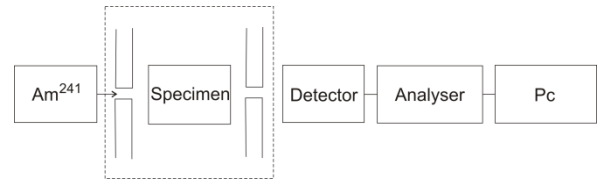


Fig. 2 Block diagram of the density analyzer (BAHYL 1992).

RESULTS AND DISCUSSION

The average moisture content of the test specimens before the pressing was 15.5 % (Table 1). The acclimated specimens were pressed under conditions described in the methods. Mechanical, moisture and heat loading acting in interactions in the pressing process caused instant as well as permanent changes in wood structure, which means also changes in wood properties. The immediate changes in wood properties directly influenced the wood compression during pressing process. The permanent modifications in wood structure and properties had impacts on dimensional stability and other properties of compressed wood.

The average moisture content of the test specimens after the pressing under various regimens ranged from 6 to 0.6 % (Table 1). The moisture content distinctly decreased with raising temperature. There was also confirmed decreasing trend in wood moisture content with prolonged pressing time. The effect of compression degree has not been confirmed unequivocally.

After removing from the pressing equipment, the springback of each specimen was determined according to the Eq. (1). The thickness change was expressed relatively to the initial thickness H_0 , representing 16 mm under 20% compression and 12 mm under 40% compression. The results are illustrated in Fig 3.

Fig. 3a demonstrates that the dimensional stability of poplar wood compressed by 20 % was mostly affected by the pressing time. After 12 min of pressing, all poplar specimens manifested absolutely perfect dimensional stability for all pressing temperature variants. Good dimensional stability was also obtained for the pressing time of 10 min. With the time reduced to 8 min, the dimensional stability was reduced, showing also distinct impacts of pressing temperature. In this case, reaching dimensional stability required a temperature of 220°C .

For 40% compression, there was observed a similar trend, however, the overall dimensional stability of specimens was worse than in the preceding case (Fig. 3b). The moisture in the specimens compressed by 40% was concentrated at the specimen's centre – not possible to escape outside the wood, and caused the considerable springback after the removal from the pressing equipment.

Compared to beech and spruce wood compressed under the same conditions (REŠETKA 2012), the

poplar wood manifested the poorest dimensional stability.

The results show that the dimensional stability was primarily affected by the pressing time. The role of pressing temperature at range 160–220 °C was only secondary if the specimens were heated over the whole thickness profile. Considering also other properties, mainly the colour of wood surface,

appropriate pressing temperature was found 180 °C and appropriate pressing time 10–12 min for the specimens of relevant thickness. In case when the wood colour surface does not play a role, the temperature of 220 °C guarantees a good dimensional stability for all pressing periods. In this case, however, there is a possible risk of considerable thermal degradation of surface wood layers.

Table 1 Moisture content values in specimens in particular phases of experiment (n = 6).

Pressing time [min]	Statistical characteristics of m. c.	Pressing temperature [°C]							
		160	180	200	220	160	180	200	220
		Moisture content before pressing ($\varphi = 70\%$, $t = 20\text{ °C}$)							
	\bar{x} [%]	15.60							
	s [%]	0.39							
	n	144							
		After pressing				Conditioning after pressing ($\varphi=65\%$, $t=20\text{ °C}$)			
		Compression by 20 %							
8	\bar{x} [%]	5.94	3.48	3.88	1.36	8.98	8.51	8.46	7.99
	s [%]	1.42	1.31	1.78	1.11	0.41	0.56	0.28	0.52
10	\bar{x} [%]	3.95	2.45	1.33	1.35	9.01	8.42	8.42	7.37
	s [%]	1.00	1.14	1.42	1.15	0.27	0.43	0.59	0.23
12	\bar{x} [%]	3.54	1.95	1.26	0.65	8.57	8.24	7.95	7.23
	s [%]	0.99	1.52	1.23	0.82	0.36	0.41	0.63	0.40
		Compression by 40 %							
6	\bar{x} [%]	6.88	4.62	3.63	1.79	9.36	8.60	8.53	7.76
	s [%]	1.21	2.11	1.68	1.59	0.19	0.13	0.29	0.64
8	\bar{x} [%]	4.31	2.74	2.07	1.27	8.88	8.29	8.08	6.93
	s [%]	1.87	1.22	1.58	0.81	0.20	0.26	0.67	0.62
10	\bar{x} [%]	3.33	2.90	1.23	0.81	8.58	8.01	7.78	6.86
	s [%]	1.42	2.04	1.18	0.76	0.18	0.31	0.59	0.59

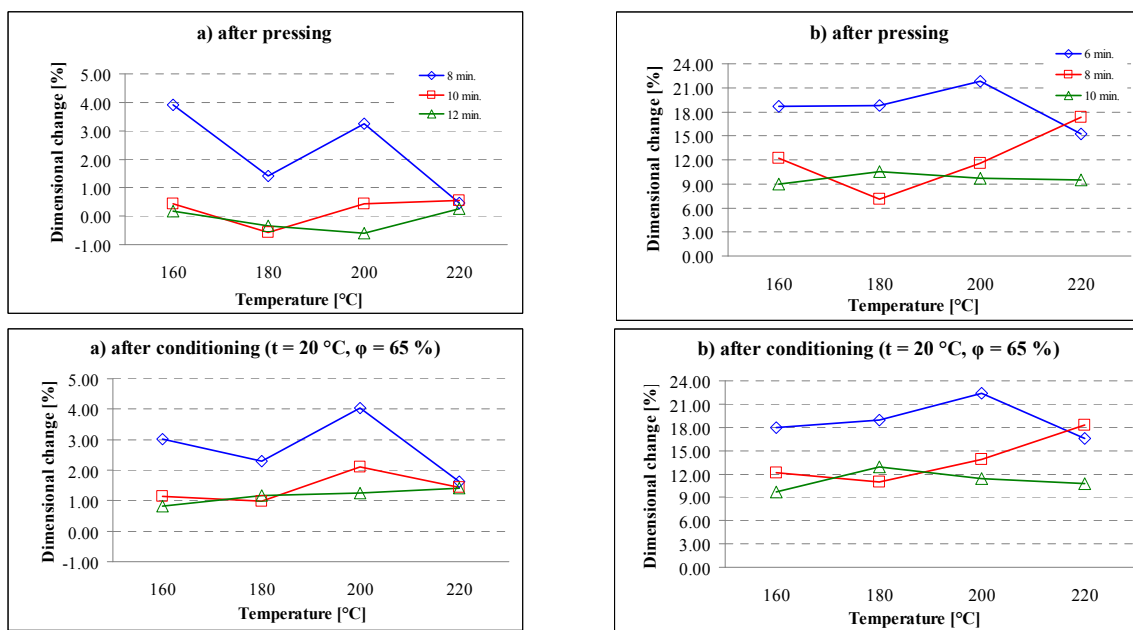


Fig. 3 Thickness variation in pressed specimens corresponding to various pressing conditions after removal from the pressing equipment and after conditioning. a) compression by 20 %, b) compression by 40 %.

Then the compressed specimens were conditioned at a relative air humidity $\varphi = 65\%$ and temperature $20\text{ }^{\circ}\text{C}$. Equilibrium moisture content in wood under these conditions is 12% . The average moisture content in the compressed specimens after the conditioning under the same conditions ranged between $9\text{--}6.5\%$ according to the pressing variant (Table 1). Therefore, the specimens displayed their sorption capacity reduced by 25 to 45% , independent on the compression degree. The results show that the wood sorption capacity significantly decreased with increasing temperature and prolonged pressing time. The specimens manifested a good dimensional stability also after the conditioning, with dimensional changes very small in comparison with the dimensional changes occurring immediately after removal from the pressing equipment (Fig. 3). As the dominant factor affecting the dimensional stability was again identified the heating time. Temperatures within the interval $160\text{--}220\text{ }^{\circ}\text{C}$ were sufficient when these values were reached in the whole body across its cross-section.

The causal factors for small springback after the load removal and re-conditioning are elastic strains (instant and time-elastic) and restoration of hydrogen bonds. The renewed hydrogen bonds enable reorganisation of macromolecular and submicroscopic structures and conformations. The result is renewal of hygroscopic deformation of wood – wood “swelling”.

The molecular mechanisms underlying changes in wood associated with temperature is different from the changes associated with moisture. Wood heating accelerates the movements of its basic elements (thermal movements), with inducing significant physical and chemical changes in this material (KAČÍKOVÁ and KAČÍK 2011).

Wood polymers are in general characterised with three temperature ranges and the three corresponding states – glassy state, viscoelastic (transitory) state and viscous flow (rubbery state) (KÚDELA 1992). For some polymers, IRVINE (1984) reports even five possible temperature ranges. Five temperature ranges are also observable in lignins of some broadleaved woody plants (KUBO *et al.* 1997). The different ranges are associated with different polymer properties and performance. From this viewpoint is important T_g temperature (glass transition).

In case of dry hemicelluloses and lignin, $T_g > 100\text{ }^{\circ}\text{C}$ (IRVINE 1984, SOLÁR 1997, OLSON and SALMÉN 1997 and others). The last-cited works, however, are showing evidence for an especially significant dependence of T_g on moisture content. The temperature range for T_g is from 60 to $100\text{ }^{\circ}\text{C}$ for wet lignin, and from 0° to $100\text{ }^{\circ}\text{C}$ – dependent on moisture content for hemicelluloses. With increasing moisture content increases also the difference in T_g between the two discussed wood constituents. It is because the hemicelluloses in wood are highly hygroscopic and

they absorb the considerable water amounts.

In this temperature range, T_g values cannot be observed for cellulose – due to the high crystallinity of this component. WOODWARD (1980) reports for cellulose a glass transition T_g value of $230\text{ }^{\circ}\text{C}$. Some authors cited in LINDSTRÖM *et al.* (1987) report $200\text{ }^{\circ}\text{C}$ for T_g of dry cellulose, with other T_g values being inversely dependent on moisture content.

The glass transition of wood in plasticization process is supposed to be controlled primarily by the T_g of lignin. In case of wet poplar wood, the T_g range is $68\text{--}80\text{ }^{\circ}\text{C}$ (OLSSON and SALMÉN 1997). Apart from moisture content, T_g is also affected by the duration of thermal or hydrothermal treatment. T_g values also depend on the presence of methoxyl groups in wood lignin, They are less abundant in poplar than in beech wood (OLSSON and SALMÉN 1997), hence the plasticization of poplar is worse than of beech under the same conditions.

Reduction of wood hydrophilicity and permanent dimensional stabilisation of wood after pressing requires reaching the rubbery state. For reaching the rubbery state of lignin in pressing wood with low moisture content, there are necessary substantially higher heating temperatures ($180\text{--}200\text{ }^{\circ}\text{C}$) – documented with the results of ITO *et al.* (1998b), INOUE *et al.* 1998 and DWIANTA *et al.* 1999.

For the initial moisture content of 15% (air-dried wood) significantly decreasing during pressing, the pressing temperatures from 160 to $220\text{ }^{\circ}\text{C}$ were verified as sufficient. These values should guarantee wood polymers being at the third transition phase – rubbery state during wood pressing. This is true, however, only under the assumption that the body has been heated across the entire cross-section.

The pressing parameters also affected the compressed wood density. The Table 2 shows that the average density of poplar wood compressed by 20% was $590\text{ kg}\cdot\text{m}^{-3}$. Compression by 40% resulted in average density of $693\text{ kg}\cdot\text{m}^{-3}$.

The results show that the density of compressed poplar wood predominantly depended on the compression degree, dimensional stability and moisture variation during pressing. Under the same compression, higher density was attained in specimens with better dimensional stability.

After conditioning at $\varphi = 65\%$, the moisture content of specimens was somewhat higher compared to the value occurring after the removal from the pressing equipment, At the same time increased also the springback, so the result was only a negligible gain in density of the acclimated specimens. Statistically significant differences observed in some cases are practically irrelevant.

The density patterns across compressed specimens and across re-conditioned specimens revealed that the compressed wood density varied along the pressing direction. At 20% compression, the

highest density values were attained in surface layers (cca 1–2 mm), decreasing inwards the specimen. Within the outer 3–4 mm layer, the density was higher than the average density of the relevant specimen (Fig. 4). This means that the compression by 20% influenced primarily the surface layers – as these were plasticized more quickly. Fig. 4 demonstrates a good symmetry of density patterns without significant changes associated changes in other pressing parameters.

The density patterns along the pressing direction observed in specimens compressed by 40% were similar (Fig. 5), showing, however more variability

and asymmetry. We assign it to expansion of water vapor in specimens removed from the pressing equipment, causing the springback of the compressed layer. Similar density distribution in compressed poplar wood has been reported by WANG and COOPER (2005).

The final density of compressed wood and its distribution is important from the viewpoint of wood mechanical properties. The mechanical properties of wood improve linearly with increasing density, equally in normal and in compressed wood (BLOMBERG 2006, KÚDELA 2010).

Table 2 Density of specimens in particular phases of experiment: initial moisture content 15.6%.

Pressing time [min]	Statistical characteristics of density	Pressing temperature [°C]							
		160	180	200	220	160	180	200	220
		Density before pressing ($\varphi = 70\%$, $t = 20^\circ\text{C}$)							
	\bar{x} [g·cm ⁻³]	0.522							
	s [g·cm ⁻³]	0.030							
	n	288							
		After pressing				Conditioning after pressing ($\varphi=65\%$, $t=20^\circ\text{C}$)			
	n = 12	Compression by 20 %							
8	\bar{x} [g·cm ⁻³]	0.585	0.598	0.585	0.589	0.606	0.611	0.601	0.613
	s [g·cm ⁻³]	0.037	0.035	0.042	0.035	0.039	0.038	0.037	0.035
10	\bar{x} [g·cm ⁻³]	0.604	0.590	0.595	0.582	0.627	0.611	0.614	0.608
	s [g·cm ⁻³]	0.022	0.035	0.043	0.030	0.025	0.039	0.043	0.034
12	\bar{x} [g·cm ⁻³]	0.586	0.589	0.604	0.583	0.610	0.612	0.626	0.609
	s [g·cm ⁻³]	0.031	0.040	0.027	0.037	0.035	0.040	0.027	0.034
	n = 12	Compression by 40 %							
6	\bar{x} [g·cm ⁻³]	0.679	0.670	0.659	0.681	0.705	0.688	0.670	0.701
	s [g·cm ⁻³]	0.082	0.084	0.107	0.103	0.079	0.082	0.101	0.100
8	\bar{x} [g·cm ⁻³]	0.715	0.724	0.696	0.659	0.737	0.739	0.715	0.684
	s [g·cm ⁻³]	0.089	0.078	0.056	0.090	0.083	0.076	0.052	0.087
10	\bar{x} [g·cm ⁻³]	0.736	0.695	0.687	0.712	0.759	0.715	0.707	0.739
	s [g·cm ⁻³]	0.065	0.063	0.059	0.068	0.059	0.057	0.062	0.066

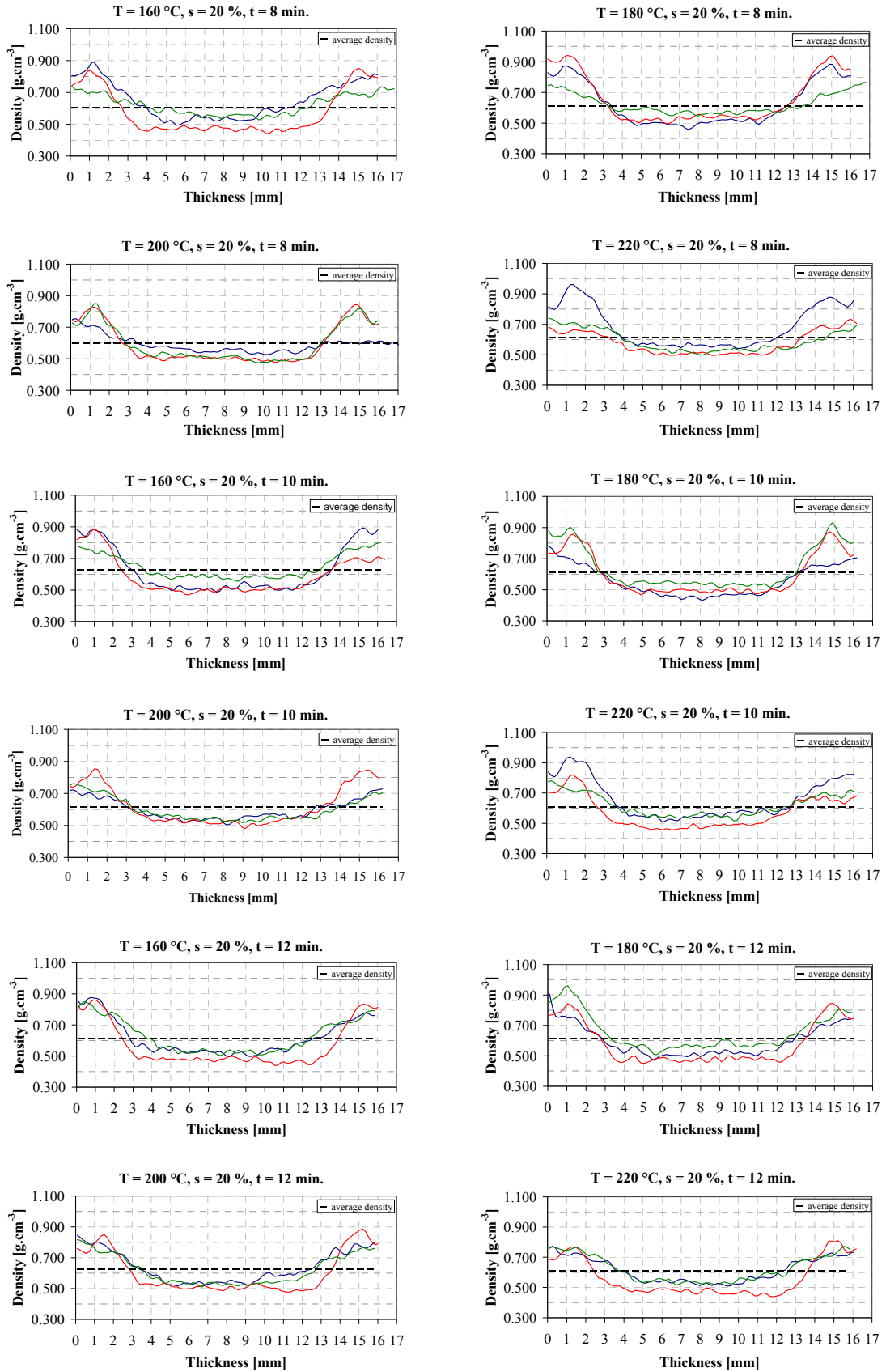


Fig 4 Density profile in specimens in individual phases of experiment (compression 20 %).

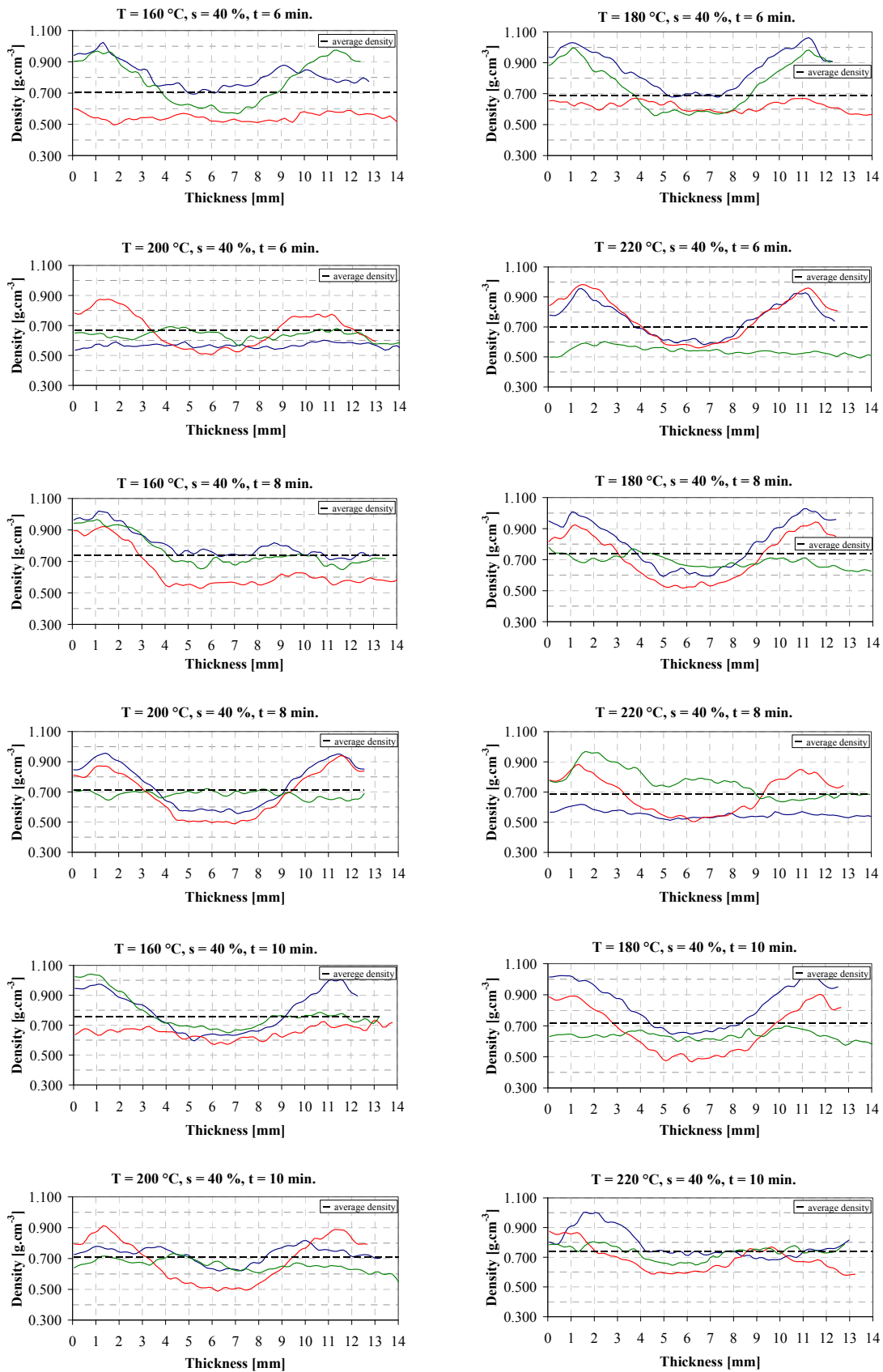


Fig. 5 Density profile in specimens in individual phases of experiment (compression 40 %).

COCLUSIONS

The experimental results have confirmed that the dimensional stability of the tested poplar specimens was significantly influenced by pressing time, and in case of shorter pressing periods, also by temperature. The best dimensional stability was obtained with the most prolonged pressing periods regardless the temperature ranging 160–220 °C. In case of shorter pressing periods, the dimensional stability increased with increasing temperature.

The results also confirmed non-uniform density distribution across the specimens along the pressing direction. The density profiles show evidence for the most intensive densification in the surface layers.

REFERENCES

- BAHÝL, V. 1992: Analyzátor hustotného profilu aglomerovaných materiálov. *Drevo*, 47(1):48–49.
- BÄCHLE, F., NIEMZ, P. & SCHNEIDER, T. 2007: Physical-mechanical properties of hard- and softwood heat treated in an Autoclave. In: European Conference on Wood Modification 2007. Bangor, UK, BC, pp. 177–182.
- BLOMBERG, J., 2006: Mechanical and Physical Properties of Semi-Isostatically Densified Wood. Skellefteå, Luleå University of Technology, Division of Wood Science and Technology, 28: 62 pp.
- BLOMBERG, J., PERSSON, B. & BEXELL, U. 2006: Effects of semi-isostatic densification on anatomy and cell shape recovery on soaking. *Holzforschung*, 60:322–331.
- CLAIR, B., ARINERO, R., LÉVÊQUE, G., RAMONDA, M. & THIBAUT, B. 2003: Imaging the mechanical properties of wood cell wall layers by atomic force modulation microscopy. *IAWA Journal*, 24(3): 223–230.
- DWIANTO, W., MOROOKA, T., NORIMOTO, M. & KITAJIMA, T., 1999: Stress relaxation of sugi (*Cryptomeria japonica*, D. Don) wood in radial compression under high temperature steam. *Holzforschung*, 53: 541–546.
- ESTEVEZ, B. M. & PEREIRA, H. M. 2009: Wood modification by heat treatment. *BioResources*, 4(3): 370–404.
- HIGASHIHARA, T., MOROOKA, T. & NORIMOTO, M. 2000: Permanent fixation of transversally compressed wood by steaming and its mechanism. *J. Jap. Wood Res. Soc.*, 46(4): 291–297.
- CHUCHRĽANSKIĽ, P. N. 1953: Lisovanie dreva. Bratislava, Práca, 156 pp.
- INOUE, M., KODAMA, J., YAMAMOTO, Y. & NORIMOTO, M. 1998: Dimensional stabilization of compressed wood using high-frequency heating. *J. Jap. Wood Res. Soc.*, 44(6): 410–416.
- IRVINE, G. M. 1984: The significance of the glass transition of lignin and hemicelluloses and their measurement by differential thermal analysis. *Tappi J.*, 67(5): 118–121.
- ITO, Y., TANAHASHI, M., SHIGEMATSU, M., SHINODA, Y. & OHTA, CH. 1998a: Compressive-moulding of wood high-pressure steam-treatment. Part 1. Development of compressively moulded squares from thinnings. *Holzforschung*, 52(2): 211–216.
- ITO, Y., TANAHASHI, M., SHIGEMATSU, M. & SHINODA, Y. 1998b: Compressive-moulding of wood high-pressure steam-treatment. Part 2. Mechanism of permanent fixation. *Holzforschung*, 52(2): 217–221.
- JOHANSSON, D., PERSSON, M. & MORÉN, T. 2006. Effect of heat treatment on capillary water absorption of heat-treated pine, spruce and birch. In: Wood Structure and Properties'06 (Eds.: Kurjatko *et al.*), Zvolen: Arbora Publishers, pp. 251–255.
- KAČÍKOVÁ, D. & KAČÍK, F. 2011: Chemické a mechanické zmeny dreva pri termickej úprave. Zvolen: TU vo Zvolene, 71 pp.
- KUBO, S., ISHIKAWA, N., URAKI, Y. & SANO, Y. 1997: Preparation of lignin fibers from softwood acetic acid lignin. Relationship between fusibility and the chemical structure of lignin. *Mokuzai Gakkaishi*, 43(8): 655–662.
- KÚDELA, J. 1992. Štúdium vplyvu teploty na vlastnosti dreva. In: Wood burning '92. Zvolen, Technická univerzita vo Zvolene, pp. 201–222.
- KÚDELA, J. 2005: Vlhkostné a tepelné namáhanie bukového dreva. Zvolen, Technická univerzita vo Zvolene, 141 pp.
- KÚDELA, J. 2010: Mechanické vlastnosti dreva. In: Parametre kvality dreva určujúce jeho finálne použitie. Zvolen, Technická univerzita vo Zvolene, pp. 101–127.
- KÚDELA, J. & REŠETKA, M., 2012: Influence of pressing parameters on dimensional stability and selected properties of pressed beech wood. I. Dimensional stability and density. *Acta Facultatis Xylogologiae*, 54(1): 15–24.
- KÚDELA, J. & REŠETKA, M. 2012: Influence of pressing parameters on dimensional stability and selected properties of pressed beech wood. II. Density profiles and hardness. *Acta Facultatis Xylogologiae* (in print).
- LINDSTRÖM, T., TOLONEN, J. & KOLSETH, P. 1987: Swelling and mechanical properties of cellulose hydrogels. Part VI. Dynamic mechanical properties. *Holzforschung*, 41(4): 225–230.
- NAVI, P., GIRARDET, F. 2000. Effect of thermo-hydro-mechanical treatment on the structure and properties of wood. *Holzforschung*. 54(3): 287–293.
- OLSON, A. M. & SALMÉN, L. 1997: Humidity and temperature affecting hemicellulose softening of wood. In: Mechanical Performance of Wood and Wood Products. Wood Water Relations. Copenhagen, COST Action E8, pp. 267–279.
- PALKO, M., ZEMĽAR, J. & VACEK, V. 2012: Vplyv lisovacích parametrov na zmenu tvrdosti lisovaných dýh. *Acta Facultatis Xylogologiae*, 54(1): 55–62.
- REINPRECHT, L. & VIDHOLDOVÁ, Z. 2011: Termodrevo. OSTRAVA, ŠMÍRA-PRINT, s.r.o., 89 pp.
- REŠETKA, M. 2012: Zmeny v dreve v procese lisovania za rôznych teplotných a vlhkostných podmienok. [Diz. práca]. Drevárska fakulta. Technická univerzita vo Zvolene. 120 s.
- SEBORG, R. M., MILLETT, M. A. & STAMM, A. J. 1962: Heat-stabilized compressed wood. FPL, Report No. 1580, p. 22.
- SOLÁR, R. 1997: Zmeny lignínu v procesoch hydrotermickej úpravy. Zvolen, Technická univerzita vo Zvolene, 57 pp.
- STAMM, A. J. & SEBORG, R. M. 1941: Resin treated, laminated, compressed wood. *Trans. Am. Inst. Chem. Eng.*, 37: 385–397.
- WANG, J. Y. & COOPER, P. A. 2005: Effect of grain orientation and surface wetting on vertical density profiles of thermally compressed fir and spruce. *Holz Roh- u. Werkstoff*, 63: 397–402.
- WOODWARD, C. 1980: Fractured surfaces as indicators of cell wall behavior at elevated temperatures. *Wood Sci.*, 13(2): 83–96.

Acknowledgement

This contribution /publication is the result of the project implementation: Extension of the Centre of Excellence „Adaptive Forest Ecosystems“, ITMS: 26220120049, supported by the Research & Development Operational Programme funded by the ERDF.

NANO-ZINK AS AN AGENT AGAINST WOOD DESTROYING FUNGI

RÓBERT NÉMETH¹, MIKLÓS BAK¹, BOB MBOUYEM YIMMOU¹, KÁROLY CSUPOR¹,
SÁNDOR MOLNÁR¹ & LEVENTE CSÓKA²

¹Institute of Wood Science, University of West Hungary, Sopron, Hungary, nemethr@fmk.nyme.hu

²Institute of Wood and Paper Technology, University of West Hungary, Sopron, Hungary

Abstract

Nanotechnology presents a tremendous opportunity to boost the field of wood preservation through implementing modern and unique metal biocides with improved properties. This study evaluated resistance of spruce, beech, poplar and pine wood treated with 0.220 and 0.055 % (m/m) zinc nanoparticles against *Poria placenta* a brown rot fungus a zinc tolerant organism. Results showed that nano-zinc inhibited brown rot in the case of spruce, beech and poplar. Retention was proportionate with the preservative concentration and higher for softwoods compared to hardwoods. Although softwood specimens demonstrated a better retention than hardwood specimens, nano-zinc solution achieved a positive reduction in percentage mass loss for both groups (spruce, or poplar and beech). In this study, nano-zinc concentration was quite low, related to previous studies where up to 5 % (m/m) nanoparticles concentrations were used for decay tests, demonstrating a satisfactory performance. Overall, zinc nanoparticles possessed favorable properties for wood protection against fungal decay from *Poria placenta*. Furthermore zinc nanoparticles showed good performance both for softwoods and hardwoods.

Key words: wood preservation, durability, biodegradation, nano-zinc, *Poria placenta*.

INTRODUCTION

Utilizing nanomaterials to create a new generation of novel cost-effective products is a key issue identified by the U.S. forest products industry (TAPPI 2005). Nanopreparations of metals, such as zinc, may possess unique characteristics that are totally different from the characteristics of the elemental metal.

A further study, that evaluated silver formulations in combination with copper or zinc nano-metals against termites, showed inhibition of termite feeding by zinc nanoparticles with and without silver (GREEN & ARANGO 2007). The potential activity of nano-copper particles for wood protection was investigated by WEITZ *et al.* (2011) using mini-agar slant and wood block tests with *Gloeophyllum trabeum* or *Trametes versicolor*. They reported that nano-copper has potential as a wood protectant, but much more research will be required to understand the properties of this material. Applying nano-silver treatment before densification can result in optimal physical and mechanical properties of densified poplar wood (*Populus alba*) (RASSAM *et al.* 2011). Over 20 field stake trials were carried out in well-known sites such as Gainesville, Florida, Hilo, Hawaii and the Dorman and Saucier sites in Mississippi as well as tests from Australia and New Zealand. In addition, 4 ground proximity tests from Hawaii and 3 ground proximity tests from Mississippi were conducted. Micronized formulations of copper showed good performances in all field trials with standardized tests. In some tests

they performed better than the amine soluble counterparts which were used as a control (MCINTYRE & FREEMAN 2011).

Provided that nanoparticles of copper, boron and zinc show original properties they may play an important role for developing new wood protection systems. In preliminary studies on nanometal preparations, nano-zinc oxide demonstrated some unique characteristics deemed worthy of further study. The objective of this study was to evaluate the preparation of 20 to 40 nm zinc nanoparticles for the capacity to prevent decay by a brown rot fungus (*Poria placenta*) which is Zinc tolerant.

Applications of zinc nanocrystals act as an antimicrobial, anti-biotic and anti-fungal (fungicide) agent when incorporated in coatings, bandages, nanofiber, nanowire, plastics, alloy and textiles and further research is being done for their potential electrical, dielectric, magnetic, optical, imaging, catalytic, biomedical and bioscience properties.

MATERIAL AND METHODS

Test materials and apparatus

The test fungus for this study was *Poria placenta*. The culture medium was a malt agar medium. The medium was prepared by warming the mixture in a boiling water bath, stirring until completely dissolved. A sufficient quantity of the medium was placed in each culture to provide a minimum depth of 3 mm to

4 mm when in-use. The vessels were closed and sterilized in an autoclave at 121 °C for 20 minutes, then they were cooled in their in-use position.

The species of softwood used were: spruce (*Picea abies*) and pine sapwood (*Pinus sylvestris*). The species of hardwood used were: poplar (*Populus×euramericana* cv. Pannonia) and beech (*Fagus sylvatica*). They were susceptible of attack by fungi and have been thoroughly soaked by the preservative solution. The dimensions of each specimen, measured at 12 % (m/m) moisture content, were 40 × 15 × 7 mm (L × T × R). The specimens were divided into:

Treated test specimens: These soaked specimens were subjected to attack by the wood destroying fungi. Eight treated test specimens were used for each preservative concentration, for each timber species.

Untreated test specimens: Four non-soaked test specimens of the same wood species as the treated test specimens. They were placed in culture vessels containing the same wood destroying fungus as for the treated test specimens.

Nano-zinc solution was used as test preservative. The preservative sample was representative of the product to be tested. A nano-zinc solution was prepared from zinc acetate, NaOH and alginic acid from brown algae. Zinc nanoparticles had a size distribution between 20 and 40 nm. The nano-zinc solution was divided in two equal volumes. One of them was diluted to one quarter using distilled water. This process provided two nano-zinc concentrations: 3.4×10^{-2} M (0.22% m/m) for the higher concentration (1:1, non diluted), 8.5×10^{-3} M (0.055%) for the lower concentration (1:4, diluted).

Soaking was carried out in descending order of concentration, starting with the pure nano-zinc solution (1:1, concentration = 3.4×10^{-2} M, 0.22% m/m) and ending with the diluted nano-zinc solution (1:4, concentration = 8.5×10^{-3} M, 0.055% m/m). For each concentration test specimens kept dry and of known mass (m_0) were soaked in the preservative sample for 1 minute and removed from the solution successively. Following this soaking treatment, the test specimens were immediately weighed to ascertain the mass after soaking. (m_1).

Two test specimens treated with the same concentration were placed in the same inoculated

culture vessel. One untreated test specimen was placed in the same inoculated culture vessel for a control. After introduction of the test specimens, the culture vessels were placed in the climate chamber at a constant temperature of 23 °C for 16 weeks.

Following incubation, the specimens were oven dried and reweighed (m_2). The percentage mass loss was calculated.

Governing equations

Chemical retention was calculated using the following equation:

$$R = \frac{m_1 - m_0}{V} \quad (1)$$

R: Amount of chemical retention of nano-zinc for wood specimens [kg/m³]

m_1 : Weight of sample after soaking [g]

m_0 : Weight of sample before soaking [g]

When considering wood preservation through soaking with the nano-zinc solution, percentage weight losses were evaluated using the following equation:

$$PWL = \frac{m_0 - m_2}{m_0} \times 100 \quad (2)$$

PWL: Percentage weight loss after 16 weeks incubation [%]

m_2 : Weight of sample after 16 weeks incubation [g]

m_0 : Weight of sample before soaking [g]

RESULTS AND DISCUSSION

Chemical retention

The amounts of chemical retention for tested specimens are shown in Table 1. There were notable differences in chemical retention based on wood species as well as on nano-zinc concentration. The retention was increasing quite proportionately with the preservative concentration as the mean ratio of nano-zinc retention between 0.220 and 0.055% is 4.29. This result complied with the ratio of nano-zinc concentrations used during our experiments 0.220/0.055= 4. It showed that the decay specimens effectively absorbed the nano-zinc solution.

Table 1 Average retention level with their ratio.

Treatment group	Average retention level (kg/m ³)		
	Nano-zinc concentration		Ratio of retention between high (0.22%) and low concentration (0.055%)
	High concentration 0.220% (m/m)	Low concentration 0.055% (m/m)	
Pine	0.284	0.067	4.19
Spruce	0.276	0.057	4.79
Beech	0.177	0.043	4.09
Poplar	0.175	0.042	4.10

Table 2 Percentage mass loss about the decay specimens and their ratio.

Treatment group	Percentage mass loss					
	Nano-zinc concentration		Ratio of percentage mass loss			
	High concentration 0.220% (m/m)	Low concentration 0.055% (m/m)	Control	C2:C1	Control:C1	Control:C2
pine	2.48	3.27	3.05	1.32	1.23	0.93
spruce	3.26	4.62	38.49	1.41	11.80	8.33
beech	13.10	14.93	23.01	1.14	1.75	1.54
poplar	12.35	8.91	22.55	0.72	1.82	2.53

Still the retention levels (0.037–0.309 kg/m³) were very low as compared with the decay test carried out by KARTAL *et al.* (2009) on Southern yellow pine, during which the average retention level expressed as metal oxide of nano-zinc varied from 4.61 to 6.39 kg/m³, (1% m/m concentration). Equally (CLAUSEN *et al.* 2010) nano-zinc impregnated Southern pine at 1.60 kg/m³ retention level (1% m/m concentration), displayed leach resistance in laboratory tests and following outdoor exposure for 12 months.

Decay results

Table 2 shows the mean percentage mass loss of the specimen test at higher (0.220%, m/m), lower (0.055%, m/m) nano-zinc concentration and at control. There were prominent differences in percentage mass loss based on wood species and on preservative retention.

For example at nano-zinc concentration of 0.220% (m/m) pine, spruce, beech and poplar test specimens showed 2.48, 3.26, 13.1 and 12.35% of percentage mass loss respectively. Then at nano-zinc concentration of 0.055% (m/m) pine, spruce, beech and poplar test specimens showed 3.27, 4.62, 14.93 and 8.91% of percentage mass loss respectively. All the specimens except poplar showed a decreasing decay as a result of increasing nano-zinc concentration. Only pine and spruce specimens exhibited a percentage mass loss lower than 5% for both preservative concentrations.

In the case of control samples, pine specimens were discarded due to an unacceptable percentage mass loss of 3.05% meaning an ineffective virulence from the fungi culture during our decay test of pine wood. In this case, ineffective virulence was caused by a strong mould growth on the surface of the control specimens. The other specimen test exhibited more than 20% mass loss for control test.

Tests of pine specimens showed a decrease in % mass loss with an increase in nano-zinc concentration, but it was discarded due to the poor culture virulence observed during the control test. There were discrepancies in the decay test of poplar as the lower preservative concentration was more effective than the higher one. There was a decrease in % mass loss associated with an increase in the nano-zinc concentration for spruce and beech specimen tests.

Beech and spruce samples demonstrated good preservative performance as the preservative effect was balanced with increasing the nano-zinc concentration. Therefore the higher nano-zinc concentration solution was more effective than the lower one and even much more effective than the control with a ratio 1:1.75 and 1:11.8 respectively for beech and spruce samples.

Contrarily to some previous studies (KARTAL *et al.* 2009), our results indicate that nano-zinc formulation of zinc metal may inhibit degradation of wood by brown rot fungi even at very low concentrations. During those studies, nano-zinc had already demonstrated unexpected and unique properties such as low leachability, increased termite mortality, inhibition of termite feeding and degradation by white-rot fungi. If their size is smaller than the diameter of pores in the bordered pits or in the wood cells, complete penetration and uniform distribution in wood can be expected (AKHTARI & AREFKHANI 2010). However, in solid wood (with a small amount of trace elements Mn, Fe, Co, Ni, Cu, Zn, Mo, Pb, etc), which have physiological influences on the mycelium growth of fungi, the additional treatment of wood tissue with nano-particles of silver, copper, zinc, aluminium or other nanobiocides can be effective only if their concentration is under-threshold toxicity range (WAZNY & KUNDZEWICZ 2008).

Environmental concerns

Nano-zinc solution was produced at the University of West Hungary, at Sopron. Preservative preparation was carried out at the Laboratory of Wood Chemistry at the Institute of Wood and Paper Technologies on the seventh of March 2011. A nano-zinc solution was prepared from zinc acetate, NaOH and alginic acid from brown algae. Thus the nanoparticles were produced in a so called green process in line with the sustainable philosophy.

According to the work of MÖLLER *et al.* (2012) the scientifically sound investigations of nanoparticles are lacking behind the product development activities of the industry. Several products containing nanoparticles are already available on the market, but the possibility of ecotoxicity could not be precluded yet. The widely used nano-silver for instance is still considered as a potential hazardous material against useful bacteria in the nature. Concerning the zinc nanoparticles no clear evidence could be found in the

literature; however zinc oxide has to be considered to be a relevant ecotoxic material as it is harmful against water-flea (MÖLLER *et al* 2012).

The leachability and efficacy of southern yellow pine treated with copper, zinc or boron nanoparticles against mould fungi, decay fungi and Eastern subterranean termites was studied by KARTAL *et al.* 2009. Results showed that nano-copper with and without surfactant, nano-zinc, and nano-zinc plus silver with surfactant resisted leaching compared with metal oxide controls. Nearly all nano-boron and boric acid was released from the treated wood specimens during leaching.

Since a predicted wide spread use of engineered nanoparticles in consumer products will lead to an inevitable increase in exposure rates in occupational, public and environments, it is crucial that the possible risks to human health and the environment be identified and mediated (MCCRANK 2009). Thus it is important to undertake relevant research on the toxicity and effects of nanoparticles in general.

CONCLUSIONS

The nanoform of zinc (20–40 nm) was evaluated for resistance against fungal decay from *Poria placenta* for spruce, beech, poplar and pine wood specimens. Treatment with nano-zinc showed favourable decay resistance especially in spruce and beech with a significant reduction in mass loss (0.66–6.60 %) and (7.16–18.25 %) as compared to (31.92–45.05 %) and (13.15–32.97 %) for untreated controls.

The effectiveness of the treatment was proportionate with the preservative concentration (0.055–0.220 %, m/m).

Though there was a minimum percentage mass loss of 1.12 % could be obtained from a poplar decay specimen, there were several discrepancies within the data which showed a very large normal distribution between 1.12 and 21.66 % mass loss for the treated decay specimens. Furthermore lower nano-zinc concentration (0.055 %, m/m) was more effective than the higher one (0.220 % m/m) with mean percentage mass losses of 8.91 and 12.35 %.

Owing to an ineffective virulence of the fungi culture towards pine decay specimens, with a mean percentage mass loss of 3.05 % for control specimens, no reliable comparison resulted from the decay test. The mean percentage mass loss of the treated specimens was 2.48 and 3.27 % for higher and lower nano-zinc concentrations, still in the same range with the control specimens. This test should be repeated for accurate data analysis.

Although softwoods decay specimens demonstrated a better retention than hardwoods specimens, nano-zinc solution achieved a positive reduction in percentage mass loss for both groups of spruce and beech. In this study, nano-zinc concentration was quite low (0.055–0.220 %, m/m),

related to previous studies where up to 5 % (m/m) nanoparticles concentrations were used for decay tests, demonstrating a satisfactory performance.

Therefore higher nano-zinc solution concentrations may exhibit unpredictable and promising properties against fungal decay. Still there is some indication that nano-zinc treated beech, poplar and pine specimens may not have been quite as effective as treated spruce specimen under the same conditions, and these differences may need further exploration.

The intrinsic properties of pit membranes arise at a scale of tens of nanometers, yet their effects on hydraulics are mediated by every level of vascular organization in the plant (CHOAT *et al.* 2008). The microdistribution and leachability of nano-zinc particles during the treatment needs to be investigated for a better understanding of the factors affecting its effectiveness. Because of their small size nanoparticles have many physicochemical properties that differ from those of their bulk forms (e.g., quantum confinement, surface plasmon resonance, and superparamagnetism effects). Not all of these properties are necessarily beneficial.

The authors recommend performing further investigations regarding the recycling possibilities and the release of particles during combustion.

REFERENCES

- AKHTARI, M. & AREFKHANI, M. 2010: Application of nanotechnology in wood preservation. International Research Group on Wood Protection, IRG/WP 10-30542.
- CHOAT, B.; COBB, A.R. & JANSEN, S. 2008: Structure and function of bordered pits: new discoveries and impacts on whole-plant hydraulic function. *New Phytologist* 177 (5): 608–626.
- CLAUSEN, C.A. 2010: Characterizing Wood Protection Properties of Nano-Metals. USDA Forest Service, Forest Products Laboratory, Madison, Wisconsin, Research In Progress RIP-4723-014.
- GREEN, F. & ARANGO, R.A. 2007: Wood protection by commercial silver formulations against Eastern subterranean termites. International Research Group on Wood Protection. IRG/WP/ 07-30422.
- KARTAL, S.N.; GREEN, F.III. & CLAUSEN, C.A. 2009: Do the unique properties of nanometals affect leachability or efficacy against fungi and termites? *International Biodeterioration & Biodegradation* 63 (4): 490–495.
- MÖLLER, M., R. GROB, K. MOCH, S. PRAKASH, CH. PISTNER, P. KÜPPERS, A. SPIETH-ACHTNICH & A. HERMANN 2012: Analyse und strategisches Management der Nachhaltigkeitspotenziale von Nanoprodukten – NachhaltigkeitsCheck von Nanoprodukten. Texte Nr. 15/2012. 2012 Umweltbundesamt.
- MCCRANK, J. 2009: Nanotechnology applications in the forest sector. Natural Resources Canada.
- MCINTYRE, C.R. & FREEMANN, M.H. 2011: Standardized field trials with micronized copper. IRG/WP 11-30564.
- RASSAM, G.; REZA, H.; TAGHIYARI JAMNANI, B. & KHAJEH, A.M. 2011: Effect of Nano-silver treatment on densified poplar wood properties. Part Two: Spring back,

compression set, impact load resistance and hardness. IRG/WP 11-40568.

TAPPI (Technical Association of Pulp and Paper Association Industry) 2005: Nanotechnology for the forest products industry: vision and technology roadmap. Report of the Nanotechnology for the Forest Products Industry Workshop, Lansdowne, VA., October 17–19, 2004. TAPPI Press, Atlanta, GA, USA, 102 p.

WAŻNY, J. & KUNDZEWICZ, A. 2008: Conditions and possibility of nanobiocides formulation for wood protection. International Research Group on Wood Protection, IRG/WP 08-30467.

WEITZ, I.S.; KNANI, K.; MAOZ, M.; FREITAG, C. & MORRELL, J.J. 2011: The potential for using CuO nanoparticles as a wood preservative. IRG/WP 11-30569.

Acknowledgement

This research – as part of the project TAMOP 4.2.1/b-09/1/KONV-2010-0006 – was sponsored by the EU/European Social Foundation. The financial support is gratefully acknowledged.

ENVIRONMENTAL LIMITS TO SUSTAINABLE YIELDS OF WOOD FOR MATERIALS AND ENERGY

JANIS ABOLINS & JANIS GRAVITIS

Latvian State Institute of Wood Chemistry, Riga, Dzērbenes iela 27, LV – 1006, Latvia, jgravit@edi.lv

Abstract

In the proposed paper, sustainability is defined as availability of permanent long-term yields of wood biomass. A simple analytical model of biomass accumulation is used to consider the basic factors limiting sustainable flows of biomass as a renewable resource for bio-refineries and bio-energy from forestry without compromising the ecological services and the capacity of biosphere. Attention is paid to estimating the “footprint” of employing the biomass – a product of photosynthesis, for economic needs of humans. The analytical expressions describing time-dependent relations between the amount of harvested biomass and land area necessary to provide sustainable yields are presented in units of normalised scales of time and stock related to the age of the stand at the maximum of current annual biomass increment.

Key words: wood biomass, sustainable yields, bio-energy.

INTRODUCTION

Approaching the limits allowed for consumption by the reserves of non-renewable resources requires reconsidering conditions under which the essential necessities of humans and the global economy can be satisfied by sustainable use of the renewable resources. Products of photo-synthesis, particularly wood along with other ligno-cellulosic biomass regarded as a universal renewable source of chemicals and fuels, are expected to sustain the needs of the existing economic system when oil and gas are used up. Compared to other species of floras the ecological role of tree populations is more substantial for biodiversity and stability of the biosphere. At the same time the global forest presents a permanent source of valuable raw materials for diverse products under condition of rational and sustainable harvesting practices. Above and beyond, wood buildings and construction articles of wood render a healthy space for living and is a kind of storage of recyclable carbon dioxide.

Accumulation of biomass expressed in terms of the rate of growth representing efficiency of photosynthesis distinctive to particular species is one of a number of key factors, along with presence of nutrients, the flow of solar energy (insolation), and land territory, limiting availability of the renewable resource for sustainable annually harvested yields. The energy flow being limited for given geographical latitude, nutrients and water can be supplied, to reasonable extent, by human activity while the territory – a limited natural asset has to be partitioned compromising the different vital needs of humans and other beings comprising the biosphere. To avoid exceeding the limits in a finite world it is necessary to

be aware of the limits to growth (MEADOWS *et al.* 1972, MEADOWS *et al.* 1992) and the limits beyond which the use of a renewable resource makes it non-renewable.

Being a product of photosynthesis fuelled by the energy of solar radiation, the biomass presents storage of primary energy and carbon dioxide released at burning. As a source of renewable energy the biomass can be regarded as a result of energy transformation and the energy content of biomass compared with results of other transformers. The physical processes comprising photosynthesis are similar to the elementary actions in photoelectric transformers. Efficiency of energy transformation of the latter being by order of magnitude higher, photosynthesis has the advantage of the transformed energy being simultaneously accumulated in biomass while the final result, apart from the available radiation, strongly depends on accessibility of water and nutrients.

Using biomass as the source of primary energy to generate electricity is not reasonable because of a rather low transformation efficiency of presently available technologies. Advancement of thermoelectric energy transformers might encourage cogeneration by burning biomass under condition of priority to heat generation. Assessment of sustainable yields of wood biomass from forest plantations presenting a number of equal-size stands of sequential ages up to the felling age is presented hereafter.

THE BASIC CONCEPTS

The generalised relations for current annual increment (growth rate) and stock of a forest stand:

Wood the Best Material for Mankind

J. Kúdela & M. Babiak (eds.), 2013, pp. 65–68

© Arbora Publishers, Zvolen, Slovakia

ISBN 978-80-968868-6-9

$$\frac{dS}{dx} = 4 \cdot (1 - e^{-ax}) \cdot e^{-ax} \quad (1)$$

$$S(x) = S_{\infty} (1 - e^{-ax})^2 \quad (2)$$

where $a = \ln 2$, obtained in an earlier study (ABOLINS & GRAVITIS 2011) are further employed to derive general expressions for sustainable yields optimised with respect to most efficient land-use.

The normalised current annual increment dS/dx (Eq. 1) and stock S (Eq. 2) as functions of time x normalised with respect to the time at which the maximum growth-rate is reached are shown in Fig. 1 (curve 1 and curve 2, respectively) along with the mean annual increment:

$$\frac{\overline{dS}}{dx} = \frac{S(x)}{x} \quad (3)$$

As shown in the previous study (ABOLINS & GRAVITIS 2011), the value of stock (normalised with respect to maximum value S_{∞} at infinity) at time $x = 1$ when the growth-rate reaches maximum is equal to $S|_{x=1} = 0.25$ and to $S|_{x \approx 1.81} \approx 0.5$ at the time when the maximum of the mean annual increment is reached (Fig. 1, curve 3).

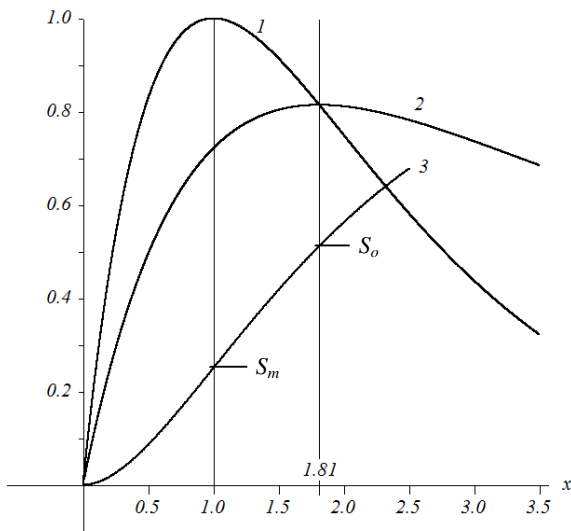


Fig. 1 Rate of growth (current annual increment), Eq. 1 (curve 1), mean annual increment, Eq. 3 (curve 2), and stock, Eq. 2 (curve 3) as functions of normalised time x . The increments are presented in units of the maximum growth-rate, stock – in units of S_{∞} .

Felling the stand at the time of the maximum of mean annual increment provides the maximum yield per unit area of the forest land. Equation (3) shows the maximum productivity of the total land area of equally sized subdivisions occupied by stands of all ages up to the felling age if x is assumed to be the number of subdivisions of the total land area under forest (ABOLINS & GRAVITIS). The limits for

sustainable yields are determined by the maximum of the mean annual increment. The latter depends on a number of factors including the biological potential of the particular species, fertility of the site, climate, etc. the cumulative effect of which is exposed through the time necessary to reach the growth-rate maximum. B. Zeide is likely the first having suggested using the age at the maximum growth-rate as the intrinsic time unit of the particular stand (ZEIDE 2004). Normalising time with respect to the growth-rate maximum provides a convenient generalised time-scale for analysis of biomass accumulation and the limits of sustainable yields.

METHODS

The maximum (limiting) yield (Eq. 3) of wood biomass expressed in generalised units under condition of sustainable harvesting at maximum land productivity is given by

$$Y(x) = \frac{S(x)}{x} = \frac{(1 - e^{-x \ln 2})^2}{x} \quad (4)$$

providing $Y(x)|_{x=1.81} \cong 0.2823$ in the scale where $S_{\infty} = 1$ (ABOLINS & GRAVITIS 2011). Since the actual value of S_{∞} is not known another unit has to be defined as the measure of stock. The stock at unit time $x = 1$ equal to $0.25S_{\infty}$ is a reasonable choice for the purpose. In the scale of the new stock units equation (2) is substituted by

$$S(x) = 4(1 - e^{-ax})^2 \quad (5)$$

The limit of sustainable annual yields is about twice the amount of stock at the age of growth-rate maximum: $Y(x)|_{x=1.81} \cong 2.0438 Y(x)|_{x=1} \cong Y_o$. In the real time scale $t = t_m x$ sustainable yield is a function of the productivity (S_m) and the age (t_m) at growth-rate maximum:

$$Y(t_o) = \frac{S(t_o)}{t_o} \cong \frac{S(t_o)}{1.81 \cdot t_m} \cong \frac{2.0438 \cdot S_m}{1.81 \cdot t_m} \cong 1.129 \frac{S_m}{t_m} \quad (6)$$

where $t_o = 1.81 t_m$ is the optimum harvesting age providing maximum sustainable yield per unit area of the plantation comprising stands of sequential ages up to the felling age, t_m and S_m – the age and stock at growth-rate maximum, respectively.

RESULTS AND DISCUSSION

Results are presented in Fig. 2 and Fig. 3. The maximum sustainable yield $Y_o = Y(t_o)$ as function of the age at which a particular stand reaches the maximum growth-rate is shown (Fig. 2) in units of the stock $S_o \cong 2.04 S_m$ (Eq. 6) at optimum felling age $t_o = 1.81 t_m$.

The curve explains the advantage of fast-growing species with respect to land-use efficiency allowing

for maximum sustainable yields at shorter rotations. The actual values of the stock unit S_o are of different magnitude depending on species and site quality. Nevertheless, only the ones having the ages at maximum growth-rate close to each other are of significance at choosing between species grown to supply biomass for general purpose.

In Fig. 3 the mean annual increment is shown as a function of normalised (intrinsic) age of any particular stand: curve 1 presents the relative value of the mean annual increment in units of the maximum current annual increment reached at $x = 1$ (see Fig. 1, curve 1), curve 2 – in units of the maximum value of the mean annual increment itself reached at the normalised age $x = 1.8$. Presenting the mean annual increment in terms of the current annual increment maximum (Fig. 3, curve 1) allows ascribing to it an absolute value while presenting it in units of its own maximum (Fig. 3, curve 2) is useful to assess the productivity with respect to delayed or early felling. As seen from the shape of curve 2, the rise of productivity to maximum is faster compared to decline after the maximum, which means that delayed felling affects the productivity to a lesser extent and is less critical in the case of species growing slower.

The amount of sustainable annual yield Y_o of wood biomass from a limited land area of forest depends on the size of the plot A , rotation (felling age) t_o , and the stock S_o when felling at the age of the mean annual increment maximum:

$$Y_o = \frac{A}{t_o} S_o \quad (7)$$

In the real time scale $t_o = 1.8 t_m$ and Eq. 6 (with account of $S_o \cong 2S_m$) is transformed into:

$$Y_o = 1.129A \frac{S_m}{t_m} \quad (8)$$

Eq. 8 presents the maximum sustainable annual yield from plantation of total area equal to A obtained under condition of rotation being equal to the age at maximum of the mean annual increment. If the stand of the forest plantation plot A_o is harvested at a different age, Eq. 8 should be substituted by:

$$Y_o(x) = A_o f(x) = A_o \frac{S(x_c)}{x_c} \quad (9)$$

where x_c is the felling age or, in terms of the maximum annual increment S_m , by:

$$Y_o(x_c) \cong 4 \frac{S_m}{t_m} \cdot \frac{(1 - e^{-x_c \ln 2})^2}{x_c} \quad (10)$$

Function $f(x)$ is the function describing the mean annual increment presented by curve 2 in Fig. 3. The normalised values of stock S_m and S_o are represented by cross-points of curve 3 with lines $x = 1$ and $x = 1.81$, respectively (Fig. 1).

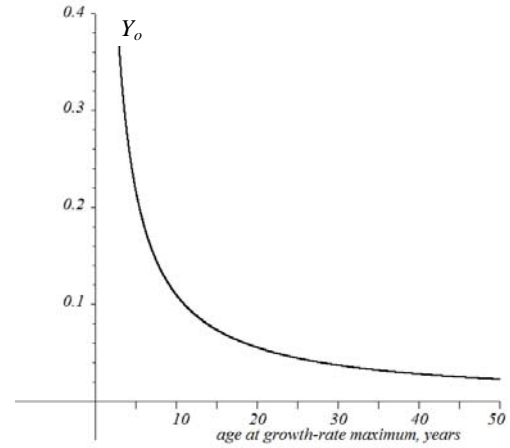


Fig. 2 Maximum yield per unit area of the plantation Y_o , Eq. 6, in units of stock at the age of maximum growth-rate as a function of the age at growth-rate maximum t_m .

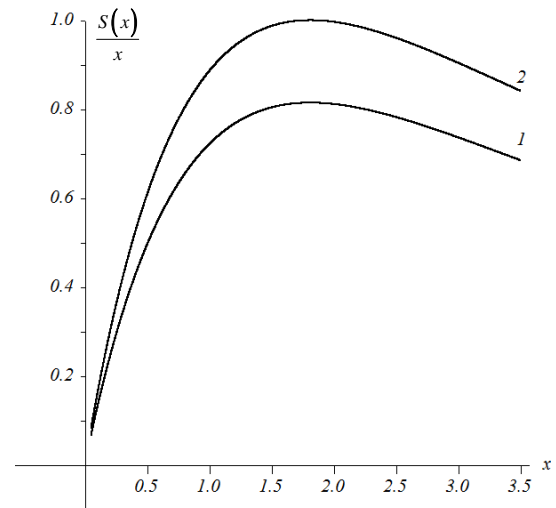


Fig. 3 Mean annual increment as function of normalised age: 1 – in units of maximum current annual increment S_m , 2 – in units of maximum mean annual increment.

CONCLUSIONS

The general patterns of biomass accumulation by natural forest stands derived on the basis of the analytical model of the rate of growth represented by Eq. 1 allow being easily characterised in terms of normalised units providing grounds for diagnostic calculations applicable to a wide range of biological species and factors limiting expectations. The normalised (intrinsic) time scale and normalised scale of the rate of biomass accumulation (the rate of growth) are essential elements of the model expanding its application.

Two empirical quantities specific to a particular stand from field measurements are required to calculate any other quantity of interest one of them being either the age or the stock at maximum growth-rate (see Eq. 10).

The highest (limiting) sustainable yields are obtained from plantations comprising equal-size stands of sequential ages when being harvested at the age of mean annual increment maximum providing the highest yield per unit forest-land area (Eqs. 7–10; Fig. 3, curve 2).

The total forest area and the age of growth-rate maximum are the ultimate factors limiting yields of general purpose wood biomass for chemicals and energy.

REFERENCES

ABOLINS J. & GRAVITIS J. 2011: A Simple Analytical Model for Remote Assessment of the Dynamics of Biomass Accumulation. In: Progress in Biomass and Bioenergy Production, Dr. Shahid Shaukat (Ed.), InTech, 91–106.

Available from:

<http://www.intechopen.com/books/progress-in-biomass-and-bioenergy-production/a-simple-analytical-model-for-remote-assessment-of-the-dynamics-of-biomass-accumulation>.

MEADOWS D. H., MEADOWS D. L., RANDERS J. & BEHRENS W. W. 1972: *The Limits to Growth*. Universe Books.

MEADOWS D. H., MEADOWS D. L. & RANDERS J. 1992: *Beyond the Limits*. Chelsea Green.

ZEIDE, B. 2004: Intrinsic units in growth modeling. *Ecological Modelling*, 175: 249–259.

Acknowledgements

The study has been supported by Latvian State Institute of Wood Chemistry (Research Project 08-12) and the National Research Programmes of renewable resources.

DEVELOPING OF A NEW PHOTO ANALYTICAL METHOD FOR MEASURING OF WOOD STACKS

ZOLTÁN PÁSZTORY, MÁRTON EDELÉNYI, JÁNOS BOROS & ZOLTÁN KÖVÁRI

University of West Hungary, Faculty of Wood Science, 4. Bajcsy Zs. Sopron Hungary 9400, pasztory@fmk.nyme.hu

Abstract

The wood assortment with smaller diameter is not measured one by one log, but in stack. The stacks could be very different depending from the diameter, the length, the site quality (the place where the timber have grown), the wood specie even the standards quality of the stacking work.

In the praxis, a fixed exchange rate between the stacked meter (stack loose volume) and the solid wood volume are used for decades. This rate has very range scatter because of the mentioned parameters.

Photo analytical method was developed and implemented for determining the individual exchange rate of each stack. According to the result of this developing project, the solid wood volume become measurable. The accuracy of the new photo analytical method is significantly higher than that of the traditional method.

Key words: stacked wood, exact loose volume of the stack, butt edge.

INTRODUCTION

In the Hungarian forestry praxis high amount of cutting wood is produced as stacked assortment especially in case of broad leaved wood species. The ratio of this stacked wood can be reach the 60–70 percent depending on the age of the stand class, the increment- selection thinning or final harvest and the quality of the soil the climate condition of territory and wood specie.

The stacked wood was used widely in the last decades such as raw material of particle board fiber board paper round firewood pit wood. Almost every stacked assortment had an own prescription related to the diameter shape and other parameters. According to these prescriptions the forest companies produced separately each assortment. The assortment had the evaluated exchange ratio between stacked volume and solid volume (MALTAMO *et al.* 2004, BARRET 1945, SCHNUR 1932).

The determination of this individual rate related to the given stack was investigated by (BARROS 2008, MACLEAN and MARTIN 1984, SMITH 1979, KEEPERS 1945). In that time the technology could not ensure the opportunity to work out an automatic high level solution.

In consequence of decreasing the producing costs of stacked wood the number of separated assortment was reduced to only one type of stacked wood. The consumers used the same type of stacked wood for fueling power plants and producing middle density fiber board or particle board and other products. There are consumptions that can tolerate the presence of bark on the stacked wood such the power plants contrasted with others which would have used the barked stacked wood like paper industry. In the letter

case the buyers do not pay for the bark and calculate the volume without bark. On the other hand the power plants can burn the fuel wood in the same way as the bark. Although the ash content of bark is considerable higher than the wood and the fuel value is lower related to the volume.

The mixing of different stacked wood assortments causes the uncertainty of exchange rate calculated earlier. In addition the quality and dimension of forest stands was changed in the last five decades also. These changes influenced rather detrimental the quality of wood and parallel the exchange rate.

Next to the mentioned influencing factors the informatics technology developed very fast in the last decades. There are high tech equipment's available on the market which can help to evaluate a newer wood stacks volume measuring method.

The remote sensing image technology is used for similar goals also (PEKKARINEN 2002, MÄKELÄ and PEKKARINEN 2001) for estimating wood quantity on the site.

It is true that the oven dry mass is widely used accounts, but the measurement of moisture content comprises failures.

The project aimed to develop a new and fast way of measuring solid cubic meter of stacked wood. To know the massive quantity are needed two important information: the exact loose volume of the stack and the exact exchange rate related to the current stack.

METHOD OF MEASURING SYSTEM

The wood assortment to be measured is given either on the field of forest or on the track during transportation. The developed system presented in this paper related to the measurement stacks on a track.

Wood the Best Material for Mankind

J. Kúdela & M. Babiak (eds.), 2013, pp. 69–72

© Arbora Publishers, Zvolen, Slovakia

ISBN 978-80-968868-6-9

Generally the end of the stack in the butt edge is plane in both case mentioned above. Since the butt edge is like a cross section of the stack it is presumable that wood surface ratio corresponding with the ratio of solid wood content in the whole volume. Principally the cross section ratio can change along the stack, but the measurements shows quite low differences in case of one meter long stacks. In case of fuel wood it is used longer stacks increasingly for the sake of reduce the production loading and unloading expenses. The longer stacks can be reached even the four meter length. In this length the surface ratio can be highly different between the two butt edges of the stack. However two third of stacked wood intended for industrial use is one meter long in Hungary.

On the basis of all these the determination of solid wood content is confined to determination of wood surface ratio. Presently it is practicable to take high resolution pictures of butt edge of the stack and the computer technique provides the effective image processing. As a first step it has to make a scale right image from the photo has taken the butt edge surface of the stack. The scale right photo means that the units on the picture are correct and same on the whole picture in other words the pixel sizes are known. The transformation can be made by base points which coordinate is known (Figure 1). Because the system was developed for measuring stacks on truck the measurement can be made repeatedly on a same site e.g. in a gate of the factory. For this reason the camera was fixed outside in an appointed place.

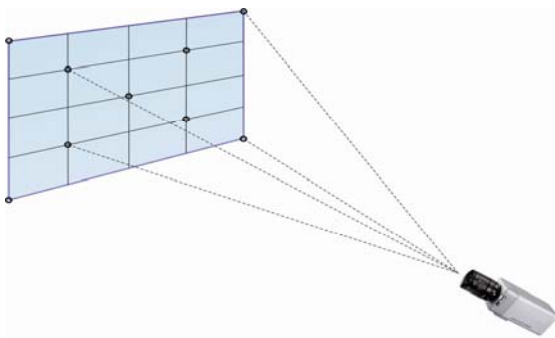


Fig. 1 Transformation of the pictures.

Tracks have to stop before the camera next to a designated line providing the same distance between the camera and the surface of the stack. After setting the base points on the transformation parameters they are saved to the computer in a configuration file. During the measurement it is not to be necessary to indicate the base points again it can be used the saved transformation parameters set before.

By the transformation process it is reduced the errors of the camera and the lens by means of precise base points.

The Usage of the Measuring System

Existing of this scale right image the second step is the image processing and analyzing the pixels on the right scale image. For achieving the best accuracy measurement results and most wide usefulness of the system it was plan more image analyzing techniques. Two main options are available for the user. The first analyzing group related to the colors of pixels what aims the classification of pixels according to the coordinate of color decide which ones belonging to the wood surface and which to the space between wood logs. Generally the butt surface is brighter than the parts between logs. We have developed a technology that can divide the pixels belonging to the butt surface from the pixels belonging to the holes. The pixel ratio belongs to the wood surface gives the correct exchange rate.

Automatic setting

The system contains an intelligent algorithm what is able to examine the color range of all pixel of the image and select automatically the pixels belong to the wood surface. This algorithm is very useful if the contrast is high between the wood surface color and the other parts of the pictures (Figure 2). The high contrast is achievable in case of fresh cut wood assortment and by good lighting conditions.

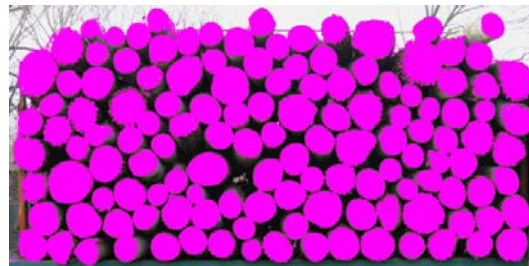


Fig. 2 Automatic classification of pixels.

Sampling

Other method is the sampling technique which gives the opportunity for the user to choose a pixel belong obviously to a wood surface by means of the cursor. The system analyzes the color coordinate of the pixel was chosen and search for the pixels on the image have a same coordinate within a set tolerant band. The tolerant band is adjustable in a wide range of color parameters. If the first sample does not select all the pixels belong the wood surface with the appropriate tolerant than the user can chose on other one sample pixel similarly to the first one. With this sampling technique can be a very accurate result but it need more time and attention.

Sampling group

This solution is similar to the “Sampling” technique but the chosen sample is not only one pixel but a pixel group. The selection of sample pixels is made with a selecting circle with adjustable diameter. The color

coordinates of the selected pixels is widen with the tolerance mentioned above and the pixels of image are classified. This technique is faster than the others but need also a good quality image.

Average measurement

In case of rectangular shape it can be measured the length and height of stacked block in more places. The single height dimensions are averaged likewise the width and the multiplication of these two numbers give the surface of the stack. The vertical lines mean the measurement point and values of height and horizontal lines mean the width of the stack (Figure 3). The lines are fixed distance from each other for the sake of fair measurement. To calculate the solid wood content need a given exchange rate. Many company has own exchange rate comes from the earlier standards or from the praxis.

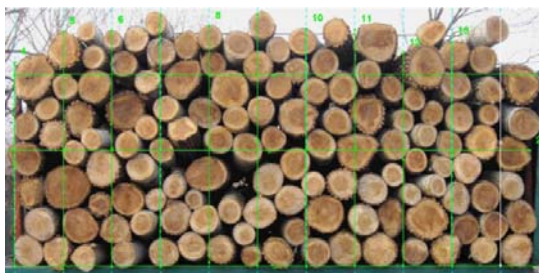


Fig. 3 Average measurement of the sizes of the stack.

Diameter measurement

The scale right image conceals the opportunity for measuring a linear distance on the pictures. It is very easy way for measuring the diameter of logs. By drawing the lines from the one side of the log surface to the opposite side the system calculate the length of lines and save them to a database (Figure 4). This database can be saved from the program e.g. in excel file format. This is a possible way for controlling the numbers of the logs and compare to the consignment. The processing proceeds with the data recording. The results coming from the image processing and the data related to the stacked unit. In case of track freight it can be recorded the data related to the transport gods such as name of contractor number plate and other data. The results and data are saved in a pdf form file and a data base form.

The saved data contain the original picture and the processed picture. By means of saved picture can be repeat the measuring process later in case of control or complaint.



Fig. 4 Measurement of diameters.

To the realization of measuring method on truck should install a suitable camera to the place where can stopped the trucks loaded with wood assortment. The truck has to stay on a designated space. The camera is controlled by the computer, so the operator takes the picture from the office. For precise measurement result the accuracy of track position is important. If the track stays ten twenty or thirty centimeter closer or farther from the designated position than geometrical error will be occurred.

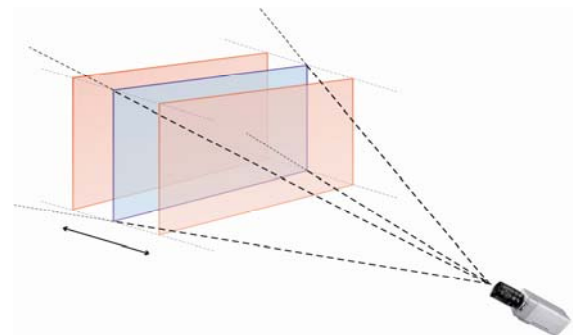


Fig. 5 Position error of the truck causes measurement error.

The degree of the error depends on the position difference and from the distance between the camera and the image plane.

The further the camera is fixed the smaller is the relative error (Table 1).

Table 1 Effect of the position error in case of different camera distance.

Camera distance from the image plane [m]	Position difference [cm]							
	-30	-20	-15	-10	10	15	20	30
	Surface difference in %							
10	5.9	4.0	3.0	2.0	-2.0	-3.0	-4.0	-6.1
15	4.0	2.6	2.0	1.3	-1.3	-2.0	-2.7	-4.0
18	3.3	2.2	1.7	1.1	-1.1	-1.7	-2.2	-3.4
20	3.0	2.0	1.5	1.0	-1.0	-1.5	-2.0	-3.0
25	2.4	1.6	1.2	0.8	-0.8	-1.2	-1.6	-2.4

In the table 1 is visible the measure of errors in dependence of camera distances and the position errors. In case of 25 meter camera distance the 10 cm position error causes 0.8% difference. If the real image plane is further from the right position the camera sees smaller the same surface size than it is; consequently it will measure less amount of solid wood. In this case the system will measure -0.8% less surface size. This error related to the surface, the linear error is much less.

If the position error raises to 20 or 30 cm the surface difference will raise also to -1.6% or -2.4% in case of 25 meter camera distance. The camera fixed only 10 meter from the image plane causes 2% surface difference what is much higher in 10 cm position error. The measure of surface difference is extreme high if the position error achieves the 30 cm. The difference is not the same in both position error directions. If the stuck surface is further with 30 cm than the designated position the surface difference is higher in percentage than the stuck would be closer to the camera.

Summarizing the facts explained above it is much advantageous to fix the camera further from the designated truck side position.

CONCLUSIONS

The punctuality of the new method is higher than that of the traditional survey at least 2–3 times. With comparison of the traditional method this system is significantly faster because of the automatically process steps. System is controlled from the office what is more comfortable for employee. The measured stack data are in digital form from the beginning of process related to the pictures and other data of transportation.

Main advantages of the photo analytical method:

- higher punctuality,
- faster survey method,
- easier documentation,
- digital technology,
- stock registering opportunity,
- easy statistical report,

Disadvantages of the photo analytical method:

- higher technology level and higher prices,
- need of educated operator,

REFERENCES

- BARRETT L. I., BUELL J. H., RENSHAW J. F. 1941: Some Converting Factors for Mixed Oak Cordwood in the Southern Appalachians. *J. Forest.* 39(6): 546–554.
- BARROS M. V., FINGER C. A. G., SCHNEIDER P. R., SANTINI E. J. 2008: Fator de Cubicáco Para Toretas de Eucalyptus grandis e Sua Variáçáo Com o Tempo de Exposicáo ao Ambiente (Cubivation Factor of Stacked Wood of Eucalyptus grandis and its Variation with the Time of Exposition to the Environment. *Ciencia Florestal* 18: 109–119.
- KEEPERS C. H. 1945: A New Method of Measuring the Actual Volume of Wood in Stacks. *J. Forest.*, 43(1): 16–22.
- MACLEAN G. A., MARTIN G. L. 1984: Merchantable Timber Volume Estimation Using Cross-Sectional Photogrammetric and Densitometric Methods. *Can. J. For. Res.* 14(6): 803–810.
- MALTAMO M., EERIKÄINEN K., PITKÄNEN J., HYYPPÄ J., VEHMAS M. 2004: Estimation of timber volume and stem density based on scanning laser altimetry and expected tree size distribution functions. *Remote Sensing of Environment* 90: 319–330.
- MÄKELÄ H., PEKKARINEN A. 2001: Estimation of timber volume at the sample plot level by means of image segmentation and Landsat TM imagery. *Remote Sensing of Environment* 77: 66–75.
- PEKKARINEN A. 2002: Image segment-based spectral features in the estimation of timber volume. *Remote Sensing of Environment* 82: 349–359.
- SCHNUR, G. L. 1932: Converting Factors for Some Stacked Cords. *Journal of Forestry*, 30(7): 814–820.
- Smith V. G. 1979: Estimating the solid wood content of stacked logs with minimum total cost. *Can. J. For. Res.* 9: 292–294.

DETERMINATION OF FRACTURE PROPERTIES UNDER MECHANICAL STRESS

SEBASTIAN CLAUB, PIERRE WATSON, SAMUEL AMMANN & PETER NIEMZ

ETH Zurich, Institute for Building Materials, Wood Physics, HIF E.251, Schafmattstrasse 6, CH 8093 Zurich

Abstract

To gain a better understanding of the influential factors in delamination, three commonly used wood adhesives, one-component polyurethane adhesive, polyvinyl acetate adhesive and melamine-urea formaldehyde resin as well as solid wood control samples were tested on beech wood in opening-mode (mode I) fracture using a compact tension (CT) test. The purpose of this study was to characterize the fracture properties of glued wooden laminates in different climate conditions. The results showed that the adhesive type and moisture content of the test samples had a large effect on the fracture characteristics. The performance of the different adhesive types varied greatly between adhesives and at different climate conditions with the significant indicators being low wood failure percentage, fracture toughness values lower than solid wood, and prominent adhesive failure.

Keywords: wood laminate, adhesive, fracture toughness, delamination.

INTRODUCTION

Delamination usually leads to failure of the structure and can occur subcritically at loads lower than the stated critical load of the overall structure (BUCUR 2011). The exact reasons for delamination processes are not yet known due to the lack of reliable mechanical tests to characterize the fracture properties of the adhesive joints.

Many factors can cause delamination such as faulty bonding, the element structure, high stresses, and fatigue due to climatic stresses. Delamination caused by moisture is especially pronounced in cross-laminated wood materials with strongly divergent swelling and shrinking properties parallel and perpendicular to the plane such as in parquet and solid wood panels. The dimensional changes vary depending on the principle directions of the wood which can lead to residual stresses in the laminate. Large cross-sections also have a large impact by multiplying the residual stresses in the laminates into high stresses large enough to cause significant damage.

The bond line in glued laminates serves as a stress intensifier by causing a pronounced moisture profile. This moisture profile is generally caused by an increased diffusion resistance or humidity dependence of the adhesive. These differences in moisture and stress can lead to a reduction in adhesion, cohesion, or complete failure of the wood at the joint (BUCUR 2011).

Wood itself is considered a brittle-elastic material with nonlinear-elastic behavior (SMITH and VASIC 2003). For simplification purposes, the behavior of wood can be characterized with linear-elastic fracture

mechanics by assuming that the plastic and inelastic zones are small compared to the test sample geometry. In wood, crack propagation is a result of cell wall fracture or intercellular separation (KEUNECKE *et al.* 2007). Oftentimes the crack surfaces do not completely separate but are still jointed by fibers of the tracheid cells. These additional connections, called fiber bridges, dissipate fracture energy and lead to fracture toughening, which results in non-linear behavior.

The objective of this work is to determine the fracture properties of adhesive joints of several different commonly used wood glues under mechanical stress. The results from these experiments will help give a better understanding of laminate and adhesive properties and their relation to delamination.

MATERIALS AND METHODS

The tests were performed on samples from beech wood, *Fagus sylvatica* L. The wood came from two boards from the same tree from the canton of Zurich, Switzerland. The average measured density of the wood, calculated according to DIN 52 182 (1976), was $628 \pm 20 \text{ kg/m}^3$.

The boards were cut into slats for acclimatization in order to ensure a stress-free initial condition before gluing and cutting. The slats were conditioned at standard climate (20 °C, 65 % relative humidity) until the moisture content in the wood was constant (changing less than 0.1 % per day). This led the samples to have a moisture content of approximately 13 %. Once acclimated, the slats were glued together using three different wood adhesives, according to manufacturer guidelines.

The three adhesives used were one-component polyurethane adhesive (1C-PUR), polyvinyl acetate (PVAc), and melamine-urea formaldehyde resin (MUF) combined with hardener. The technical specification of the three adhesives can be seen in Table 1.

The CT test samples were then cut from the glued slats according to the shape and dimensions shown in Fig. 1 (a) with the glue line in the center of the test sample. The test samples were oriented between RL and TL such that the annual rings are approximately at a 45° angle. The actual angle varied between 30° and 75°. The test samples were then subjected to the treatments described in DIN EN 302-1 (2011). Unglued samples were also tested as a control to compare the performance of the glued laminates with that of solid wood.

Compact Tension Test

Using the Deben Microtest Tensile Stage Controller (Deben UK Ltd, Suffolk, UK), the samples were subjected to mode I tension until fracture while recording the force applied by the device Fig. 1(b). At least 15 samples were tested for each adhesive and treatment type. The crack tip of each test sample was sharpened with a razor prior to testing to ensure a crack tip radius of < 0.25mm according to DIN EN ISO 12737 (2005).

A rounded crack tip can inhibit crack propagation through crack tip blunting. The test machine was set to a maximum force of 300N with an adjustable displacement speed of 0.1, 0.2, 0.5, 1, and 1.5 mm/min and a refresh rate of 5Hz (sample every 200 ms). The displacement was applied to the holes of the test samples with a maximum displacement of 10mm. The speed was set so that fracture occurred 30–90 seconds after beginning the test which translated to a speed of approximately 1mm/min. This speed was fast enough to prevent creep from occurring but also slow enough to keep the test in quasi-static mode.

The parameter of interest was the stress intensity

factor for mode I, K_I , which can be calculated using DIN EN ISO 12737 (2005). As there are no standards for calculation of fracture toughness in wood, this standard was used instead and was adapted to wood test samples. The compact tension (CT) test is a simple, standard method of measuring the stress intensity factor of a material by analyzing the force vs. displacement plot to obtain the critical force (F_C).

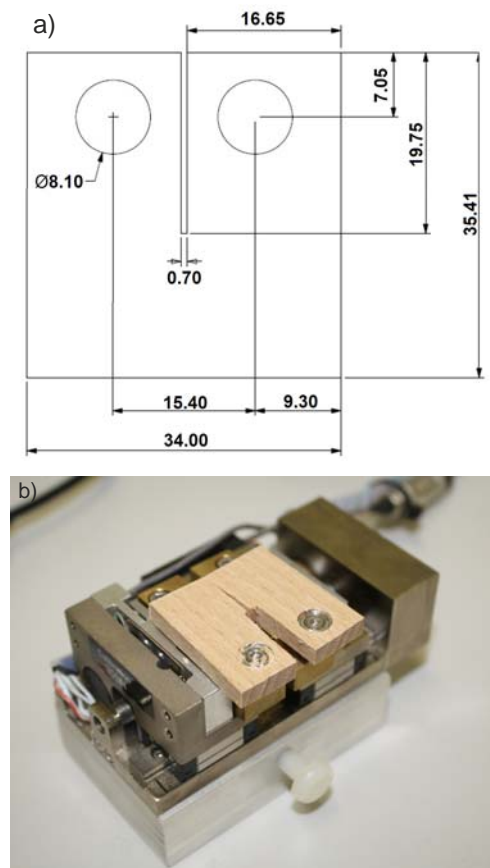


Fig. 1 (a) Shape and dimensions of the tested samples. (b) Compact Tension test of a solid wood sample on the Deben Microtest Tensile Stage Controller. The two pins set in the holes of the wood sample displace outwards causing fracture of the specimen.

Table 1 Technical Specifications of the three adhesives used in testing. The moisture requirements are listed as: 1st value - % R.H. of the wood samples to be glued, 2nd value - difference in % R.H. between the two wood samples to be glued. Data from Technical Specification Sheets. +Data from KONNERTH *et al.* (2007), *Data from Wood Physics Group, ETH Zurich.

	1C PUR	PVAc	MUF
Type	isocyanate prepolymer	starchbased	polycondensation
Amount Applied (g/m ²)	140–180	120–200	340–440
Mixing Ratio	–	–	100 g adhesive + 50 g hardener
Working Time (minutes)	70	7	120
Press Time (hours)	3	1.25	14
Curing Time (hours)	12	168	18.5
Pressure Applied (N/mm ²)	0.6–1	0.6–0.7	0.8–1.2
Viscosity (MPa·s)	24000	8000	3000
Density (kg/m ³)	1160	–	1280
Moisture Required (%)	>8, Difference < 4	6–12	>6, Difference < 4
E-modulus (MPa)	971 ± 67*	1500+	2550 ± 53*

With the conditions of linear elastic fracture mechanics (LEFM) and plane strain satisfied, the calculated K_{IC} from F_C is equal to the fracture toughness (K_{IC}). The equation below (Eq. 1) was used to calculate the K_{IC} of the test specimen with a sample thickness (B), a distance (W) between the point of applied force and the end of sample and a crack length (a).

$$K_{IC} = \frac{F_C}{B\sqrt{W}} \cdot \frac{2 + \frac{a}{W}}{\left(1 - \frac{a}{W}\right)^{3/2}} \cdot \left[0.886 + 4.64\left(\frac{a}{W}\right) - 13.32aW^2 + 14.72aW^3 - 5.60aW^4\right] \quad (1)$$

Prior to the CT test, the kiln drying method in DIN 52183 (1977) was used to determine the humidity of the test samples.

Wood Failure Percentage

The wood failure percentage was calculated using ASTM D 5266 (2005). After CT testing, the fractured test samples are divided along the fracture line and the percent of adhesive on both sides of the fracture surface was calculated as a percent of total area. The following criteria were used: 100 % percent adhesive on both sides of the fracture surface equals 0 % wood failure, 0 % adhesive on both sides of the fracture surface equals 100 % wood failure, 100 % adhesive only on one fracture surface equals 0 % wood failure with adhesive failure.

RESULTS

The glued samples showed varying fracture toughness values depending on the adhesive and treatment type. The obtained results are summarized in Table 1. The A1 samples performed better with higher K_{IC} than the other two treatment types. The box plot in Fig. 2 clearly shows the significance of treatment type on fracture toughness and it shows that an increase in moisture content caused a decrease in fracture toughness for all adhesive types. As also seen, MUF always performed better and the PUR always performed worse than the solid wood controls.

The PVAc samples performed similarly to the control except in A2 when it displayed exceptionally low F_C and K_{IC} values. The p-values in Table 2 firm this observation statistically. The fracture toughness of the PVAc was so low in A2 that 9 samples were broken while being attached to the testing machine. The PUR samples were also fragile in A2 and 2 samples were broken while being attached to the testing machine.

A literature comparison on fracture toughness for the glued samples is difficult as not many similar experiments have been done. There exist other studies on the fracture properties of wood adhesive but not many are tensile tests as most wood adhesives are tested in shear. The fracture properties are given in shear resistance, shear strength, work to fracture, etc. which are difficult to translate into the fracture toughness notation used in this study. Also, with the large number of commercial wood adhesives, an exact comparison of the adhesive is difficult.

For the PVAc samples, the water affected the quality of the adhesive causing softening of the bonds and a reduction in adhesion as was observed in this study. Water enters the polymer network and due to hydrolysis, the carbon – carbon bond between the monomers is cleaved (DUNKY and NIEMZ 2002). Previous studies have observed this reduction in strength due to water (TANKUT 2007 and SCHRÖDTER and NIEMZ 2006). In a previous investigation by KURT and UYSAL (2009), it was observed that PVAc completely lost its bonding strength after 7 days submerged in 20°C water which is very similar to what was observed after the A2 treatment.

Water also affected the adhesion strength of PUR, but to a lesser degree than in PVAc. PUR is more water resistant than PVAc and actually uses the moisture content in the wood for the curing process with the isocyanate polymer end (CLAUB *et al.* 2011). Thus, a drop in fracture toughness and wood failure percentage in A2 was observed with PUR but was not as pronounced as with PVAc. A decrease in the number of samples with adhesive failure was even observed in the A2 and A3 treatments.

Table 2 CT Test results showing mean ± standard deviation. The P-Value compares glued samples and the corresponding control samples by means of a t-test. N/A stands for "Not Applicable".

		n	F_C (N)	K_{IC} (MPa√m)	Wood Failure (%)	Adhesive Failure (n)	P-Value
Control	A1	25	84.34 ± 22.35	0.83 ± 0.22	N/A	N/A	N/A
	A2	26	32.25 ± 5.49	0.32 ± 0.05	N/A	N/A	N/A
	A3	25	76.74 ± 23.00	0.75 ± 0.23	N/A	N/A	N/A
PUR	A1	20	62.71 ± 24.49	0.61 ± 0.24	10 ± 25	4	< 0.01
	A2	18	20.82 ± 4.76	0.21 ± 0.05	0	1	< 0.01
	A3	18	48.77 ± 16.49	0.48 ± 0.16	0 ± 5	0	< 0.01
PVAc	A1	19	89.79 ± 26.26	0.88 ± 0.26	40 ± 20	8	0.46
	A2	11	8.05 ± 4.52	0.08 ± 0.04	0	10	< 0.01
	A3	18	71.90 ± 19.39	0.71 ± 0.19	30 ± 20	12	0.5
MUF	A1	20	99.83 ± 19.28	0.98 ± 0.19	60 ± 25	0	0.018
	A2	18	38.87 ± 7.35	0.38 ± 0.07	35 ± 30	1	< 0.01
	A3	19	92.75 ± 15.05	0.91 ± 0.15	60 ± 30	0	0.01

The bonding performance of the MUF was the least affected by water as expected due to its increased water resistance. As explained by KURT and UYSAL (2009) and DUNKY and NIEMZ (2002), the addition of melamine to urea-formaldehyde increases the moisture stability of the adhesive because the double bonds in the melamine stabilize the carbon – nitrogen bond between the melamine and formaldehyde groups and increase the resistance to hydrolysis from water. As a result, the MUF samples performed better than the other glues and the solid wood samples in A2 and A3.

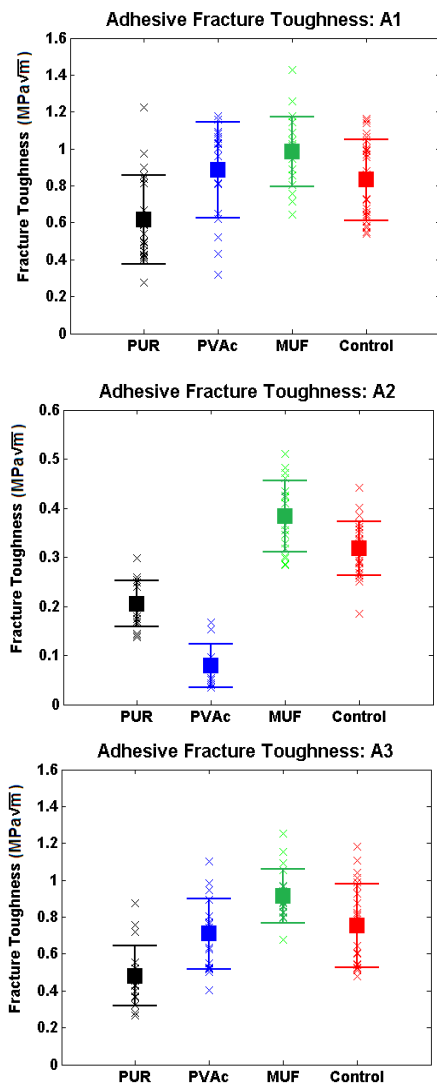


Fig. 2 Fracture toughness plots for each glue and treatment type. The plots show the mean and standard deviation of each glue type compared with the control samples. The “x” signifies the fracture toughness of MUF of an individual sample.

This observation is significant because one would expect that if the wood was weaker than the glue, the wood would fail at its normal F_C before the adhesive and thus, the samples would have the same K_{IC} as the solid wood samples. Instead, the wood is able to withstand a higher K_{IC} when glued than unglued. A

possible explanation for this is that the sharpened crack tip was cut into the glue line and thus 1) higher forces were required for crack initiation in the tougher MUF and 2) higher forces were required for crack initiation in the blunted wood. Oftentimes, the crack would initiate and propagation in the wood and ignore the preexisting, sharpened crack in the glue. The crack would have experienced crack tip blunting as it was not sharpened with a razor and the blunted curvature of the crack would reduce the stress intensity factor. Once the crack initiation had begun in the glue, it had a tendency to veer into the wood due to the lower toughness of the wood.

The wood failure percentage varied significantly between the glues (Fig. 3(a)). MUF always had the highest wood failure percentage and PUR had the lowest except in A2 when both PVAc and PUR had equally low values of less than 10 %. The A2 treatment caused a decrease in all the wood failure percentages. The A3 treatment caused a decrease in the wood failure percentage of PUR and PVAc but did not affect the wood failure percentage of MUF. PUR had only one sample with a wood failure percentage higher than 50 % and MUF had the majority over 50 %.

Besides the wood failure percentage, the percentage of samples with adhesive failure was counted and can be seen in Fig. 3(b). PVAc showed the highest number of samples with adhesive failure, particularly in A2, when the percentage of samples with adhesive failure reached over 90 %. PUR had occasional adhesive failure, which amounted to less than 20% of the samples. MUF had only one sample with adhesive failure.

Although it is difficult to compare the failure behavior of samples tested with different test setups, the results of wood failure percentage for the A1 and A3 revealed a similar tendency regarding the different adhesives like those found by SCHMIDT *et al.* (2010) and CLAUB *et al.* (2011). The two previous studies, however, tested the adhesives in shear rather than in tension, and the exact adhesive type and manufacturer differed between the experiments. Despite these differences, the same general trend of wood failure percentage was observed with the stiffer polycondensation resins as MUF mostly causing higher wood failure percentages compared to PUR or PVAc.

The fracture characteristics of the glued samples varied largely between the three adhesives. The PUR samples fractured along the glue line with unstable crack propagation. The PVAc samples fractured partially along the glue line with adhesive failure and partially in the wood with some fiber bridging.

The MUF samples had the most favorable fracture characteristics with almost entirely wood failure with fiber bridging. The wetness of the A2 samples exaggerated the fracture characteristics seen in A1; the PVAc exhibited complete adhesive failure

and the MUF exhibited even more pronounced fiber bridging. The PUR samples in A2, however, still displayed approximately 0% wood failure as seen in A1.

The shape of the force vs. displacement curve (Fig. 4) was dictated by the fracture and material characteristics for each adhesive and treatment type. The elastic section of the curve varied between the dry (A1 and A3) and wet (A2) conditions. The A1 and A3 samples displayed a similar, linearly increasing slope, whereas the A2 samples displayed a more gradual, curvier slope. The shape of the curve during and after fracture relates directly to the fracture characteristics.

The PUR, being weaker than the wood, caused sudden brittle fracture along the glue line. Without fracture in the wood, fiber bridging was not possible and thus complete failure of the sample upon reaching F_C was observed. Only short displacements (< 1 mm) were required for fracture and failure of the samples and the treatments A2 and A3 led to similar force curves but with reduced peaks (F_C).

reaching F_C . Instead, a gradual, descending force plot was observed with increasing displacement. The A2 samples adhesively failed almost immediately which led to gradual sloping curves with very low peaks.

The MUF samples displayed mostly brittle fracture with significant fiber bridging leading to a slow, gradually decreasing force after the initial drop at fracture. The climate treatments affected the samples mainly by reducing the peaks of the curves. The PVAc and MUF samples required larger displacement (1–2 mm) before fracture occurred.

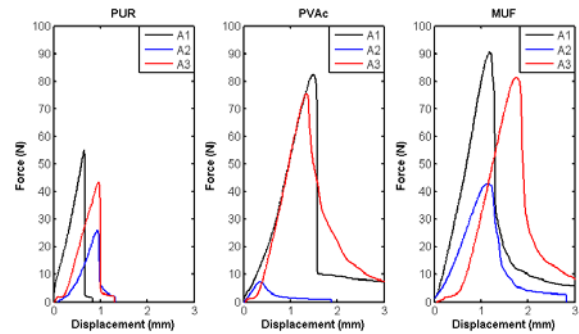


Fig. 4 Force vs. displacement curves for typical samples for each glue and treatment type. Information about the fracture and material characteristics can be deduced by the shape of the curve.

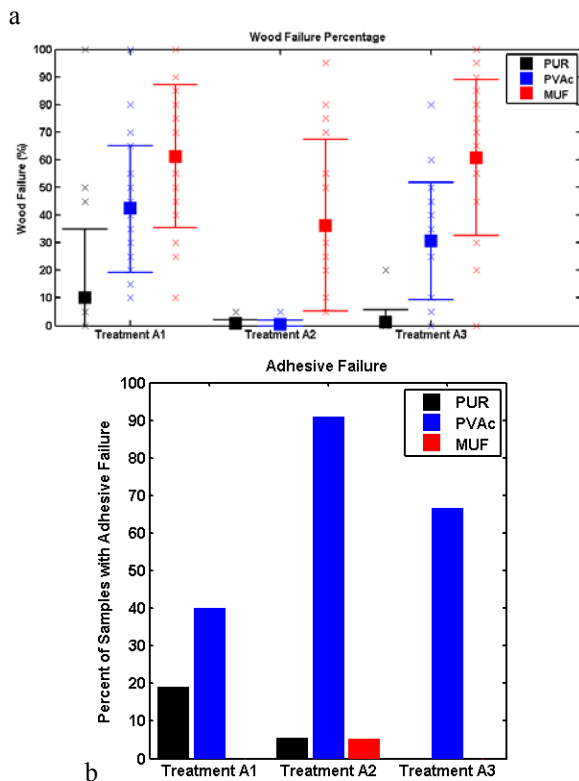


Fig. 3 (a) Wood failure percentage for each glue and treatment type plotted as mean and standard deviation. The “x” signifies the wood failure percentage of an individual sample. (b) Percentage of samples with adhesive failure for each glue and treatment type. Missing bars for a treatment type signifies that no samples displayed adhesive failure for that glue and treatment.

The fiber bridging present in the PVAc samples prevented complete failure of the sample upon

CONCLUSION

The fracture properties of adhesive joints under tensile stress in mode I depend on adhesive type, climate treatment, and moisture content. Increased moisture content had the effect of reducing the fracture toughness, reducing the wood failure percentage, and causing more quasi-ductile behavior from the wood. MUF performed the best for all treatment types due to its high fracture toughness, its resistance to water, and the presence of fiber bridging during fracture leading to fracture toughening and slow crack propagation. PUR performed poorly for all treatment types due to its low fracture toughness leading to glue line failure and rapid crack propagation. The performance of PVAc bond lines depended significantly on the moisture content of the wood. The PVAc performed similarly to solid wood during normal climate tests with slow crack propagation, but when subjected to high moisture content, the adhesive bond between the PVAc and the wood failed and the samples were easily broken with minimal force. The PVAc samples that were wetted and then dried displayed a much higher rate of adhesive failure despite having similar fracture toughness values as the solid wood samples. Thus, laminates with a high moisture content particularly with PVAc and laminates glued together with PUR increase the probability of delamination by increasing the chance of failure in the adhesive.

REFERENCES

- ASTM D 5266 (2005): Standard Practice for Estimating the Percentage of Wood Failure in Adhesive Bonded Joints.
- BUCUR V. 2011: Delamination in Wood, Wood Products and Wood-Based Composites. New York : Springer.
- CLAUß S., JOSCAK M. & NIEMZ P. 2011: Thermal stability of glued wood joints measured by shear tests. *European Journal of Wood and Wood Products*, 69:101–111.
- DIN 52182 1976: Testing of wood; determination of density.
- DIN 52183 1977: Testing of wood; determination of moisture content.
- DIN EN 302-1 2011: Adhesives for load-bearing timber structures - Test methods - Part 1: Determination of n longitudinal tensile shear strength.
- DIN EN ISO 12737 (2005): Metallic materials - Determination of plane-strain fracture toughness.
- DUNKY M. & NIEMZ P. 2002: *Holzwerkstoffe und Leime: Technologie und Einflussfaktoren*. Berlin, Heidelberg, Berlin : Springer.
- KEUNECKE D., STANZL-TSCHEGG S. & NIEMZ P. 2007: Fracture characterisation of yew (*Taxus baccata* L.) and spruce (*Picea abies* [L.] Karst.) in the radial-tangential and tangential-radial crack propagation system by a micro wedge splitting test. *Holzforschung*, 61:582–588.
- KONNERTH J., GINDL W. & MÜLLER U. 2007: Elastic Properties of Adhesive Polymers. I. Polymer Films by Means of Electronic Speckle Pattern Interferometry. *Journal of Applied Polymer Science*, 103: 3936–3939.
- KURT S. & UYSAL, B. 2010: Bond strength/disbonding behavior and dimensional stability of wood materials with different adhesives. *Journal of Applied Polymer Science*, 115: 438–450.
- SCHMIDT M., GLOS P. & WEGENER G. 2010: Gluing of European beech wood for load bearing timber structures. *European Journal of Wood and Wood Products*, 68:43–57.
- SMITH I. & VASIC S. 2003: Fracture behavior of softwood. *Mechanics of Materials*, 35(8): 803–815.
- TANKUT N. 2007: The effect of adhesive type and bond line thickness on the strength of mortise and tenon joints. *International Journal of Adhesion & Adhesives*, 27: 493–498.
- WANG L., LU Z. & ZHAO G. 2003: Wood fracture pattern during the water adsorption process. *Holzforschung*, 57:639–643.

COMPOSITES OF STEAM EXPLODED BIOMASS

JANIS GRAVITIS¹, JANIS ABOLINS², GALINA DOBELE¹, RAMUNAS TUPCIAUSKAS¹, ANDRIS VEVERIS¹,
MARTINS ANDZS³, ANNA PUTNINA⁴ & SILVIJA KUKLE⁴

¹Latvian State Institute of Wood Chemistry, 27 Dzerbenes Str. Latvia LV-1006; jgravit@edi.lv

²Institute of Atomic Physics and Spectroscopy, University of Latvia

³Latvia University of Agriculture, Forest Faculty, Dep. of Wood Processing

⁴Riga Technical University, Institute of Textile Materials Technologies and Design

Abstract

Steam explosion pre-treatment of biomass presents one of advanced techniques for transformation and functionalization of the components of natural polymers and allows to extract easily hemicelluloses and destructed fragments of lignin from the processed mass. Depending on the treatment severity, the fibres of cellulose are reduced to micro-fibrils and nano-size whiskers. The complex physical and chemical modification proceeding at steam explosion pre-treatment of wood biomass is used to improve the properties of the diverse composite materials made of the renewable resource for a variety of purposes e.g. hemp and flax fibres for electro-spinning, hemp and flax shives as heat insulating composites. Considering bio-refineries based on biomass pre-treatment by steam explosion, the effects of steam explosion severity on mass recovery and properties of processed wood biomass and composite products including self-binding fibreboards made thereof are presented and discussed with respect to applications. The paper includes published results and is kind of a review of the authors' results reflecting the research directions.

Key words: steam explosion, bio-composites, lignin, fibre materials.

INTRODUCTION

Natural wood is a complex and multifunctional composite material used by humans for a vast variety of their needs from the source of energy to the stuff for arts competing successfully with other substances and modern synthetics. During millennia humans have learned to improve and modify the natural properties of wood for special needs by special treatment and selection.

Plywood and a variety of pressed boards are well-known composite materials widely used in building constructions and furniture. Developed technologies allow to utilize low-quality wood and waste from sawmills to make useful products.

Some adhesive substance is the usual other component used to make composite boards the main ingredient of which is wood or other kind of biomass. Presently phenols are the main source of industrially used adhesives. About 95 percent of phenol produced in North America is derived from cumene oxidation. Cumene is made from petrochemicals – benzene and propylene for which reason the costs of these chemicals are driven by the price of oil. As the oil prices increase dramatically, the costs of wood composites (plywood, oriented strand board (OSB), medium density fibre board (MDF), etc.) rise dramatically too – the prices of phenol-based adhesive resins show a direct correlation with the oil market prices. The other major adhesive component is formaldehyde produced from natural gas. However, in 2004 the International Agency for Research on

Cancer has classified formaldehyde as human carcinogen.

Along with economic considerations suggesting to reduce the costs adhesives by using aromatics from renewables at stable pricing of feedstock carbon lately is growing the interest in cheap self-binding (self-adhesive or synthetic binderless) wood composites. Studies results of which are presented hereafter have been taken on as an attempt to use lignin extracted from wood after steam explosion (SE) auto-hydrolysis (GRAVITIS 1987) as the adhesive in hot-pressed wood boards. Many advanced green and high value products can be produced from renewable biomass, e.g., heat insulating materials, electro- and nano-spinning materials, wood ceramics, etc.

Zero Emissions and Biorefinery concepts (PAULI 1998, GRAVITIS 1999, GRAVITIS *et al.* 2008) emphasize the shift from traditional linear industrial model in which wastes are considered the norm, to integrated technologies systems in which everything has its use. It advocates an industrial transformation whereby businesses emulate the sustainable cycles found in nature and where society minimizes the load it imposes on the natural resource base and learns to do more with what the earth produces. In this way, industries are reorganized into clusters such that each industry's wastes/by-products are fully matched with the input requirements of another industry, and the integrated whole produces no waste of any kind. ZERI concentrates attention on utilization of renewable biomass using biorefinery. The Laboratory of Eco-Efficient Conversion of the Latvian State Institute of Wood Chemistry defines biorefinery as a

cluster of technologies integrating biomass conversion into transportation fuels, power, chemicals, and advanced materials within the framework of zero emissions and is based on two – materials and energy - platforms. The biorefinery concept is the analogue of today's petroleum refineries producing multiple fuels and products from petroleum. Industrial biorefineries have been identified as the most promising route to creation of a new domestic biobased industry. By producing multiple products, a biorefinery takes advantage of the differences in biomass components and intermediates to maximize the value derived from the biomass feedstock. Biorefinery gives answer to how to substitute fossil oil with renewable biomass, particularly protecting environment. „Zero Emissions” and „Biorefinery” are keywords of the 21st century.

MATERIALS AND METHODS

Commercial chips of birch (*Betula pubescens*) and grey alder (*Alnus incana*), wheat straw, and birch wood veneer as well as extracted SE lignins, were used in this research. Hemp and flax fibers and shives also being studied.

The SE material for hot-pressed board samples was studied by an L&W Fibre Tester analyser to determine such fibre parameters as length, width, shape factor (the ratio of projected to actual length), coarseness (mass per unit length), and ratio of *finer* (fibres less than 0,2 mm), of the steam-exploded wood biomass and extracted cellulose.

A Mettler Toledo TGA/SDTA851 thermal gravimeter and a Mettler Toledo DSC822 differential scanning calorimeter were used to detect thermal effects (loss of mass) and glass transition temperature T_g in samples of the extracted lignins.

The lignin in hot-pressed board samples was evaluated from infrared spectra recorded by a Perkin Elmer “Spectrum One” Fourier transform spectrometer. The 32 repeated infrared absorption spectrum scans at the rate of $0.2 \text{ cm}^{-1}/\text{s}$ at resolution of 4 cm^{-1} of each of the three samples prepared for the purpose covered the range from 450 to 2000 cm^{-1} . The Spectrum 5.0.1 (Perkin Elmer Instruments LLC) software was used for correction of the base line and normalisation of the spectra.

The SE lignins were studied using pyrolysis-gas chromatography/mass spectrometry (PY-GC/MS) FRONTIER LAB PY-2020 ID, Shimadzu GCMS-QP 2010.

SEM micrographs were obtained by Vega TS 5136 scanning electron microscope (SEM) operating at 15–20 kV, after sputter coating with gold.

Mechanical properties (modulus of elasticity and bending strength (EN 310:1993) internal bonding, etc. of hot-pressed board samples were tested by a universal ZWICK/Z100 machine for testing material resistance at the LSIWC and MeKa institute. The

materials were pressed in a “Joos” single-stage hydraulic hot-press.

The testing results of the board and plywood samples were compared with European standards (EN 312: 2003, EN 622-2:2004, EN 314-2:1993).

Steam explosion unit and fractionation of SE biomass

Steam explosion (SE) is principally a rather simple process but complicated in technical details. The biomass is treated with saturated steam, usually at pressures up to 4 MPa. The treatment time varies from some seconds to some minutes. After the treatment, within a split second, the biomass is decompressed (exploded) to the pressure of ambient atmosphere. The diagram of the SE process is shown in Fig. 1. The steam is generated by heating water in the boiler. Upon reaching the necessary steam parameters the sample is filled into the reactor and treated by steam at needed temperature and pressure. After having been subject to treatment for a chosen duration the sample is forced out into receiver where-from it further proceeds to the separation column. SE simulation and energy demand evaluation was performed (ABOLINS and GRAVITIS 2009). Fractionation sequence of SE biomass is showed in Fig. 2.

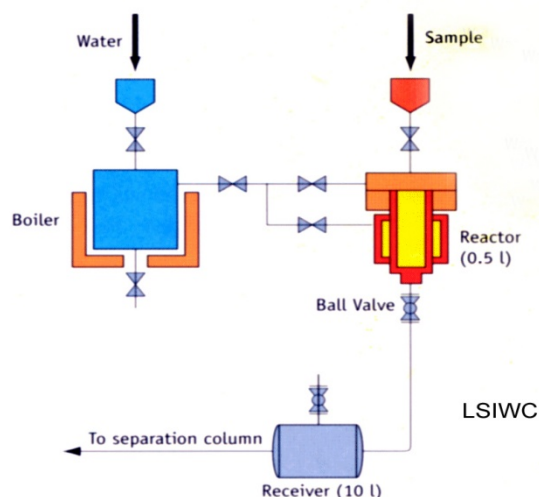


Fig. 1 Experimental SE unit.

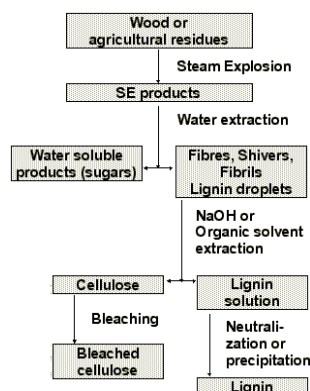


Fig. 2 Fractionation of SE biomass.

RESULTS AND DISCUSSION

Case study of grey alder pre-treatment by SE for self-adhesive composites (TUPCIAUSKAS *et al.* 2012)

A batch steam explosion pre-treatment (SE) was applied to grey alder (*alnus incana* (L.) Moench) chips to obtain self binding fibrous lignocelluloses' complex. For SE was used water vapour without any chemical catalyst. The structural impact of SE on the chips investigated by such aspects as: mass loss (depending on severity of SE, moisture and size of chips); changes of microstructure; components output; changes of bulk density. The study pursued information about the pre-treated lignocelluloses' complex which further was used for binder-less board production. Mass loss of the chips mostly depends on pre-treatment conditions and increases with increasing SE severity. The bulk density of the pre-treated chips decreases at least by 1.5 times and depends on the size of chips and the severity of SE. The microstructure of pre-treated lignocelluloses' complex is greatly modified; however it includes the same amount of lignin and cellulose as untreated wood.

Recently SE receiver cascade have been used.

Self-binding fiber boards (GRAVITIS *et al.* 2010)

Sulphur-free lignins open the way for replacement of phenol-formaldehyde resins to bind different wood composites (fibre boards, plywood, etc.). The main results are related to the reduction of formaldehyde emissions during production and from the finished composites. The SE is a route to self-binding composites via sulphur-free SE lignin. The self-binding grey alder fiber board properties are demonstrated in Table1.

Sulphur-free lignin studies by Pyrolysis-gas chromatography/mass spectrometry (Py-GC/MS)

Py-GC/MS was employed to examine sulphur-free SE lignins. Lignins were performed by Py-gc/MS method using a Frontier Lab Micro Doble-shot Pyrolyser (Py-2020iD). Pyrolysis temperature was 500°C. The volatile compounds emitted from pyrolysis samples were separated by gas chromatography (GC) and identified by mass spectrometry (MS). The SE lignins were characterized by Shimadzu GC/MS 2010 (Japan, capillary column RTX-1701, 60 m × 0.25 mm × 0.25 μm). The temperature of the injector and the ion source was 250°C, ion energy EI – 70 eV. The MS scan range was m/Z 15-350. The carrier gas was helium at a flow rate of 1 ml*min⁻¹, and the split ratio 1:30.

Table 1 Properties of self-binding grey alder fibreboard samples.

Pressing conditions		Board samples properties					
T °C	Pressure MPa	Density g cm ⁻³	Swelling %	Water absorption %	Bending strength N mm ⁻²	Modulus of elasticity N mm ⁻²	Internal bonding N mm ⁻²
170	8	1.34 ± 0.04	8 ± 1	7 ± 3	32 ± 5	4700 ± 1300	0.6 ± 0.6
170	5	1.27 ± 0.04	9 ± 1	10 ± 3	29 ± 5	4100 ± 1200	0.8 ± 0.6
190	8	1.24 ± 0.18	11 ± 1	17 ± 6	14 ± 5	2600 ± 1300	0.4 ± 0.4
190	5	1.30 ± 0.03	10 ± 1	11 ± 2	16 ± 1	3590 ± 330	0.9 ± 0.2

The principal self-binding composite production chain is shown in Fig.3

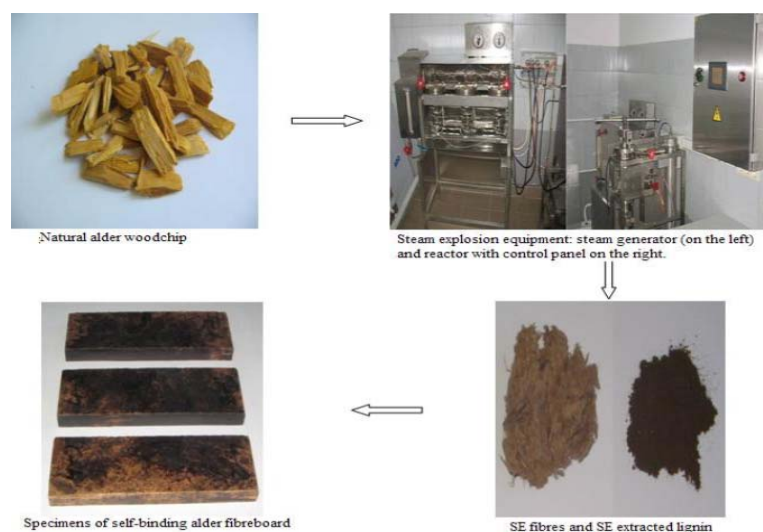


Fig. 3 An illustrative display of processing the self-binding hot-pressed boards from SE materials.

The oven program was 1 min isothermal at 60°C, then 6°C·min⁻¹ to 270°C, and finally 10 min at 270°C. Library MS NIST 147.LI13 was used. If all volatile compounds are arbitrary 100%, Py-GC/MS allow detecting content of all identified compounds in relative %.

The non-sulphur SE lignins of grey alder (235°C, 3.2 MP, N1 – 1min, N2 – 2min, N3 – 3 min.), birch (N4-1min.), Bjorkman birch (N5), and wheat straw (N6-1min.) were analysed.

Py-GC/MS is a powerful analytical tool and gives information about carbohydrate impurities, and content of phenyl/benzyl-, Guaiacyl(G)-, Syringyl(S)-derivatives (Table2).

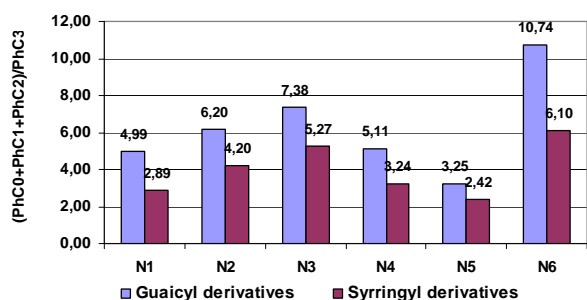


Fig. 4 Phenyl (Ph0)+ Phenylmethane(Ph1) + Phenyl-ethane (Ph2) / Phenylpropane (Ph3) ratio for phenols calculated on the basis of Py-GC/MS.

These phenomena could be considered as a consequence of the cleavage of native β-aryl-alkyl bonds in lignin and conforming cleavage and degradation of SE lignin side chains during pyrolysis SE hemp shives as a heat insulating composite (ANDZS *et al.* 2012)

Compared with synthetic insulation materials hemp shives – the residue presenting a mixture of fragmented bits of hemp stalks and short fibres left after decortication and removal of the long fibres, have a lower resistance to heat transfer but being permeable are ideally suited for breathable constructions. The micro-porous stalk particles have a very fine capillary structure and are highly hygroscopic. These properties make them an excellent natural insulator and moisture buffer. SE conditions of hemp (*Cannabis sativa*) are presented in Table 3.

Table 2 Component proportion in the volatiles (%).

Component and derivatives	Grey alder lignin			Birch lignin		Wheat straw lignin
	SE			SE	Bjorkman birch	SE
	N1	N2	N3	N4	N5	N6
Identified (% from pyrogram)	99.81	99.85	99.81	99.83	98.63	99.84
Sum (CO ₂ , H ₂ O, CH ₃ OH, CH ₂ O)	46.38	50.74	53.86	47.21	38.24	57.48
Carbohydrates	1.92	2.07	2.29	1.63	5.67	2.27
Lignin (including derivatives)	51.42	46.86	43.57	51.29	54.39	39.92
Phenyl and benzyl derivatives	2.95	2.97	2.93	1.47	1.42	4.10
Guaiacyl derivatives	13.22	13.57	12.88	10.11	13.22	23.91
Syringyl derivatives	35.25	30.32	27.76	39.71	39.75	11.91

Table 3 Steam explosion parameters.

Sample	Time, min.	T, °C	Pressure, MP.	Severity
R-00	0.0	235	3.2	1.87
R-05	0.5			3.67
R-10	1.0			3.98
S-30	3.0			4.45
S	sheared dried 2.5 cm pieces of stalks			
R	dry industrial dressing residues			

SE severity is an empirical parameter (Heitz *et al.* 1991), including temperature and time of the SE treatment.

Increasing of SE treatment time generates more guaiacyl- and syringyl- derivatives with shortened side chains (PhC0 +PhC1+PhC2)/PhC3 (Fig. 4).

Properties of SE shives are presented in Table 4. Pre-treatment by steam explosion improves the insulating properties of hemp shives increasing resistance to heat transfer from 13.2 to 23.2 m·K·W⁻¹ the improvement being achieved along with higher mass recovery at decompressing the biomass as soon as the pressure is reached. Density and heat conductivity of the exploded mass increase with the time the biomass is held under high temperature and pressure in the reactor. Therefore, any protracted treatment of shives being prepared for heat insulation should be avoided.

SE for composite as a natural fibre materials (PUTNINA *et al.* 2012)

Cellulosic fibres in micro- and nano-scale are attractive to replace man-made fibres for reinforcement to make environmentally friendly (green) products. Sustainability, industrial ecology, eco-efficiency, and green chemistry are guiding the development of the next generation of materials, products, and processes.

Hemp (*Cannabis sativa*) is one of the fastest growing plants with a potential in various industrial areas and it is suitable for temperate climate. Inside the hemp stems are bast fibres and the woody core. Hemp shives most widely used for bedding, mulch, chemical absorbents, and building materials (hemp-concrete, insulating filler), but they are not as widely used as a source of fibre. Therefore it is important to find new applications.

Table 4 Properties of SE hemp biomass.

Property		Samples			
		R-00	R-05	R-10	R reference
Mass recovery, %		97.58	93.77	86.96	100
Density, g cm ⁻³		0.043	0.063	0.089	0.064
Heat conductivity λ , W/(m·K)		0.043	0.045	0.055	0.076
Particle size, mm	< 0.2	1.51 %	1.67 %	3.44 %	1.08 %
	0.2-0.4	2.30 %	2.87 %	5.15 %	1.0 %
	0.4-0.6	3.14 %	4.55 %	6.50 %	1.10 %
	0.6-0.8	3.61 %	4.50 %	6.73 %	1.48 %
	0.8-1.0	6.46 %	13.48 %	11.71 %	4.86 %
	1.0-2.0	32.18 %	29.72 %	32.25 %	35.65 %
	> 2.0	50.79	43.20 %	34.21 %	54.83 %

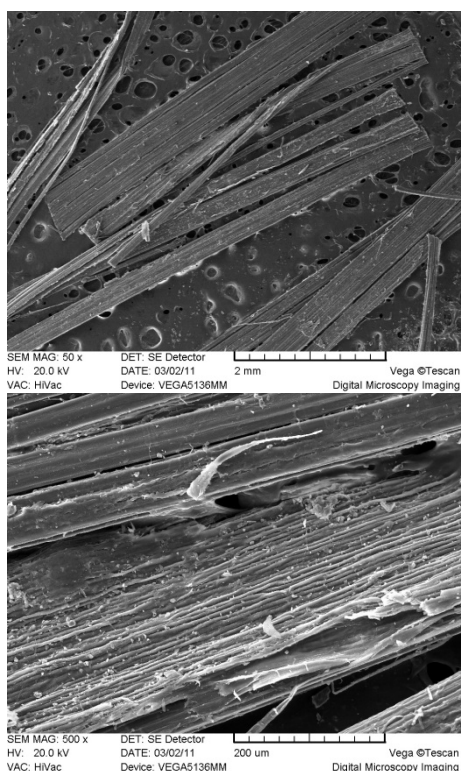


Fig. 5 SEM micrographs of hemp fibres control group sample before SE.

Several methods are used to extract highly purified micro-fibrils from the plant cell wall. They are generally based on successive chemical, chemical-physical and mechanical treatments. The steam explosion treatment (SE) is currently still being extensively studied as a promising pre-treatment method.

During the SE, the shives is exposed to high-pressure steam followed by rapid decompression resulting in substantial breakdown of the lignocellulosic structure, hydrolysis of the hemicelluloses fraction, depolymerisation of lignin components and defibrillation. By SE lignin is broken down making cellulose accessible for preparation of suspension or solution to further processing by electro-spinning. Electro-spinning (also, on deeper structural level – nano-

spinning) of natural fibres is a novel process for producing superfine fibres by forcing a solution through a spinneret with an electric field. Presently at Riga Technical University Institute of Textile Materials Technologies and Design in cooperation with the Laboratory of Biomass Eco-Efficient Conversion of the LSIWC has been realized SE pre-treatment of hemp fibres. The next step could be SE fibres electro-spinning. Effects of pre-treatment intensity, temperature, and pressure of steam explosion process were studied.

The hemp SE fibres characteristics were measured using scanning electron microscopy (SEM) and Fourier transform infrared spectroscopy (FTIR). SEM micrographs before (Fig. 5) and after (Fig. 6) SE treatment revealed principal changes of fibres ultrastructure.

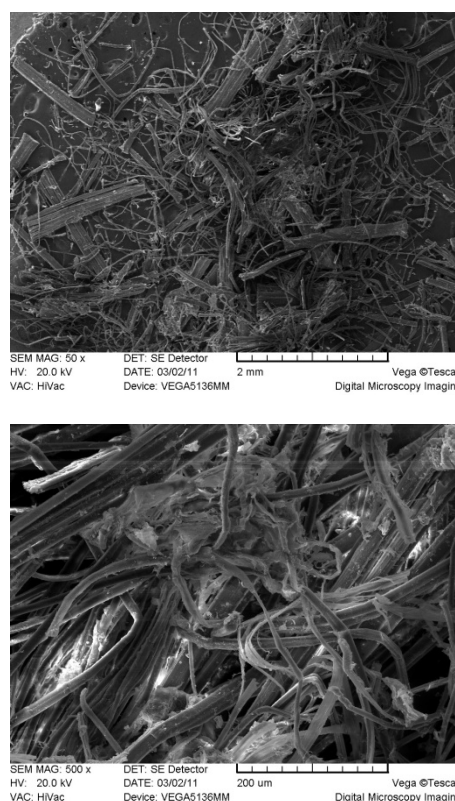


Fig. 6 Hemp fibres sample after SE (220 °C, 23 bar, 60s).

CONCLUSION

Steam explosion technique is the biomass materials pre-treatment method which corresponds to biorefinery and zero emissions concept demands. SE non sulphur chemically active lignin open road as new adhesive for composites: different boards, plywood, OSB, etc. Sulphur free lignin is key in production of self-binding boards and in processing and finished composites formaldehyde emissions are on zero level. SE demonstrated its potential in processing of insulating and textiles materials from hemp and flax. The electro-spinning will be perspective for cellulose materials after SE.

REFERENCES

- ABOLINS J. & GRAVITIS J. 2009: Energy from Biomass for Conversion of Biomass. *Latvian Journal of Physics and Technical Sciences*, 46(5): 16–23.
- ANDZS M., GRAVITIS J., VEVERIS A. & ABOLINS J. 2012: A novel ecological heat-insulating composite of steam exploded biomass. Accepted to 20th Annual Internationale Conference on Composites and Nano Engineering, Beijing, China, July 22–28.
- GRAVITIS J. 1987: Theoretical and applied aspects of the steam explosion plant biomass autohydrolysis method. *Review. Wood Chemistry* 5: 3–21 (in Russian).
- GRAVITIS J. 2008a: Biorefinery: Biomaterials and Bioenergy from Photosynthesis, Within Zero Emissions Framework. In: *Sustainable Energy Production and Consumption. Benefits, Strategies and Environmental Costing*. NATO Science for Peace and Security, Barbir F., Ulgiati S., (Eds.), Springer, 327–337.
- GRAVITIS J., ABOLINS J. & KOKOREVICS A. 2008b: Integration of biorefinery clusters towards zero emissions, *Environmental Engineering and Management Journal*, 7(5): 569–577.
- GRAVITIS J., ABOLINS J., TUPCIAUSKAS R. & A. VEVERIS 2010: Lignin from steam-exploded wood as binder in wood composites. *Journal of environmental engineering and landscape management*, 18(2): 75–84.
- HEITZ, M., E. *et al.* 1991: Fractionation of *Populus tremuloides* at the pilot plant scale: Optimization of steam pretreatment conditions using STAKE II technology. *Biores. Technol.* 35: 23–32.
- PAULI G. 1998: *Upsizing: The Road to Zero Emissions. More Jobs, More Income and no Pollution*, Greenleaf, Sheffield.
- PUTNINA A., KUKLE S. & GRAVITIS J. 2012: Innovative Technologies based on Latvian Renewable Natural Resources. Accepted to 3rd International Conference on Integrative Approaches Towards Sustainability „Sustainable development, knowledge society and smart future manufacturing Technologies”, Jurmala, Latvia, June 27–30.
- TUPCIAUSKAS R. *et al.* 2012: Grey Alder Pretreatment by Steam Explosion for Self Adhesive Composites. Submitted to 8th meeting „Northern European Network for Wood Science and Engineering (WSE) in Lithuania, 2012, October 27–28.

Acknowledgments

The studies have been supported by the National Research Program on sustainable use of local resources, new products, and technologies, and by EU Framework 7 Wood Wisdom program, Project ProLignin.

THERMAL INSULATION CAPACITY OF CHIPPED OAK BARK IN DIFFERENT COMPRESSION LEVEL

ILDIKÓ RONYECZ & ZOLTÁN PÁSZTORY

University of West Hungary, Faculty of Wood Science, 4. Bajcsy Zs. Sopron Hungary 9400

Abstract

Nowadays it is emphasized the importance of improving thermal property of different insulation materials. The forest companies and wood working factories, especially sawmills, produce high amount of wood bark in different shapes. The CO₂ balance of wood bark is excellent facing other generally used insulation materials. The bark is mainly “byproduct” of wood industry and the bark insulation can be reuse on the end of its life cycle.

In the present research investigated the thermal insulation capacity of chipped sessile oak bark (*Quercus petraea*). The compression level of chipped bark influences the thermal conductivity of bark-air composite system, shows the experiments. Thermal conductivity decreases as the thickness of the system is decreasing from 10 cm to 6.5 cm. After a special compression point, the thermal conductivity of bark-air system turn to increase.

Keywords: bark, oak, thermal insulation.

INTRODUCTION

In the last decades CO₂ emission is in the center of interest. Buildings energy consumption for heating and cooling is responsible for one third of this emission. Because of the rising energy prizes more interest is attended to the energy efficiency of homes, thus the improvement of different insulation materials is in the focus of researches (GRÖSCHE 2009; OMER 2009). Utilization of wood became more and more popular in the building industry because of its low CO₂ emission and low energy consumption during processing. Wood is recyclable and able to reduce environmental damage by bonding CO₂ from the air (RONYECZ 2011) in contrast with other building materials such as concrete stone brick and metals and plastics. Wood based materials have low energy demand during product processing, thus represent lower environmental load than that of silicate basic materials.

The bark is the most important protecting layer of the living tree. Bark separates wood part of the plant from outer world and shelters from bad weather conditions or biological attacks like pests and fungus (MOLNÁR *et al.* 2007).

The bark can be divided into two parts: the outer bark (phloem) and inner bark (ritidoma). The inner bark can be quite thick and contain long fibers especially in case of some broad leaved wood species, although there might be significant differences among species (MOLNÁR 2004). Some bark types are rich in fibers e.g. black locust poplar oak others contain lower amount of fibers e.g. pine (LOTOVA 1987).

The yearly harvested wood quantity contains 500–600 thousand m³ bark in Hungary (BÖRCSÖK 2010). Bark content can occupy 10–20% of the whole volume of the tree (SOPP and KOLOZS 2000). The living bark has an important role, it protects the wood against many outer impacts and provides habitat for several ecosystems as well (MICHEL *et al.* 2011, MACFARLANE and LUO 2009). Bark protects the cambium from harmful effect of forest fire (BAUER *et al.* 2010, WANG *et al.* 2011). During the wood processing the bark mostly constrained to a by-product position. Many alternative researches have done to find appropriate use of bark mainly in North America and Europe in the last decades. Because of the small dimensions and the low firmness the bark can be used in chopped form. The bark of processed wood is mostly used for energy production (RAGLAND *et al.* 1991), mulching in other words soil covering (CMGP 2009, SÁRI 2007, HARKIN *et al.* 1971) different types of coating (GERENCSÉR 2010), or production of medicaments (LIU *et al.* 2007, VASCONCELOS *et al.* 2011).

Present research aimed at to find an alternative use for wood bark on the field of energy saving as thermal insulation material. It was investigated the thermal conductivity of chipped oak bark in different compression level.

MATERIALS AND METHODS

One of the most popular wood species is the oak in the Hungarian forests. More than one fifth of Hungarian forest is oak (Table 1), however it imply the sessile the pudenkulate and downy and red oak

Wood the Best Material for Mankind

J. Kúdela & M. Babiak (eds.), 2013, pp. 85–88

© Arbora Publishers, Zvolen, Slovakia

ISBN 978-80-968868-6-9

species. The oaks have a distinguish position in the harvested wood quantity. In addition the prizes of oak logs are one of the highest between the temperate forest species. For these reasons was chosen the bark of sessile oak to be investigated. The bark ratio is quiet high in the case of sessile oak; it can reach 15-18% depending on the age and diameter of the tree. Inner bark content is high also, but the ratio is variable depending on the age of the timber.

The sample pieces were chipped with a hammer grinder chipping equipment without sieve. The lack of the sieve causes that the size of chipped particles become significantly different. We did not use regrinding technology and did separate neither the bigger nor the smaller particles from the fraction. Particle sizes are shown in the Table 2 and Figure 1 shows the view of chipped particles. The tight long shape inner bark fibers are similar to the wood wool. Outer bark fragments implying different sizes, but mainly with clod shapes.

The heat flow through chipped bark sample made of oak bark was measured. To ensure the perpendicular heat fluxes to the surface, the width was at least 5 times higher than the thickness. The lateral heat fluxes will be reduced by use of insulation at the sides. The side insulation boundary keeps the form of wood bark chips.

The initial oak bark samples dimensions were 500 mm × 500 mm × 10 mm. The coefficient of thermal conductivity was determined by

measurement of the steady state heat flow through the sample.

$$Q = \frac{\lambda \times A \times \Delta T}{d}$$

Where: d is the thickness of the model and ΔT is the temperature difference between hot and cold sides in degrees Kelvin. The measuring heat flux meter was positioned in the middle of hot plate with the size of 120 × 120 mm. These Q values were obtained under steady state conditions for ΔT differences between two sides of the sample.

Thermal conductivity measuring instrument executes the measurement per minute automatically. In the experiments was used the same amount of chipped bark in the different compression level.

The initial thicknes of chiped bark sample was 10 cm as a first step of research progress. After the first measurement the sample thickness was decreased to 9.5 cm. The 10 cm thick bark-air composite system was compressed to 9.5 cm. The measurement was done repeatedly in the above mentioned way. Sample thickness was decreased with 0.5 cm in every next measurement stages till 6 cm. At the last compression steps was possible to be done with special local compression technique, because the high compressive strength of the chipped bark. The further compression had endangered the sensible heat flux meter built in the hot plate.

Table 1 Distribution of wood species in the Hungarian forests and the gross amount of harvested wood in Hungary (source: MOLNÁR 2009).

Wood Species	1000 m ³	%	1000 ha	%	Bark content %
Oak	1089	16.6	380.6	21.9	15
Black locust	1206	18.2	385.0	22.2	20
Poplar	1076	16.2	165.1	9.5	15
Turkey Oak	832	12.6	198.1	11.4	16
Beech	649	9.8	109.5	6.3	5
Hornbeam	309	4.7	104.3	6.0	8
Other deciduous trees	509	7.7	168.5	9.7	–
Pine	938	14.2	226.7	13.0	10
All	6609	100	1737.8	100.0	–



Fig. 1 Structure of chipped oak bark.

Table 2 Particle size in the wood chips without phloem.

	Size of particles (mm)
Thickness	1–26
Width	1–27
Length	1–100

RESULTS

Because of the high number of measurement and the stable steady state heat flow the time of the measurement sequence took a long time. The final result comes from the average value of the last 100 measurement.

The measurements were performed between 6–10 cm samples of varying thickness. The results are shown on the graph in Figure 2.

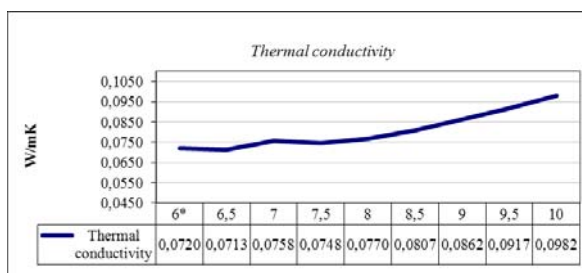


Fig. 2 Thermal conductivity of chipped oak bark depending on the compression level.

Thermal conductivity decreases as the thickness of the system is decreasing from 10 cm to 6.5 cm. After a special compression point the thermal conductivity of bark-air system turn to increase. The curve between 10 and 7.5 cm draw clearly the physical phenomenon, but in higher compression level than 6.5 cm it turning to increase again.

CONCLUSIONS

The oak chipped bark has a better insulation capacity if the compression level is increasing from 10 cm to 6.5 cm. Further compression causes the thermal insulation capacity turning to rise again. The minimum thermal conductivity point of investigated air-chipped bark system seems to be around 6.5 cm with the value of thermal conductivity 0.0713 W/mK, in this point the bark-air ratio of the system achieve the ideal proportion. We would emphasize that the fraction of the chips importantly influences the system properties including the coefficient of thermal conductivity and the ideal proportion of lowest value. The exploration of the effect of fraction needs further investigation. According to the results we can state that the thermal conductivity of chipped bark is not far from the commonly used insulation materials such as polystyrene and rock or glass wool. Thermal conductivity of chipped bark is almost the same level as the insulation material made of natural fibers or paper fibers. More details are needed to be explored for developing higher insulation efficiency of insulation system based on wood bark. We would conclude by saying that the results of this research have an importance in two main fields. The first one: Thermal conductivity of chipped wood bark is

almost the same than that of the commonly used insulation materials.

The second one: The research results prove that it is possible to use natural raw material with low energy consumption for producing a competitive and environment friendly products.

The competitiveness has to come not only from the performance of the product but the ratio of environment pollution (including the energy consumption) and the performance of the product in the future.

REFERENCES

- BAUER G., SPECK T., BLÖMER J., BERTLING J. & SPECK O. 2010: Insulation capability of the bark of trees with different fire adaptation. *J Mater Sci.* 45: 5950–5959
- BÖRCSÖK Z. 2010: Erdő- és fagazdálkodás, (Forest and Wood Management) Digital lecture notes, Sopron.
- Colorado Master Gardeners Program (2009): Mulching with Wood/Bark Chips, Grass Clippings, and Rock, Colorado State University Extension.
- GERENCSÉR, K. 2010: Fűrészipari technológia. (Saw mill technology) Elektronikus oktatási segédlet, Sopron.
- GRÖSCHE P. 2009: Measuring residential energy efficiency improvements with DEA. *J. Prod. Anal.* 31: 87–94.
- HARKIN M. J. & ROWE W. J. 1971: Bark and its possible uses. Forest Service US. Madison.
- LIU Z., ZHANG X., CUI W., ZHANG X., LI N., CHEN J., WONG W. A. & ROBERTS A. 2007: Evaluation of short-term and subchronic toxicity of magnolia bark extract in rats. *Elsevier* 49, 160–171.
- LOTOVA L.I. 1987: Anatomiya kory khvoynikh (Anatomy of Bark in Conifers), Moscow: Nauka, 1987.
- MACFARLANE D. W. & LUO A. 2009: Quantifying tree and forest bark structure with a bark-fissure index. *Can. J. For. Res.* 39: 1859–1870
- MICHEL A.K., WINTER S. & LINDE A. 2011: The effect of tree dimension on the diversity of bark microhabitat structures and bark use in Douglas-fir (*Pseudotsuga menziesii* var. *menziesii*). *Can. J. For. Res.* 41(2): 300–308.
- MOLNÁR S. 2004: Faanyagismeret. (Wood Material Science) Mezőgazdasági Szaktudás Kiadó, Budapest.
- MOLNÁR S., PESZLEN I. & PAUKÓ A. 2007: Faanatómia. (Wood anatomy) Szaktudás Kiadó Ház, Budapest, pp. 78–84.
- MOLNÁR S. 2009: MTA: Erdőgazdálkodás és fahasznosítás: jelen-jövő. (Forest management: present and future) Conference performance, Budapest.
- OMER A. M. 2009: Energy use and environmental impacts: A general review. *J. Renewable Sustainable Energy*, 1, Article Number: 053101.
- RAGLAND K. W., AERTS D. J. & BAKER A. J. 1991: Properties of Wood for Combustion Analysis *Bioresource Technology* 37: 161–168.
- RONYECZ I., MOHÁCSI K. & PÁSZTORY Z. 2012: Néhány hazai fafaj kérgének hőszigetelő képessége. (Bark thermal insulation capacity of some domestic wood species) *Faipar, LX/1*: 16–21.
- RONYECZ, I. 2011: Faház kontra CO₂ (Wood house facing CO₂) *Gerendaházak, VI. évf. 2 szám*, 11. Oldal.

- SÁRI, J. SZ. 2007: Tőzeghelyettesítő anyagok a paprikahajtásban. (Peat substitute materials) PhD thesis, BCE, Budapest.
- SOPP L. & KOLOZS L. 2000: Fatömegszámítási táblázatok. (Wood volume calculating tables) Department of Hungarian State Forest, Budapest, pp 24–27.
- VASCONCELOS C. F., MARANHÃO H. M., BATISTA T. M., CARNEIRO E. M., FERREIRA F., COSTA J., SOARES L. A., SÁ M. D., SOUZA T. P. & WANDERLEY A. G. (2011): Hypoglycaemic activity and molecular mechanisms of *Caesalpinia ferrea* Martius bark extract on streptozotocin-induced diabetes in Wistar rats. Department of Pharmaceutical Sciences, 137(3):1533–1541.
- Wang G.G. & Wangen S.R. 2011: Does frequent burning affect longleaf pine (*Pinus palustris*) bark thickness?, Can. J. For. Res. 41: 1562–1565.

FEASIBILITY OF REINFORCING BIRCH PLYWOOD WITH HEMP FIBRES

GINTS UPITIS¹ & JANIS DOLACIS²

¹Riga Technical University, Faculty of Materials Science and Applied Chemistry, Riga, Āzenes iela 14/24-269, LV-1048, Latvia, gints.upitis@rtu.lv

²Latvian State Institute of Wood Chemistry, Riga, Dzērbenes iela 27, LV – 1006, Latvia, dolacis@edi.lv

Abstract

The present paper reflects searches for solving the problems of enhancing the strength of plywood, reinforced with hemp fibres. A radical possibility of obtaining a new environmentally friendly material with enhanced strength characteristics is shown. The modern developing society has faced the problem of ever increasing demands for the energy intensity of production and the limited potentialities of meeting them. Recently, the worldwide demand for the sources of natural renewable resources has grown, governed by the energy saving and environmentally friendly technologies of their production, and the feasibility of their processing to environmentally friendly, biodegradable materials with a high added value due to the decrease of material and energy costs. One of such resources is hemp, which is rather profitable, requires much less amounts of artificial fertilisers than other cultures, has a favourable effect on the agroecosystem, improves the soil structure, and inhibits weeds, pests and diseases. Hemp fibre is one of the strongest natural fibres and its characteristics (high tensile strength, wet state strength, etc.) make it technically feasible for the production of different industrial products.

It is shown that the reinforcement of birch five-layer plywood by hemp textiles with a cell size of 8 mm makes it possible to produce an environmentally friendly composite material. Optimal ratios of the components and the binder for producing a composite material of birch plywood, reinforced by hemp textiles, with enhanced mechanical characteristics in bending σ_{bend} up to 13.2 % and modulus of elasticity up to 10.3 % have been found. The given composite material can be used for the production of curved-glued furniture and other goods from plywood.

Keywords: Reinforced plywood, hemp, phenol-formaldehyde resin, polyvinyl acetate glue.

INTRODUCTION

The modern developing society has faced the problem of ever increasing demands for the energy intensity of production and the limited potentialities of meeting them. In recent years, the worldwide demand for the renewable sources of natural resources is growing, governed by the energy saving and environmentally friendly technologies of their production, and the feasibility of their processing to environmentally friendly, biodegradable materials with a high added value due to the decrease of material and energy costs. Particular attention is being given to materials from natural fibres and their wide application in various branches of industry. One of such resources is hemp, which is rather profitable, requires much less amounts of artificial fertilisers than other cultures, has a favourable effect on the agroecosystem, improves the soil structure, and inhibits weeds, pests and diseases. Hemp fibre is one of the strongest natural fibres and its characteristics (high tensile strength, wet state strength, etc.) make it technically feasible for the production of different industrial products. Hence, hemp is regarded as one of the most promising sources of renewable resources as a

component for producing a wide range of manufactured goods.

Recently, the cultivation of the technical culture of hemp in the area of hundreds of hectares has been common in Latvia. For processing hemp products (fibres and stems) into innovative products, universal studies on the sorts cultivated in local climatic and soil conditions, and their comparative analysis are required. It is shown that the mechanical characteristics of hemp fibres depend on both the sort and the growing conditions (FREIVALDE *et al.* 2010). In recent years, crops of hemp for technical purposes are receiving wide acceptance worldwide; especially inexpensive this production is in China, Bangladesh and India (SMALL *et al.* 2002). Hemp crops become popular also in the south of the USA and Canada (SMALL *et al.* 2002, EHRENSING 1998). In Bolton's (1995) opinion, hemp, so that to become competitive, should meet the following requirements: the material should be produced in sufficiently large volumes; the price should be low enough; the fibre characteristics should be stable within the whole service life, and the used technologies of treating the new raw material should be reasonable and approbated for its processing. When selecting technical sorts of hemp,

in contrast to narcotic strains, an important factor is the substantial volume, occupied by the lignified part of the cross-section of the stem of the latter (MEIJER 1995). One of the reasons for the wide use of hemp fibre is its length. The length of the primary bast fibres in bark reaches 5–40 mm, which are joined in fibre bundles and can reach the length of 1–5 m (average length of secondary bast fibres is about 2 mm). For example, hardwood fibres are much shorter, namely, about 0.55 mm and are connected with a considerable content of lignin (BOLTON 1995). Hemp fibre can potentially substitute other fibres of plant origin, but cannot compete with minerals from glass fibre, as well as aluminium and other metals. Tests of polymer coatings and films, reinforced with mesh knit fabric, have been carried out in Uzbekistan (RAKHIMOV *et al.* 2008). Studies on the physico-mechanical properties of plywood, reinforced with glass fibre, using phenol-formaldehyde resins as a binder, have been successfully carried out in the Czech Republic (KRÁL *et al.* 2008).

MATERIALS AND METHODS

In the present study, searches for solving the problem

of enhancing the strength of glued birch five-layer plywood, reinforced with a hemp textile, are considered. One of the methods is to reinforce the glued plywood with separate hemp fibres and a hemp textile. To optimise the conditions of the formation of such a composite material, the multi-factor analysis was employed (Tables 1 and 2).

As a binder, a mixture of phenol-formaldehyde resin and polyvinyl acetate glue PVA was used. The variation levels of the variable factors were chosen based on the earlier experiment.

The experiment was planned as a multi-factor experiment with 5 variables (Table 3).

For each group of the variable factor of the experiment, 10 samples 200 mm in length and 50 mm in width were made, in which the direction of the fibres of the veneer of the outer layers of the sheets was parallel to the sample's length, and the same number of samples, in which the direction of the fibres of the veneer of the outer layers of the sheets was perpendicular to the length of the sample. For all samples, birch rotary cut veneer with a width of 1.5 mm was used.

Table 1 Factors, influencing the physico-mechanical characteristics of plywood.

Constant factors			Value
Designations	Name	Unit of measurement	
<i>x</i> 6	Moisture of veneer	%	8
<i>x</i> 7	Relative humidity of air	%	49
<i>x</i> 8	Room temperature	°C	22
<i>x</i> 9	Wood density	kg/m ³	617
<i>x</i> 10	Amount of the binder	g/m ²	170
<i>x</i> 11	Viscosity of the binder at 24°C	mPa·s	5842.2
<i>x</i> 12	Number of the veneer layers	pieces	5
<i>x</i> 13	Veneer thickness	mm	1.5
<i>x</i> 14	Veneer sheets' orientation	I – I – I	1
<i>x</i> 15	Holding time upon gluing	min/mm	5.42
<i>x</i> 16	Gluing temperature	°C	90

Table 2 Factors, influencing the physico-mechanical characteristics of plywood.

Variable factors			Value of the "0" level
Designation	Name	Unit of measurement	
<i>x</i> 1	Pressing pressure	MPa	1.5
<i>x</i> 2	Hemp mesh cell size	mm	8
<i>x</i> 3	Hemp mesh tension	N	20
<i>x</i> 4	Mass of the binder (per 100 g of resin)	g	20
<i>x</i> 5	Mass of PVA per 100 g of resin	g	12

Table 3 Intervals and levels of the variation factors.

Factors			Variation levels			Inter-vals
Designation	Name	Unit of measurement	–1	0	1	
<i>x</i> 1	Pressing pressure	MPa	1.3	1.5	1.7	0.2
<i>x</i> 2	Hemp mesh cell size	mm	4	8	12	4
<i>x</i> 3	Hemp mesh tension	N	10	20	30	10
<i>x</i> 4	Mass of the binder (per 100 g of resin)	g	17	20	23	3
<i>x</i> 5	Mass of PVA per 100 g of resin	g	10	12	14	2

To make experimental samples, a bicomponent mixture of the resin "Casco Adhesives' UF 1274" with the hardener 2545 ("Akzo Nobel") and polyvinyl acetate glue D3, group "Tempo 303" ("KLEIBERIT") were used. The samples were glued up in a hot press ("Schmersal Joos"). The physico-mechanical characteristics of the samples were determined according to the requirements of the European and Latvian standard LVS EN 310:2001 (Wood-based panels; determination of modulus of elasticity in bending and of bending strength). Based on the experimental data, a mathematical variation modelling of the intervals of variable factors was performed.

RESULTS AND DISCUSSION

Values of coefficients were calculated, and the regression equation was set up: $Y = 95.94 - 3.26 \cdot x_1 - 1.71 \cdot x_2 - 1.99 \cdot x_3 + 2.61 \cdot x_4 + 1.81 \cdot x_5$, from which it can be seen that, with decreasing factors x_1 , x_2 and x_3 and with increasing factors x_4 and x_5 , it is possible to improve the deformation indices of the hemp fibre reinforced birch plywood. Levels of significance coefficients are calculated, and the upper and lower limits of the theoretically permissible variables of the variation factors are calculated. The calculations show that, at the described conditions of the experiment, the average index of the value of the ultimate strength in statistical bending σ_{bend} for such a material increases by 13.2 %.

CONCLUSIONS

1. It is shown that, based on reinforcing birch five-layer plywood with hemp textile (mesh) with the cell size 8 mm, it is possible to produce an environmentally friendly composite material.
2. Optimal ratios of the components and the binder for producing a composite material - hemp textile reinforced birch plywood with enhanced mechanical characteristics in bending σ_{bend} up to 13.2 % and modulus of elasticity up to 10.3 % have been found.
3. The given composite material can be used for the production of curved-glued goods from plywood.

REFERENCES

- BOLTON, J. 1995: The potential of plant fibres as crops for industrial use. *Outlook Agr.*, 24: 85–89.
- EHRENSING, D.T. 1998: Feasibility of industrial hemp production in the United States Pacific Northwest. Department of Crop and Soil Science, Oregon State Univ. Expt. Sta. Bul. 681. Oregon State University, Corvallis. www.css.orst.edu/Hemp/body.html.
- FREIVALDE, L., KUKLE, S. & ULME, A. 2010: Comparative analysis of hemp fiber durability. *Scientific Journal of Riga Technical University. Material Science. Textile and Clothing Technology*, 5: 134–138.
- GROOT, B. DE, G.J. VAN ROECKEL JR. & J.E.G. VAN DAM. 1998: In: P. Ranalli (ed.), *Advances in hemp research*. Food Products Press (Haworth Press), London. p. 213–242.
- KRÁL, P. & HRÁZSKÝ, J. 2008. A contribution to the resistance of combined plywood materials to abrasion. *J. For. Sci.*, 54: 31–39.
- MEIJER, E.P.M. DE 1995. Diversity in *Cannabis*. In: Nova Institute, *Bioresource Hemp. Proc. Symp.* (Frankfurt am Main, Germany, March 2–5, 1995). 2nd ed. HempTech, Ojai, CA. p. 143–151.
- SMALL, E. & D. MARCUS 2002. Hemp: A new crop with new uses for North America. In: J. Janick and A. Whipkey (eds.), *Trends in new crops and new uses*. ASHS Press, Alexandria, VA. p. 284–326.
- RAKHIMOV, F.H., MIRZAEV, N.B. & RAFIKOV, A.S. 2008. Polymer coatings and films, reinforced with mesh knit fabric. *Plasticheskie Massy*, 9: 49–51 (in Russian).

POLYETHYLENE TEREPHTHALATE RECYCLING IN PARTICLE BOARD PRODUCTION

JÁN IŽDINSKÝ, VIKTOR TÓTH & JOZEF KÚDELA

Faculty of Wood Sciences and Technology, Technical University in Zvolen, T.G. Masaryka 24, SK-960 53 Zvolen, Slovakia
e-mail: izdinsky@tuzvo.sk, viktor.toth1989@gmail.com, kudela@tuzvo.sk

Abstract

Waste recycling does not only concern the waste disposal, it is also one of promising approaches in facing the increasing shortage in the natural raw materials. This paper presents the results of a laboratory study of how polyethylene terephthalate (PET) recycled flakes admixed into wood particle boards (PB) in different amounts and in different layers affected selected properties of the modified boards. On one hand, the PET admixture resulted in poorer mechanical properties; on the other hand, it improved the boards' resistance against water (reduced thickness swelling and water absorption). These properties also depended on the amount of PET flakes added into the boards as well as the location of this flakes within the board (surface layers, core layer).

The recent research has revealed that PET surface treatment with plasma can improve adhesion properties of this material and thus also the properties of PBs with PET admixture.

Key words: particle boards, PET, pressing process, physical and mechanical properties.

INTRODUCTION

A very serious environmental issue at the present is waste disposal. The concern is about individual components of communal waste as well as about waste produced in various industrial branches. Primary important is the problem of waste from polyethylene terephthalate (PET) packing materials, especially PET bottles. Recycling methods for PET packing materials are sought to obtain raw materials with specific secondary use. One of such possibilities arises also in wood industry (OZALP, 2011, TÓTH *et al.* 2012).

The increasing production of large-area wooden materials and the limited natural sources of wood raw material are responded by permanently increasing prices of both compact and disintegrated wood (sawdust, chips). New raw materials are necessary to substitute natural wood in production of certain types of wooden materials (especially particle boards PB). In the recent years, the research has mainly been focused on supplementing ligno-cellulose plants and their lignified parts and also supplementing old, recycled wood in wooden materials manufacturing (SAMIR *et al.* 2005, KLYOSOV 2007, LI *et al.* 2010, PANAITESCU *et al.* 2011, SOBCZAK *et al.* 2012, VRÁBELOVÁ *et al.* 2006, RÉH and VRTIELKA 2011, RÉH *et al.* 2012 and others).

Another approach is to combine wooden components with synthetic thermo-plastic materials (PP, PE, PVC, ...). In this way are obtained new materials recognised as wood-plastic composites (MORTON and ROSSI 2003, KLYOSOV 2007, AYRILMIS *et al.* 2012).

The aim of this work was to prepare a wood particle board supplemented with PET flakes and to study how the amount and allocation of PET component in wood particle boards affected selected physical and mechanical properties of such modified materials.

MATERIALS AND METHODS

The problem was investigated on five model PB variants prepared in the laboratory of the Technical University in Zvolen:

- V1 – without PET admixture – control,
- V2 – PET admixture representing 10 % in the surface layer and 0 % in the core layer,
- V3 – PET admixture representing 0 % in the surface layer and 10 % in the core layer,
- V4 – PET admixture representing 10 % in the surface layer and 10 % in the core layer,
- V5 – PET admixture representing 30 % in the surface layer and 30 % in the core layer.

The wood particles for PB production were coniferous – a mixture of spruce and fir. The average moisture content in particles adjacent to the glue line was 5.2 %, in the particles in core layers 3.9 %. The weight ratio between the surface and core layers was 40:60. We used urea-formaldehyde glue with 67% solid content. The glue proportion applied onto the surface particles represented 11 % and onto the core particles 7 %. The hardener was a 55% solution of ammonium nitrate. The PBs were also supplemented with a paraffin emulsion with 35 % solid content,

applied onto the surface and core particles in a proportion of 0.85 %.

The recycled PET waste was provided by the General Plastic Ltd, the leading PET waste processing plant in Slovakia. The proportions of individual wood particle fractions in the surface and core layers and proportions of PET flakes determined by sieving analysis are in Fig.1.

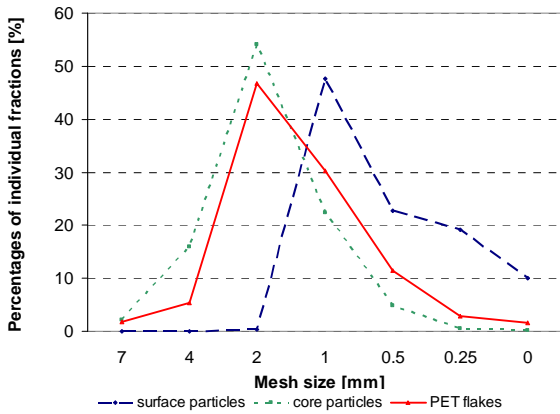


Fig. 1 Wood particles and PET flakes fractions.

The particle boards were pressed according the pressing diagram illustrated in Fig. 2, at a pressing temperature of 210 °C and a pressing factor of 14 s.

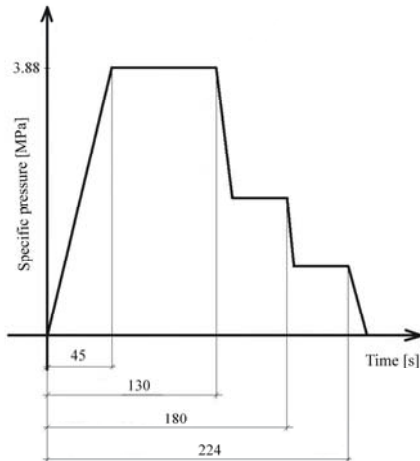


Fig. 2 Pressing diagram.

The size of the boards was 360 × 360 mm, the thickness was 16 mm. Each PB variant was produced in 3 pieces, altogether 15. The average density of the boards was 613–639 kg·m⁻³ (Fig. 3).

From these boards, there were cut specimens (see schedule in Fig. 4) for testing the following physical and mechanical properties: water absorption (WA) and thickness swelling after 24 hours (STN EN 317) and tension strength perpendicular to the plane (STN EN 319) with bending strength (STN EN 310).

Before the testing, the test specimens were conditioned at a relative air humidity $\phi = 65 \%$ and a temperature of $20 \pm 2 \text{ }^\circ\text{C}$.

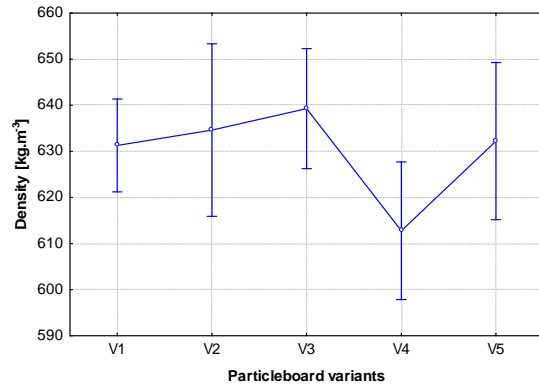


Fig. 3 Density of wood particle boards with various PET fractions.

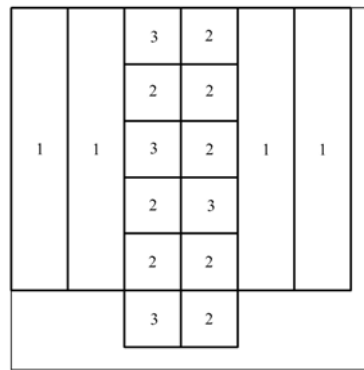


Fig. 4 Schedule for preparing test specimens (1 – bending strength, 2 – tension strength perpendicular to the plane of the board, 3 – thickness swelling and water absorption).

RESULTS AND DISCUSSION

The differences between the PB variants were examined by one-way analysis of variance. The analysis resulted in detecting differences in physical and mechanical properties between PB with and without PET admixture in all variants. In all cases, the added PET significantly reduced WA after 24h of immersion in water (Fig. 5). The 10% proportion of PET in the surface or core layers caused an 18% decrease in boards' WA. Addition of more PET flakes into the whole board profile resulted in a slight increase in WA, which we judge due to the lower density (Fig. 3) and thus increased porosity of the PBs. PET admixed in an amount of 30 % into both the surface and core layers reduced PB water absorption after 24h immersion in water by 30%.

In swelling, distinct reduction (40 %) was only observed in case of 30 % PET proportion through the whole PB volume (Fig. 6). This might have been due to the reduced soaking capacity, but we assign the main cause to the 30% reduction of swelling wood particles replaced by water resistant PET flakes.

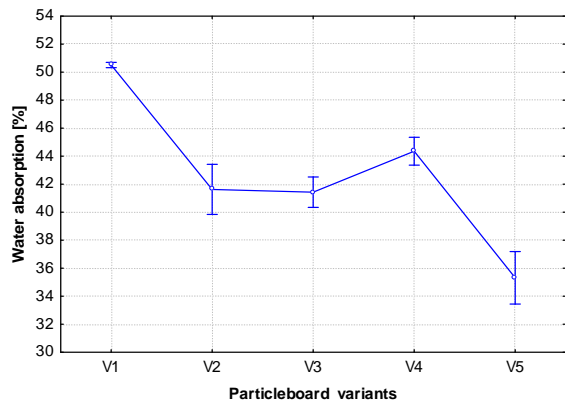


Fig. 5 Water absorption of wood particle boards differing in PET admixture, after 24h immersion in water.

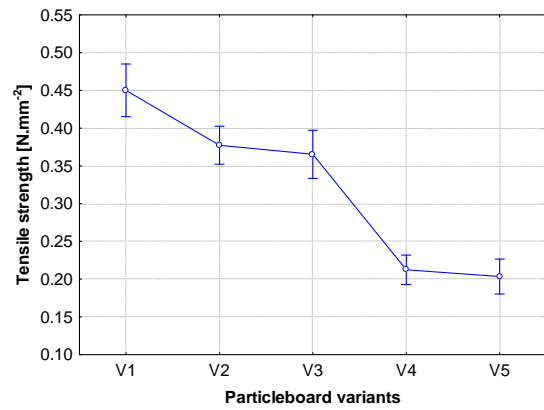


Fig. 8 Tension strength perpendicular to the plane in individual PB variants.

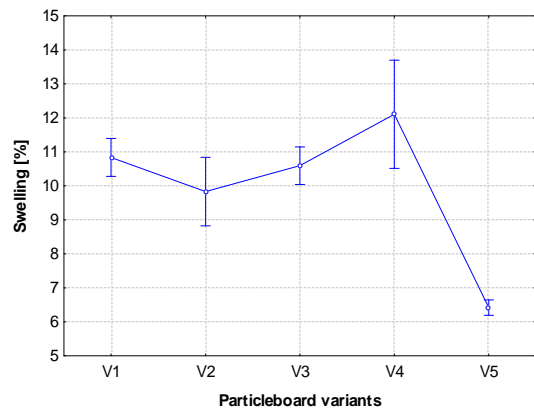


Fig. 6 Thickness swelling of wood particle boards differing in PET admixture, after 24h immersion in water.

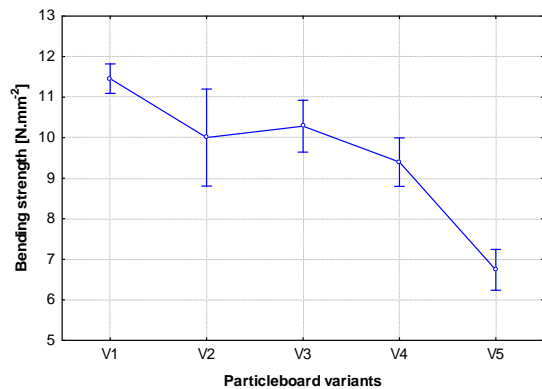


Fig. 7 Bending strength of individual PB variants.

On the other hand, the PET admixture in PBs had negative effects on mechanical properties of these boards. Bending strength decreased with increasing proportion of PET flakes (Fig. 7). The 10% PET admixture into either surface or core layers resulted in strength reduction by 12 %, the same PET proportion in both layers reduced the strength by 17 %, and the 30% PET proportion in both layers by even 42 %.

A similar trend was also observed in case of tensile strength perpendicular to the plane (Fig. 8).

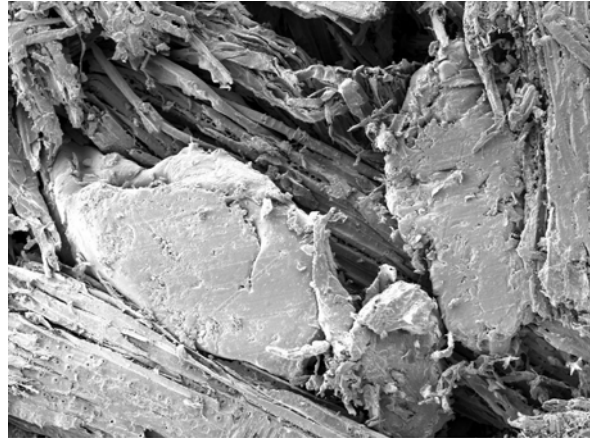
The 10% PET admixture into either surface or core layers resulted in average tensile strength reduction by 16 %, the same PET proportion in both layers reduced the strength by 53%. In our opinion, this considerable decrease was primarily due to the lower density of the boards, as the 30% PET admixture did not cause more decrease in tensile strength.

Investigating of PB structure, we detected PET flakes filling the space among wood particles (Fig. 9). In the surface layers, under a temperature of near 200 °C, some PET flakes were melting (Fig. 10) and compacted to some extent with the adjacent wood particles. The result was the substance insulating particularly the wood particles against the water. The filling of void space among wood particles and melting PET flakes on PB surface reduced the water absorption and swelling of the boards.

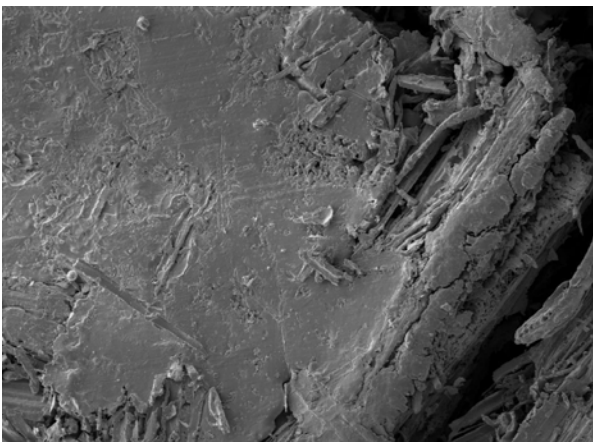
Inwards the core layers, the pressing temperature decreased to about half the value on the board surface. Under this temperature, the PET flakes maintained their original shape and did not link with the wood particles (Fig. 11). The urea-formaldehyde glue did not create glued joints between PET flakes and wood particles. We suppose that the cause may be in very low surface energy of PET causing poor wetting of this material. This affected the poor adhesion between the PET and glue in both liquid and cured state. Here we also see the cause of the PB strength decrease with increasing PET presence in the boards. This is above all evident for tension perpendicular to the plane of the board when impairment occurs in the core layer the density of which is lower than the density of surface layers (ŠTEFKA 1996). The lack of glue joints between wood particles and PET flakes exaggerated the effect of PET presence in the core layer, and this was responded by a considerable drop in tension strength perpendicular to the plane. We propose to solve this problem by surface treatment of PET flakes, especially by increasing their surface energy and, consequently, adhesion to the glue. FLORIÁN *et al.* (2012) have shown that this is possible by treating PET with plasma.



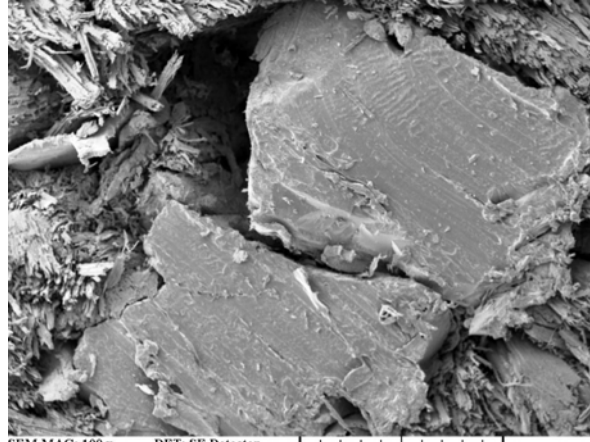
Fig. 9 Surface of particle board containing 30% PET.



SEM MAG: 200 x DET: SE Detector
HV: 15.0 kV DATE: 04/04/11
VAC: HiVac Device: TS5130
500 µm Vega ©Tescan
Katedra náuky o dreve - DF TU Zvolen

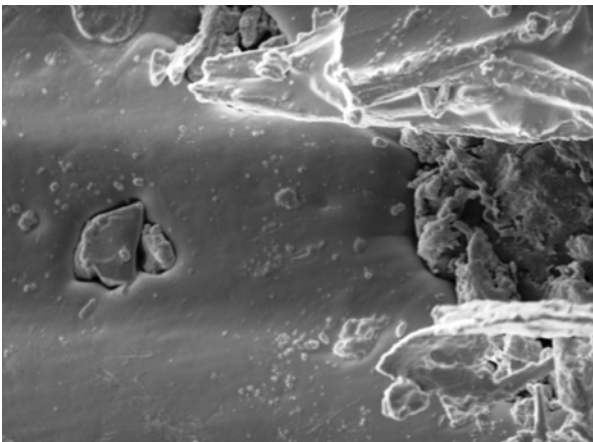


SEM MAG: 200 x DET: SE Detector
HV: 15.0 kV DATE: 04/04/11
VAC: HiVac Device: TS5130
500 µm Vega ©Tescan
Katedra náuky o dreve - DF TU Zvolen



SEM MAG: 100 x DET: SE Detector
HV: 15.0 kV DATE: 04/04/11
VAC: HiVac Device: TS5130
1 mm Vega ©Tescan
Katedra náuky o dreve - DF TU Zvolen

Fig. 11 PET flakes in the core layer are not glued with wood particles.



SEM MAG: 3.00 kx DET: SE Detector
HV: 15.0 kV DATE: 04/04/11
VAC: HiVac Device: TS5130
20 µm Vega ©Tescan
Katedra náuky o dreve - DF TU Zvolen

Fig. 10 Melted PET flakes covering wood particles on PB surface.

CONCLUSIONS

From the results of our research, we can draw the following conclusions:

- recycling of waste from PET packaging material in the particle board production proved to be highly relevant,
- addition of PET flakes reduced the mechanical properties but on the other hand improved the water resistance (reduced thickness swelling and absorption) of the boards,
- significant impact on the changes in the tested properties had the proportion of PET flakes in the particle board,
- it has been revealed that modification of PET surface with plasma could improve adhesion properties of this material and thus also the properties of wood particle boards with PET admixture,
- in our opinion, additional research focused on this subject is needed.

LITERATURE

- AYRILMIS, N., BENTHIEN, J. T. & WHITE, R. H. 2011. Properties of flat – pressed wood plastic composites containing fire retardants. *J. Appl. Polym. Sci.* 122 3201–3210.
- FLORIÁN, Š., NOVÁK, I., POPELKA, A., CHODÁK, I., ŠPIRKOVÁ, M., CHEHIMI, M. M. & KLEINOVÁ A. 2012. Surface properties of polyethylene terephthalate modified by barrier plasma. In.: 43th International Conference on Coatings Technology. Pardubice, University of Pardubice, pp. 107–116.
- KLYOSOV A. A., 2007. Wood plastic composites. New Jersey, Wiley & Soons, 698 pp.
- LI, X., CAI, Z., WINANDY, E. J., BASTA, H. A., 2010. Selected properties of particleboard panels manufactured from rice straw of different geometries. *Bioresource Technol.* 101(12): 4662–4666.
- MORTON, J. & ROSSI, L. 2003. Current and emerging applications for natural and wood fiber composites. In.: 7th International Conference on Wood Fiber - Plastic Composites. May 19–20, Madison – Wisconsin, Forest Production Society, 3
- OZALP, M., 2011: Study of the effect of adding the powder of waste PET bottles and borax pentahydrate to the urea formaldehyde adhesive applied on plywood. *Eur. J. Wood Prod.*, 69: 369–374.
- PANAITESCU, D. M., FRONE, A. N., GHIUREA M., SPATARU, C. I., RADOVICI, C. & IORGA, M. D. 2011. Properties of Polymer Composites with Cellulose Microfibrils. In: *Advances in Composites Materials – Ecodesign and Analysis.* (Ed. B. Attaf), InTech., Chapter 5, pp.103–122.
- RÉH, R., MARKOVÁ, I., VRTIELKA, J. & ORÉMUSOVÁ E. 2012. The influence of addition of hemp shives in the particleboard core layer to their heating value and energy efficiency. In: *Wood and Fire Safety* (Ed. Osvald, A.). Ostrava, Šmíra – Print, pp. 239–244.
- RÉH, R. & VRTIELKA, J., 2011. Wheat straw as biomass for fractional utilization in particleboard. (in Slovak). In.: *Selected processes at the wood processing.* Zvolen, Technická univerzita vo Zvolene, pp. 244–252.
- SAMIR, M., ALLOIN, F., DUFRESNE, A., 2005. Review of Recent Reseach into Cellulosic Whiskers,their Properties and Their Application in Nanocomposite Field. *Biomacromolecules.* 10: 19–26.
- SOBCZAK, L., LANG, R.W. & HAIDER, A. 2012: Polypropylene composites with natural fibers and wood – general mechanical property profiles. *Compos. Sci.Technol.* 72: 550–557.
- STN EN 317. Drevotrieskové a drevovláknité dosky - Zisťovanie hrúbkového napúčania po ponorení do vody. 1995
- STN EN 310. Dosky na báze dreva - Zisťovanie modulu pružnosti v ohybe a pevnosti v ohybe. 1998.
- STN EN 319 Trieskové a vláknité dosky - Zisťovanie pevnosti v ťahu kolmo na rovinu dosky. 1995.
- ŠTEFKA, V., 1996: Profil hustoty a vlastností drevotrieskových dosák. Zvolen, Technická univerzita vo Zvolene, 13/96A, 57 pp.
- TÓTH, V., POMIKALA, R. & JERZ, J. 2012,. Pat. Slovenská republika 287936. Spôsob výroby konštrukčného prvku s povrchovou vrstvou z PET fólie, konštrukčný prvok a jeho použitie. 03. 05. 2012.
- VRÁBĽOVÁ, Z., ŠTEFKA, V. & IŽDINSKÝ, J. 2006: Využitie cirokového odpadu na výrobu plošných a tvarových aglomerovaných materiálov. *Acta Facultatis Xylogologiae Zvolen*, 48(2): 59–72.

Acknowledgements

The authors would like to thank the Grant Agency of the Slovak Republic (Projects VEGA No. 1/0345/12 and No. 1/089/13) for financial support of this work.

ABSTRACTS

UNDERSTANDING WOOD AT THE NANOSCALE - ZOOMING THROUGH WOOD CELL WALL ULTRASTRUCTURAL ORGANIZATION

RUEL K.

Like most biological materials, wood owes its structure and properties to its several levels of organization interconnected through hierarchical scales. The process of cell wall expansion during wood biogenesis decisively influences the shape of trees and also wood mechanical properties. Whether the cells undergo isotropic or anisotropic expansion will determine their biological function in the tree, such as storage, water conducting or supporting structure. It has long been clear that rationalizing trees and wood-based products properties at the macroscopic scale necessitates in depth understanding of the mode of distribution and interaction of the macromolecular constituents at the finest resolution scale. Understanding the analysis of the wood at the ultrastructural level implies visualizing and identifying the constituents *in situ* in *their native state* within the cell walls. Resolution between μm and nm can be obtained using transmission electron microscopy (TEM), and by coupling TEM to non-invasive techniques of labeling the respective distribution of the different cell wall macromolecular constituents may be achieved. Immunochemical approaches offer a large reservoir of specific markers allowing visualization, identification and semi-quantitative evaluation of the spatial distribution of the wood cell wall constituents at the sub-cellular level. It was thus possible to map the progressive spatio-temporal integration of cellulose, hemicelluloses and lignins in the developing cell walls as well as to characterize the ultrastructural alterations and compositional modifications induced by genetic modifications of the hemicelluloses or lignins biosynthetic pathways. All the observations depicting the progressive steps of the biogenetic development of the wood cell walls, their genetically controlled modification as well as their deconstruction by chemical or enzymatic processes converged to the elaboration of a dynamic hierarchical model of the constitution of the lignified wood cell wall. The informative potential of combining *in situ* methods and micromechanical measurements will be of increasing interest in the context of wood and wood-derived materials in the domains of nanotechnologies and for the processes of biomass conversion.

NANOFIBRILLATED CELLULOSE FROM WOOD AS BUILDING BLOCK IN HIGH TOUGHNESS MATERIALS

SEHAQUI H.

Materials from nanofibrillated cellulose (NFC) are an interesting alternative to oil-based materials. Nanofibrillated cellulose refers to high aspect ratio fibrils disintegrated from wood, plant resources and agricultural wastes by a high shear mechanical treatment and are obtained as an aqueous suspension. A wide selection of materials from NFC with a wide range of properties can be obtained by drying the NFC suspension by different means. For example, light-weight foams with up to 99.5% porosity and an ice template structure are obtained by freeze drying NFC suspension. NFC aerogels with a fibrillar network structure and high specific surface area can be obtained by supercritical drying, t-butanol freeze drying, or by rapid freeze drying of NFC suspension. A dense films made of NFC also called nanopaper can be obtained simply by air drying the aqueous suspension, or by a papermaking-like route involving vacuum filtration and drying. The intrinsically high mechanical properties of cellulose crystals in NFC (modulus of ca 100 GPa) and their network forming characteristics makes NFC materials of good mechanical properties (high toughness). Mechanical properties can be further increased by orientation of the fibrils.

Moreover, NFC can be used for elaboration of biocomposites. We will explore different ways of nanocomposites processing such as papermaking approach, insitu polymerization on high surface area NFC network and melt processing.

SORPTION ISOTHERMS FROM WOOD ADHESIVE FILMS

WIMMER R., KLÄUSLER O. & NIEMZ P.

Wood is a sorptive materials and most wood properties are linked closely related to water sorption. While sorption of solid wood is a common research problem, there are rarely data on the sorption behavior of cured adhesives. The study of vapor dynamics of cured adhesives is seen as new and might reveal novel insights to bonding behavior. A fully automated humidification system, called dynamic vapor sorption was used to expose cured adhesive films to relative humidity and temperature changes. The temperature-controlled incubator contained two chambers, the reference chamber and the sample chamber, within which the specified relative humidity was produced. The changes in relative humidity in each chamber occurred by mixing a specific ratio of saturated vapor and dry air. Temperature was also altered to collect separate sorption isotherms. Different theories of water sorption were applied to water adsorption data of adhesive films. For a better understanding sorption isotherms were also collected at three different temperatures over the same partial pressure range. By applying Clausius-Clapeyron equation heat-of-sorption cures of adhesive films were obtained. It is shown that the water content of adhesive films may lead to a retarded formation of the adhesive network structure, which adversely affects the strength of adhesive joints.

SPECTRAL STOCHASTIC MODELLING OF UNCERTAINTIES IN HEAT AND MOISTURE TRANSFER EQUATIONS

TRCALA M.

This paper deals with the stochastic analysis of heat and moisture transfer in wood with random input material properties. The spectral solution of this problem is based on discretization of the resulting physical fields in the stochastic dimension by the orthogonal polynomials. A Galerkin projection is applied in the stochastic dimension to obtain the deterministic set of partial differential equations that is solved by finite element method.

The main purpose of this paper is to demonstrate that the spectral method based on polynomial chaos expansion is more efficient in modelling uncertainties associated with heat and moisture transfer in wood than Monte Carlo method in terms of computational time. Numerical examples are given and there is shown that the results (mean and the standard deviation) obtained with the spectral method are in good agreement with the results of the Monte Carlo simulations.

DIAGNOSTIC CRITERIONS OF FIGURED WOOD OF EUROPEAN BEECH (*FAGUS SYLVATICA* L.) GROWING IN UKRAINE

SOPUSHYNSKYI I., ZHMURKO I., TEISCHINGER A.

The quality reflects the utility of the wood and therefore is defined by the end users. Quality criterions can only be applied for the specific purpose for which the wood is used. In Ukraine, a variety of European beech (*Fagus sylvatica* L.) represented by special wood anomalies like wave grain are typical in the mountain forest. This wood deliver high-value decorative wood for furniture, interior design, floors with highly decorative wood surfaces etc. Additionally, from a socio-economic viewpoint European beech possessing decorative features have higher economic value for the forestry and wood technology. The question of the formation of aesthetic quality and some details of wood fibres placing in the trunks of beech were debated. The length of decorative wood in the trunk, the distance to the first live crown knot, the average diameter of the crown, diameter at breast height, height of trees of beech wood and ratio of leaf indexes were analyzed. Morphological differences with cross-grained and straight grain beech wood have been established. The diagnostic parameters of decorative wood of European beech and its grading characteristics were given.

DRYING OF SIFTED WOOD WITH THE PNEUMO-IMPULSE METHOD

ANTONS A. & DOLACIS J.

Wood as one of the Latvia's main renewable energy resources, which is still in sufficient amounts and is not fully utilised, should be used rationally and efficiently. In this connection, the issue of ground wood drying, which would be efficient and energy-saving, is urgent. The present work deals with a method for drying the pine model material by the pneumoimpulse method. The model material (pine cubes $5 \times 5 \times 5$ mm) is specially prepared to carry out the studies. The object of the study is the laboratory experimental pneumoimpulse dryer, which makes it possible to study the drying regime for different types of biomass (wood chips, sawdust, lignin, corn, etc.) products. Owing to the non-stationary interaction of the drying agent's flow with the disperse material's layer, at each pulsation, the material's arrangement on the sieve varies, and the formation of large air voids (channels) throughout the layer is eliminated.

It has been found in the work that, as a result of the effect of the pulsing flow, in comparison with the stationary flow, the substance's temperature increases, and the formation of the turbulent flow zones is intensified. Applying the pulsing flow, it is possible to speed up the drying process due to the intensification of the moisture emission process, removal of the evaporated moisture from the material, and the heat and mass exchange in the fluidised bed. Drying at the impulse regimes is more efficient, on the average, by 13 %, and the air consumption, on the average, at the pulsation frequency ($H = 5-45$ Hz) is lower by 12-24 % as compared with the stationary flow regime ($H = 0$ Hz). The aim of the work is to analyse the peculiarities of the heat and mass exchange in drying processes in the pulsing air flow, employing the experimental data.

THE EFFECT OF HEAT AND AMMONIA TREATMENT ON COLOUR RESPONSE OF OAK HEART/SAPWOOD AND COMPARISON OF PHYSICAL AND MECHANICAL PROPERTIES

ČERMÁK P. & DEJMAL A.

In this paper the effect of heat and ammonia treatment on the change in colour of oak wood and comparison of physical and mechanical properties were investigated. Wood specimens were made from heartwood and sapwood. The specimens were subjected to heat treatment at 180 °C and 230 °C for 2 and 4 hours, others were treated by ammonia for 24 hours. After these processes, hardness, EMC, density and MOE of wood were tested in comparison with untreated samples. The results show that the heat treatment contributed to darkening of sapwood and heartwood and the total colour change increased up to 38.47 in the radial direction and 37.75 in the tangential direction. Previous research into ammonia treatment shows that the most significant changes were noticed after 1 day. The colour changes between sapwood and heartwood were more noticeable than in the case of heat treatment. All observed properties were decreased in the case of heat treatment. Ammonia treatment does not have a significant influence on the observed properties. The results proved that ammonia treatment is a modification that improves the decorative value but has a minimal effect on technologically relevant properties of solid wood. Nevertheless, the heat treatment can be used as comparable process for colour change of wood.

MICROWAVE RADIATION EFFECT ON AXIAL FLUID PERMEABILITY IN FALSE HEARTWOOD OF BEECH

Koiš V.

The subject of this study was to measure the fluid permeability in samples produced from beech false heartwood. The samples were divided into three groups. The first group was the reference group. The remaining two groups were exposed to microwave radiation. The process of microwave treatment was conducted using laboratory equipment at a frequency of 2.45 MHz and output of 900 W but each of the groups was exposed for a different time. The permeability was measured using distilled water in the axial direction and laboratory equipment for testing of porous materials. The last stage of the experiment was measuring of strength parallel to the grain in all three groups of samples. After the experimental part, the coefficient of stationary permeability was calculated by Darcy's law. The resulting evaluation was carried out using statistical methods. The results show that the stationary permeability coefficient is higher in all microwave treated samples. At the same time, the strength parallel to the grain decreased in these samples when compared with the reference group and the volume increased.

NUMERICAL ANALYSIS OF MODE STIRRER IMPACT ON ELECTRIC FIELD UNIFORMITY IN A MICROWAVE WOOD DRYER

SEBERA V. & NASSWETTROVÁ A.

Nonuniformity of the electromagnetic field in microwave ovens is assumed to be one of the reasons causing nonuniform drying of materials. There are several approaches that are partly able to eliminate such a negative phenomenon. One of them is a placement of mode stirrers in the microwave (MW) applicator. Therefore, the goal of this study was to numerically investigate an influence of a proposed fan-like mode stirrer on the uniformity of the electric field (EF) in an experimental MW device. This was done with the help of 3D harmonic high-frequency finite element (FE) simulation of the EF distribution in the MW applicator. Within the work, two FE models of the MW device were built, analyzed and compared to each other. The first FE model does not incorporate the mode stirrers. The other one has two mode stirrers, each placed in front of two waveguide ports. In both models, the EF uniformity is studied in ten height levels and in two mutually perpendicular directions. Change of the EF uniformity was analyzed in terms of coefficients of variation (CoV's) of the electric vector sum across the applicator. Results of simulations show that the mode stirrers decreases CoV's (EF uniformity) in 8 from 10 studied height levels ranging from 2 to 20 % and increase them in two topmost levels ranging from 3 to 7.3 %. In respect to the fact that the simulations did not consider the mode stirrers' rotation, the calculated effect might be lower than real one. However, harmonic FE analysis was shown to be an efficient way for investigating, to a degree, the mode stirrer influence on the EF uniformity in a microwave applicator.

HIGH-THROUGHPUT CHARACTERIZATION OF WOOD

VAN ACKER J., VAN DEN BULCKE J., DEFOIRDT N. & DIERICK M.

Selection and breeding of tree species requires high-throughput characterization of the wood properties in relation to both applications for material and bioenergy use. At the Laboratory of Wood Technology, advanced techniques have been developed for this purpose. First, coupled DSC-TGA can be used as a tool to obtain semi-quantitative information on the chemical composition due to the different thermokinetics of the main constituents (lignin, cellulose and hemicelluloses) and gives also a detailed view on the energetical content of the material. Scanning experiments can be set up in DSC, TGA or coupled mode, with different carrier or reactive gases, and with heating rates variable programmable from 0.01 up to 30°C/min. Second a method is developed for using short-wave infrared signals to obtain chemical information on cellulose and lignin composition in a fast and quantitative way. Third, structural properties on different scales are acquired using the multi-resolution X-ray tomography set-up developed at UGCT, the Ghent University Centre for X-ray Tomography. The system offers a large range of operation freedom, all combined in versatile acquisition routines (standard or fast scanning, tiling, helix, etc.). Simultaneously with 3D structural information, (micro)densitometrical detailing is obtained as well. Combining all aforementioned techniques allows for quantitative characterisation of key wood properties for selection and breeding taking into account not only mean values, but surely also asses variability within and between trees.

SURFACE PROPERTIES ANALYZED BY ATOMIC FORCE MICROSCOPY

LAGAÑA R., KÚDELA J., ĎURKOVIČ J.

The topic of the study deals with surface properties evaluation using AFM technique.

The first part discusses selected properties of two types of solid coatings (polyurethane and water-based) investigated in two forms: coatings applied on spruce wood surface and free films applied on glass. These properties were studied at micro and nano-scales, with the aid of an atomic force microscope (AFM). The differences in the properties between the coatings and free films showed that the properties of solid coatings were affected by the substrate properties. The results indicate that the final properties of the coatings significantly depended on the substrate – coating interaction during the curing.

The second part of the study discusses an effect of sorbus hybrids and elm disease on leaf mibrid properties. AFM technique addresses parental effects of sorbuse hybrids and reveals an influence of elm disease. AFM showed to be a useful tool for analyzing material properties at micro and nano levels.

SMOKED WOOD RESISTANCE TO SUBTERRANEAN AND DRY WOOD TERMITES ATTACK

HADI Y. S., NURHAYATI T., JASNI M., YAMAMOTO H. & KAMIYA N.

Samples from sengon (*Paraserianthes falcataria*), sugi (*Cryptomeria japonica*), and Pulai (*Alstonia* sp) woods were smoked for 3-, 8- and 15-day using mangium wood (*Acacia mangium*), and for comparison purposes polystyrene and untreated woods were prepared. All of the wood specimens were exposed to subterranean termite (*Coptotermes curvignathus* Holmgren) and dry wood termite (*Cryptotermes cynocephalus* Light) under laboratory conditions. The results showed that (1) the untreated woods had the same resistance class V or very poor resistant to subterranean termite attack. On the other hand pulai and sugi had resistance class IV or poor resistant to dry wood termite, while sengon had resistance class III or moderate resistant based on the Indonesian standard (SNI, 2006); (2) Treatment of the samples for 3 days resulted resistance class I or very resistant to subterranean termite attack; and (3) smoke treatment during 3 days for sengon and pulai, and 15 days for sugi resulted resistance class I to dry wood termite attack, and these smoked woods had the same resistance classes with polystyrene woods.

COMPARISON OF PHYSICAL PROPERTIES OF POPLAR WOOD VACUUM-PRESSURE IMPREGNATED WITH SUCROSE AND SODIUM CHLORIDE

PAŘIL P. & DEJMAL A.

This paper deals with the effect of vacuum-pressure impregnation of poplar wood (*Populus alba* L.) by aqueous solutions of sucrose and sodium chloride on its physical properties. Impregnation was conducted using laboratory vacuum-pressure equipment (JHP 1-0072). Groups of samples with different concentrations of substances in the aqueous solution were compared within each other and also with a reference (non-impregnated) group. After the quality and degree of impregnation have been assessed (WPG, etc.), the samples from all groups were experimentally tested for density, moisture absorption and dimensional changes. The obtained data were then statistically analysed and the conclusions were compared.

THE INFLUENCE OF HEAT TREATMENT ON THE RHEOLOGICAL PROPERTIES OF BEECH WOOD

ŠUCHAŇOVÁ I., LAGAŇA R. & BABIAK M.

The contribution deals with rheological characteristics of thermally treated beech wood. The specimens were oven dried, then thermally treated (160, 180 and 200 °C for 2, 4 and 6 hours), soaked into water and conditioned at the RH = 95 % and temperature of 20 °C for 21 days. The specimens were then loaded in bending with a static load.

The deflection was measured by optical system during loading and also on unloaded specimens. For the evaluation of results we used image analysis program.

The results were evaluated according to Burger's body described by two moduli of elasticity and two viscosities. All the rheological characteristics decreased with increasing temperature in comparison with untreated specimens. Because of small number of specimens the results can serve only as an orientation for planning the next experiments.